REVIEWS OF
MODERN PHYSICS

VOLUME 16, NUMBER 2 APRIL, 1944

Sound Waves in Rooms

PHILIP M. MORSE AND RICHARD H. BOLT*
Acoustics Laboratory, Massachusetts Institute of Technology, Cambridge, Massachusetts

TABLE OF CONTENTS

* Member of the Physics Department, University of Illinois, during part of the time this article has been in process of preparation.

I. INTRODUCTION

1. Historical

THE SCIENCE of architectural acoustics is a relatively small branch of physics and one which attracts the attention of few physicists; yet the field has had its share in the advances of the past decade, and some of the new results may prove useful in other fields. After the pioneer work of W. C. Sabine (S1)* at the turn of the century, very little new scientific work was done on the subject for some time, and room acoustics seemed to have become a branch of engineering (S5). During the past decade, however, scientific interest in the field has revived, largely because of the theoretical discussions of Schuster and Waetzmann (S10), and Strutt (S15), and the enlightening experimental results of Knudsen (K3, K5), Hunt (H7, H9), and others (C2, M5, M10, P7, P9, S3, W8). Considerable progress toward a fundamental understanding of the subject has now been achieved.

Ten years ago Knudsen wrote an article (K7) in these Reviews, outlining the status of the field at that time, emphasizing the inadequacy of the underlying concepts previously in vogue and pointing the direction in which new advances must be made. Since that time the advances which he foreshadowed have been sufficiently extensive and interesting to warrant another report in these Reviews.

Room acoustics is the study of the transient and steady-state behavior of sound waves in an enclosure. The scientific aspect of the field has many inter-connections with other fields of physics. The inter-relations between experimental acoustics and the advances in vacuum-tube technique are obvious, as are the relations between acoustic theory and the theory of other sorts of wave motion. Rayleigh's law for the number of electromagnetic waves in a given frequency range was first worked out for the acoustic case (R3, R4). More exact expressions for this number have been developed for use in acoustics (B6, M1, R8), and recently these expressions have been used (H10) in the study of the Bose-Einstein statistics of particles. The exchange has also been in the opposite direction; some of the theoretical techniques developed for use in wave mechanics have been applied in acoustical theory (M11, R8). Some of the results discussed in this report may, in turn, find application in other fields.

The study of sound waves is of particular importance to the study of wave motion in general, for several reasons. In the first place, sound waves have a convenient length, not being immoderately long as are most radio waves, and not being excessively short as are light and matter waves. This advantage of wave-length size more than outweighs the practical difficulties of measuring the small energies involved in acoustics, for details of wave motion may be studied by direct and obvious methods. In the second place, the objects which usually reflect and absorb sound are of about the same magnitude as the wave-lengths of sound (S7). This is the region in which the most complicated wave phenomena occur. Many problems in this region have been left undone, even though the results would have been valuable, because the need for their study in other fields was not great enough to warrant the efforts required for their solution. In the study of acoustics, however, it is impossible to avoid these problems if any scientific advance is to be made at all.

* References to the bibliography at the end of this review are given in parentheses, ( ).

2. Geometrical and Wave Acoustics

Curiously enough, though perhaps it is understandable, the concepts developed by the early workers in room acoustics, and the concepts underlying present acoustical engineering practice, completely neglect the wave properties of sound. Here, in a subject where wave properties continually obtrude, a geometrical picture of rays and sharp reflections has been used. It is to be expected that geometrical acoustics should have been first used, for the wave analysis presents so many difficulties that no initial advances could have been made without using an oversimplified picture. W. C. Sabine (S1) of course recognized effects arising from the wave nature of sound, and he pointed out some of the influences of diffraction and interference. But he set aside these complications in order to make a start on the problems, and they are set aside by most acoustical engineers even now.

Thus it is not surprising to find (H8, K7, W1) that the acoustical engineer must salt his geometrical formulas with large doses of "common sense" before they become useful in practice. In spite of the unreliability of the formulas, however, and because of his common sense, the acoustical engineer today is quite successful in designing satisfactory auditoriums and office rooms—whenever the architect gives him a chance. As Knudsen (K7) says, "The approximate theories, when used with *caution* and *understanding*, have served satisfactorily for the practical purposes of acoustical designing, and they will continue to do so until they are superseded by more exact theories."

Such a state of affairs may be satisfactory to the engineer; it is not at all satisfactory to the physicist. In order that room acoustics may advance along with the rest of physics, the wave nature of the problem must be investigated (K5, S4). It is necessary to study the normal modes of air vibration in rooms whose boundary surfaces are not simple shapes. It is necessary to study the effects of patches of absorbing material and irregularities in wall shape on the distribution of steady-state sound. It is important to study exact solutions for the transient vibrations in a room with absorbing walls; in this case the boundary conditions are dependent on the frequency of the wave, the characteristic values of the frequencies are complex, and the characteristic functions do not form an orthogonal set. It is necessary to study the transient effect when many normal modes of vibration are set into motion, each normal mode having a different decay rate and the resulting decay exhibiting interference effects. It is necessary to investigate the nature of the absorption of sound by various acoustic materials, to find how best to formulate this effect as a boundary condition of the waves, and how best to measure the effect quantitatively. In the past ten years, attacks have been initiated on some of these problems. The results will be reported in succeeding pages.

After a short summary of the results obtained by geometrical acoustics, we shall discuss the general principles underlying wave acoustics, and the way in which these principles clarify and supplement the geometrical results of the earlier workers. In the remainder of the report we shall outline the recently obtained solutions to some of the problems of wave acoustics and indicate some of the problems which still await solution. It is to be hoped that the incompleteness of these results will tempt other workers to enter the field.

3. Reverberation Time and Acoustic Criteria

Although most of the present report will be concerned with the physical problem mentioned above, some space must be devoted to discussing engineering questions since they provide criteria for determining the relative importance of the physical problems. As soon as the engineering aspect is considered, however, one must also consider the aesthetic and the psycho-physiological aspects of acoustics. Before one can apply acoustical science to the design of an auditorium, one must know what constitutes a "good" auditorium. This was partly answered by W. C. Sabine (S1), who showed that an important criterion is the nature of the transient response of a room. He distinguished between the irregular transient which constitutes an echo, and the more regular damping out of sound after the source is stopped, which he called *reverberation.* In order to measure this important effect he defined the *reverberation time:* the length of time for the mean square pressure of a suitably chosen

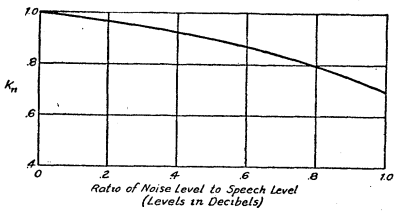

FIG. 1A. Factors determining percentage articulation in rooms (according to Knudsen, reference K3). Articulation reduction factor for noise.

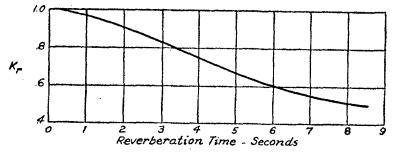

FIG. 1B. Factors determining percentage articulation in rooms (according to Knudsen, reference K3). Articulation reduction factor for reverberation.

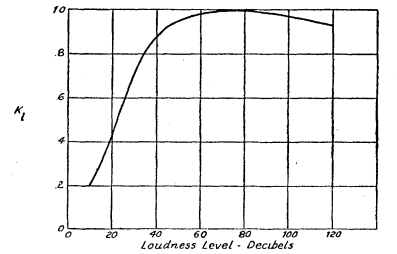

FIG. 1C. Factors determining percentage articulation in rooms (according to Knudsen, reference K3). Articulation reduction factor for loudness.

distribution of sound waves to diminish to one-millionth of its original intensity. He then collected opinions as to what values of reverberation time in various rooms were considered satisfactory. Other investigators have extended this study. In the following sections are discussed some of the criteria which guide present engineering practice.

3.1 Criteria for Hearing of Speech

The recognizability of speech in rooms has been studied quantitatively by Knudsen (K3) and Lifschitz (L3), using "articulation test" methods (F3) developed for testing transmission over telephone equipment. *Percentage articulation* (P.A.) is defined as the percentage of typical speech sounds heard correctly, when measured statistically by a number of speakers and listeners, using specially devised lists of typical syllables.[1]

The percentage articulation in a room can be estimated by means of the following equation and empirically determined factors:

$$\text{P.A.} = 96 k_l k_r k_n k_s, \tag{1.1}$$

in which the k's give the reduction as dependent on: $k_l \rightarrow$loudness, $k_r \rightarrow$reverberation, $k_n \rightarrow$noise, $k_s \rightarrow$shape of room. Values for k_l, k_r, and k_n are shown in Fig. 1 as obtained by Knudsen(K3).

We see that through k_l, Fig. 1C, the P.A. drops rapidly with decreasing average loudness below about 40 db. This is due to psychological factors such as attentiveness, and to physiological factors such as the variation of ear sensitivity with frequency which causes the weaker sounds (*b*, *v*, *th*, etc.) to drop below audibility before the average level does. On the other hand we see that k_r decreases with increasing reverberation, which is due to confusion of sounds and to masking caused by the overlapping of prolonged sounds. The k_r function in Fig. 1B is based on reverberation time at 512 c.p.s.; variation of reverberation effects with frequency will be discussed later.

Reverberation time T and steady-state sound intensity I are connected through the following (asymptotic) relation:*

$$I = (\Pi / KV)T \tag{1.2}$$

in which Π is the rate of emission of sound, K a constant depending on units, and V the room volume. The subjective quantity *loudness* is monotonically, but not linearly,[2] related to the objective quantity *intensity;* and the relation depends on frequency. These functional interrelations are shown in Fig. 2.

As a consequence of the opposing effects of k_l

[1] The commonly accepted evaluation scale for percentage articulation is:

P.A. = 96	"Perfect hearing"; some sounds are misheard even under ideal conditions, but their meaning is supplied by context.
85–96	Highly satisfactory.
75–85	Satisfactory.
65–75	Speech understandable with normal acuity and strained attention.
below 65	Unsatisfactory.

* A glossary of symbols used is given at the end of this review.

[2] Except at 1000 c.p.s.; loudness level is by definition equal to intensity level at 1000 c.p.s. See Fig. 2.

and k_r, connected through Eq. (1.2) and the functions in Fig. 2, there is an *optimal reverberation time* for a room of a given volume, i.e., a value of T for which the P.A. becomes a maximum; and the optimum varies with V. In Fig. 3A, the lower curve, marked "speech," gives the optimal reverberation time as a function of volume, according to Knudsen. This curve incorporates only the effects of k_l and k_r, as outlined above, and neglects effects of k_n and k_s.

Noise, as expressed by k_n in Fig. 1A, always reduces the P.A., because of masking of the speech sounds. However, the reduction depends to some extent on the *ratio* of noise to speech level, so that the effect of noise can be reduced by amplification of the speech, at least up to a limiting loudness level of about 80 db, beyond which k_l begins to drop off.

The effect of shape is not so well understood and requires further quantitative investigation. In "conventional" rectangular rooms, k_s probably does not differ appreciably from 1.0. In very large auditoriums, or in the presence of improperly curved surfaces, it may be as low as 0.9. In small rooms with properly shaped reflecting surfaces, k_s may be as high as 1.05. Some of the new developments reviewed later have considerably increased our knowledge of the physical behavior of sound as influenced by room shape. It is hoped that further studies may yield useful information on the influence of shape on hearing conditions.

The recent developments in room acoustics appear to have a significant bearing on the above picture, particularly through the relation between P.A. and k_r. In the first place, there is an increasing tendency to consider the decay rate[3] as more fundamental than the reverberation time. Decay rate has meaning even for nonlinear decays, whereas T is defined in terms of a linear decay of 60 db. As discussed elsewhere, a strictly linear decay is more likely to be the exception than the rule; in practice one finds both major breaks in the curve and small superposed fluctuations. There are indications that the first 30 or 40 db of decay are the most significant in determining the hearing quality. Thus a room having a rapid initial decay and a long tail of small slope would probably possess a higher P.A. than a room having linear reverberation matched to the same value 60 db down;

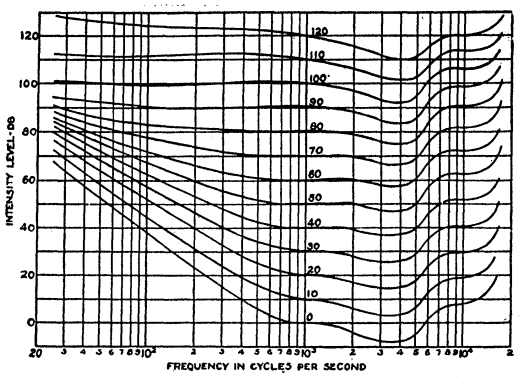

FIG. 2. Contours for constant loudness level plotted on the (intensity level, frequency) plane.

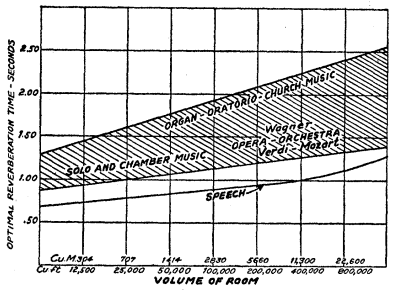

FIG. 3A. Reverberation time criteria. From reference K3. Optimal reverberation times, at 512 c.p.s., for speech and music rooms.

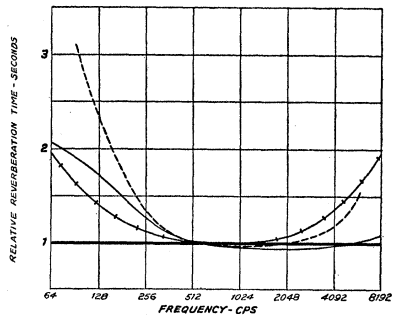

FIG. 3B. Reverberation time criteria. From reference K3. Optimal frequency characteristic of reverberation. Reduced to unity at 512 c.p.s.

——— flat criterion
——— McNair criterion for speech
—|—|—|— Knudsen criterion for speech
– – – – – – Knudsen criterion for music

[3] In this report the term "decay curve" will always mean the plot of the natural logarithm of the mean-square pressure as a function of time; and "decay rate" will mean the magnitude of the slope of this curve. In some cases the decay curve will be plotted in decibels (ten times the logarithm to the base ten), but the decay rate will always be the slope of the natural logarithm function.

yet k_r would be assigned the same value for these two cases on the basis outlined above. Modulations on the decay may also influence speech hearing, though it appears that this effect may be more important for music hearing, as will be mentioned later. But beyond the explicit influence of decay shape on P.A., one might expect the detailed nature of the decay curve to reveal other acoustic properties which in turn affect the hearing conditions. For example, strong interference effects and also the degree to which the sound energy has been mixed influence the decay curve. Decay shape and modulations are controlled by absorbing materials and their distribution and by room shape and irregularities. These relations will be developed in Chapter VII.

The above discussion implies that k_r and k_s are not strictly separable factors. In fact it may be necessary to modify the functional form of Eq. (1.1) in order to express more rigorously the dependence of P.A. on the physical properties of the room. But one can do no more than indicate the general problem at this time; there remains much experimental work to be done before we can supplant Eq. (1.1) which, when used with understanding, provides a very useful engineering guide to the design of speech rooms.

3.2 Criteria for Hearing of Music

The evaluation of speech hearing in rooms has been reduced to a fairly definite engineering practice largely because one can employ the objective measurement of percentage articulation. The evaluation for music is more difficult, and to date no comprehensive, solidly grounded criteria have been established. Objectivity is more difficult to apply; personal tastes differ and may be conditioned by experience and musical environment. And yet it is to the control of music rooms that we expect the application of recent results to be most fruitful (B1, L4, R5).

The fundamental requisites are similar to those for speech: (a) sufficient loudness for comfort and pleasure, (b) freedom from extraneous noise, (c) freedom from distortion of frequency and amplitude relationships, and (d) adequate separation of successive sounds to satisfy musical taste.

The last two requisites are the most relevant here, especially the last one which calls for proper control of reverberation time. The same underlying factors apply to music as to speech hearing. It is expected that these would lead to an optimal reverberation time for music, and that this optimum would depend on volume. But the analogy can be carried no further. We must depend on the concensus of musical taste to provide "quantitative" criteria. The present accepted practice is about as shown in Fig. 3A (K3). The optimum values form an area (instead of a single curve as for speech) because, in any given room, the most acceptable reverberation time depends on the kind of music. Fast, light, intricate music requires generally shorter T, while broad, flowing music seems pleasing in the presence of longer reverberation. For no kinds of music is the desired T as short as for speech. Figure 3A applies to 512 c.p.s.

The dependence of optimal reverberation on frequency has been studied by several investigators (W2, L2, L4, S10, L3). Knudsen (K1, K3) proposes that T should be so adjusted that all frequency components die away to inaudibility at the same instant. MacNair (M4) has proposed that the loudness of all components should decay at the same rate. Other criteria have been suggested, some being based more on results as attainable with conventional acoustic treatment than on any rational basis. In Fig. 3B are shown some of these criteria; each of these have yielded fairly satisfactory engineering results. Recently there has been a trend on the part of some investigators to favor a more nearly flat frequency characteristic, especially in rooms thoroughly treated with sound diffusing irregularities (H2). Apparently there is a connection between the degree of diffusion (as discussed in Chapter VII) and optimal decay properties. It has also been observed that the ear tolerates longer reverberation in rooms properly shaped and with surfaces "broken up" for diffusion (M5). The result is an increase in "liveness" without sacrifice in clarity or distinctness.[4]

[4] Maxfield has arbitrarily defined "liveness" L by the equation $L = KT^2d^2/V$, in which K is an empirical constant, T the reverberation time, d the distance between sound source and ear, and V the room volume. He finds that in some cases the optimal $T-V$ curve (Fig. 3A) fits an hypothesis that the ear shows preference on the basis of equal liveness.

3.3 New Trends

It now appears that reverberation time alone is not always a sufficient measure of auditorium excellence. It is desirable to have the mean square pressure as nearly uniform as possible over the seating area. It is also important to have at least a certain percentage of the sound reach the listener directly from the speaker, and less than a certain percentage reach the listener indirectly, after reflection from any single surface; these requirements are involved in the concept of liveness.[4] It is now well known that sound in many rooms does not exhibit a straight line decay curve,[3] so that the term "reverberation time" has become somewhat ambiguous. For this reason, in the present report we shall discuss the *decay rate*, the slope of the decay curve, which has meaning even for non-linear decay curves. It seems that the decay rate should be nearly constant for the first 30 or 40 db for good acoustics, except for small superposed fluctuations which appear to make the decay more pleasing to the ear. Few of these subsidiary criteria have been reduced to quantitative statements, and it is hoped that studies will soon be made to remedy this lack. Articulation tests in rooms with specially controlled acoustic properties are needed, and quantitative tests should be devised for music conditions.

We now see that acoustic excellence of rooms depends on both large scale and small scale properties of both the steady-state and the transient behavior of sound waves. The recent developments reported here lay a foundation for a detailed understanding of the physical aspects and the factors which govern even the fine details of acoustic behavior. But there remains much work to correlate these physically describable variables with acoustic excellence. The criteria for speech and music should be reexamined with these new tools. It is not too much to hope that these lines of thought, pursued cooperatively by physicist, psychologist, engineer, musician and architect may lead to rooms which not only lack acoustic faults, but which possess positive qualities for enhancing the enjoyment of music.

II. GEOMETRICAL ROOM-ACOUSTICS

Prior to the twentieth century, contributions to room acoustics were meager and qualitative (A, S5, S7, K3, W1). Probably the most significant findings were those of Joseph Henry (H3), who discussed such matters as echoes, reverberation, resonance, and the shapes of enclosures as related to acoustic properties. Many of his conclusions, though qualitative, were based on experimental observations. Other physicists of this era, particularly Tyndall and Rayleigh, recognized the problems involved in controlling sound in rooms, but no systematic investigation was made in this period.

4. Absorption Coefficient

The first controlled quantitative experiments in room acoustics were those started in 1896 by Wallace C. Sabine (S1). His immediate task was the improvement of hearing conditions in the newly-constructed Fogg Art Museum lecture hall at Harvard, but he made of this particular problem the start of a general study of the behavior of sound in rooms. By ingenious experiments and inductive reasoning Sabine arrived at the now well-known reverberation theory and the formula:

$$T = KV/\sum \alpha_j S_j,$$

in which T is the reverberation time in seconds (defined above); K is a constant depending on units, V is the volume, and S the surface area of the room. The summation in the denominator is over the different sorts of material on the wall surface; S_j is the exposed area of each type of material, and α is a constant, called the *absorption coefficient* of the material, which Sabine defined as the average ratio of absorbed to incident sound intensity for the material.

The experimental details of Sabine's work have been discussed by many writers (K3, W2, S5) and need not concern us here. However, we should review the essential concepts involved as well as the experimental limitations since these underlie the geometric theory and its inherent shortcomings. From a present-day point of view, Sabine's equipment was quite primitive. For a sound source, organ pipes were used; the sound detector was the ear, which was found to be

adequately consistent if a single experimenter carried through a complete set of measurements himself; timing of decay was recorded on a chronograph; absorption was provided by seat cushions which were available in a large number of small uniform units. These comments are not meant to detract from the importance of Sabine's contributions, which have guided admirably the acoustic planning of auditoriums during the last four decades; they are given here to indicate why the approximate geometric approach was adequate to describe the results obtained in the particular cases studied by him, but not in all cases.

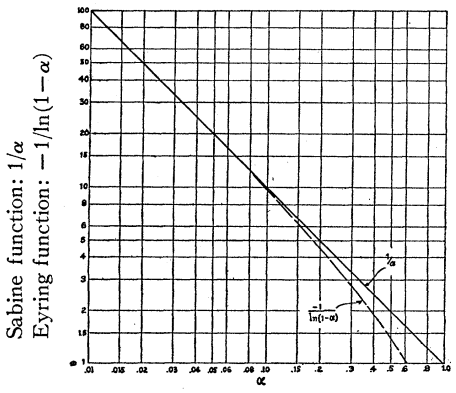

FIG. 4. Relation between Sabine and Eyring formulas for reverberation time.

5. Sabine's Approximations

Before proceeding with extensive studies of reverberation, Sabine examined the possible sources of experimental inconsistency and arrived at the following conclusions: (1) The duration of audibility of residual sound is *nearly the same* everywhere in the auditorium; (2) the duration of audibility is *nearly independent* of the position of the source; (3) the efficiency of an absorbent in reducing the duration of audibility is under ordinary circumstances *nearly independent* of its position. These results, which we shall see are invariably the prerequisites of the *geometrical* concept of room acoustics, were conditioned both by the experimental method and the choice of room conditions which were investigated. Had Sabine used a high speed instrumental means of detecting sound instead of the ear, he would have observed large fluctuations in intensity, with respect to both space and time changes. The averaging property of the ear, which smooths out space and time variations, made it possible for him to accept this elementary picture. The rooms used were moderately large and were all fairly reverberant, with reverberation times usually greater than 1.5 sec. If a wider variety of rooms had been studied, including extreme cases, no such simple conclusions as those listed would have resulted.

Sabine's choice of a standard unit of absorption is of considerable interest. He adopted an open window as a perfect absorber and assigned to it an absorption coefficient $\alpha=1$. Numerous absorbing materials were then measured by finding the area of open window which gave the same reverberation time as a particular area of the absorbing material. Sabine clearly recognized the limitations of the open window standard, in particular the influence of diffraction, which renders a small area comparatively more efficient in absorbing energy than a large window. In fact, this limitation applies to small areas of absorbing materials in general, though the diffraction effect is greater for very absorbing materials than for areas which have low values of absorption coefficient. This defect did not, however, appear to be too serious as long as the areas of window or material were not too small. Sabine concluded that, to the same order of accuracy as the other factors involved in reverberation measurements, the efficiency of an absorbent is usually independent of the area of the material exposed. This situation made it possible to apply the simple reverberation equation (2.3).

6. Geometrical Theory

Shortly after Sabine's empirical development (S2) of reverberation theory, Jaeger arrived at the same equation by a derivation similar to that used in the classical kinetic theory (J1, A1, F5). Modified derivations have since been given by Eckhard (E1), Buckingham (B14), and others (C5, C6, D2, F4, S15, S16). These derivations are based on certain simplifying assumptions (necessary in order to apply the statistical methods) which are based on the experimental observations of Sabine mentioned above. These

assumptions are essentially: (1) uniform, diffuse distribution of sound energy throughout the room at any instant; (2) equal probability of propagation of sound in all directions; (3) continuous absorption of sound by the boundaries. Clearly, the picture is strictly *geometrical;* sound energy is considered to travel in rays, and all wave phenomena are neglected. These assumptions are valid to the order of accuracy of Sabine's observations, which involved the averaging property of the ear.

These concepts lead to a simple differential equation derived from the conservation of energy.

$$\begin{bmatrix}\text{Rate of increase}\\ \text{of energy in room}\end{bmatrix}=\begin{bmatrix}\text{Rate of emission of}\\ \text{energy from source}\end{bmatrix}-\begin{bmatrix}\text{Rate of absorption}\\ \text{of energy by walls}\end{bmatrix}.$$

Let W be the energy density (assumed uniform), V the volume of the room, and Π the power of the source. Then $VdW/dt=$ the rate of increase of energy. The absorption rate is derived by calculating the fraction of energy which falls on unit area per second from a single direction, and integrating this over all angles of incidence. Then the rate at which energy strikes unit area is equal to

$$\frac{W}{4\pi}\int_0^c dr\int_0^{2\pi} d\theta\int_0^{\pi/2}\cos\varphi\sin\varphi\,d\varphi=(Wc/4).$$

The absorption rate is $(Wc/4)(\alpha S)$, since α is defined to be the fraction of incident energy absorbed by the surface area S.

The differential equation is:

$$V(dW/dt)=\Pi-(c\alpha S/4)W.$$

The solution, when the source is turned on at $t=0$, is found to be

$$W=(4\Pi/c\alpha S)[1-e^{-(c\alpha St/4V)}], \qquad (2.1)$$

and, when the source is turned off at $t=0$, it is

$$W=(4\Pi/c\alpha S)e^{-(c\alpha St/4V)}.$$

The measure of the shortness of the transient is sometimes expressed in terms of the decay constant

$$k=(c/8V)\alpha S, \qquad (2.2)$$

where the exponential factor in the transient term is written e^{-2kt}. The more usual measure of the transient duration is, however, the *reverberation time*, the time required for the energy to fall to 10^{-6} of its initial value,

$$T=(4V/c\alpha S)[\ln(10^6)]=(KV/\alpha S). \qquad (2.3)$$

In this, $K=0.049$ in English units and 0.161 in metric units. This equation is the same as the one obtained experimentally by Sabine, which emphasizes again the fact that Sabine's picture was essentially a geometrical and statistical one.

7. Other Geometrical Formulas

The first important modification of Sabine's theory was the replacement of the assumption of "continuous absorption" by that of a process of discontinuous drops in intensity during the decay. The resulting formula, due to Eyring (E3), is

$$T=KV/[-S\ln(1-\alpha)]. \qquad (2.4)$$

The Sabine assumptions of uniform distribution of energy and random flow of energy are retained, but sound energy is assumed to travel one mean free path and then to be reduced abruptly by an amount depending on the absorption coefficient of the wall. The form of the equation is similar to that of Sabine, with the simple absorption coefficient replaced by a logarithmic function. A plot of this function is given in Fig. 4, and we see that for large absorption Eq. (2.4) can differ from Eq. (2.3) by more than 100 percent. Measurements in relatively dead rooms show that the Eyring formula is very much superior to the simple Sabine one for these cases.

The Eyring formula may be deduced very simply, by a method suggested by Norris (N1). On the average, every time a travelling wave front strikes a wall, a fraction α of the energy is absorbed and a fraction $(1-\alpha)$ is reflected. The mean free path of the wave is $(4V/S)$, ($V=$volume and $S=$area of room), as used in Sabine's analysis (S1). The average number of reflections of the wave in a time t is then $(Sct/4V)$, $c=$velocity of sound, and the intensity after the time t will be

$$I=I_0(1-\alpha)(1-\alpha)(1-\alpha)\cdots=I_0(1-\alpha)^{Sct/4V}$$
$$=I_0\exp[\{Sc\ln(1-\alpha)/4V\}t].$$

Placing $I/I_0=10^{-6}$ we obtain the reverberation time given in Eq. (2.4). In Section 53 of the present Review we shall discuss the inaccuracies inherent in this method of analysis.

The Eyring formula uses an "average absorption coefficient." It is assumed that the walls are uniformly covered with material of uniform absorption or that the material is sufficiently well spread over all walls so that an average value can be taken. In this case

$$\alpha=[\sum\alpha_i S_i]/[\sum S_i].$$

For very non-uniformly placed absorbents, as when just one wall is highly absorptive and the rest are reflective, the Eyring form is seriously in error. This shortcoming led Millington (M7) and Sette (S12) to propose another form of averaging the absorption coefficient. Their equation is:

$$T=\frac{KV}{-\sum S_i \ln(1-\alpha_i)}. \qquad (2.5)$$

The main point of departure is this: Eyring's theory assumes that the energy in the room resumes uniform distribution after each set of incidences, during the discontinuous decay process; Millington and Sette follow the course of a bundle of rays through many reflections and assume that, on the average, a particular ray will strike a given surface a number of times proportional to its area. Both forms assume the Sabine geometric conditions, but the averaging is obtained differently. Eyring takes an *arithmetic* mean over the absorbing surfaces while Millington and Sette take a *geometric* mean. Since the geometric mean is always less than the arithmetic mean, it follows that the reverberation times and absorption coefficients given by the Eyring (E) and Millington-Sette (M-S) equations will be related by:

$$T_{MS}>T_E, \quad \alpha_{MS}<\alpha_E.$$

One serious defect of the M-S form is that it predicts $T=0$ if any surface, no matter how small in area, is completely absorbing.

Thus we see that each of the three equations discussed can be seriously in error in certain cases. The reason for Knudsen's remarks about "caution and understanding," mentioned in the previous section, is apparent.

All reverberation theory so far discussed has considered that energy is lost at the walls only. Actually there is some dissipation in the air in the room. Absorption in the air is negligible below 1000 c.p.s. but becomes increasingly important with higher frequencies. Above 4000 cycles the absorption in air may, in some cases, be several times the total absorption at the boundaries of the room. The nature of this absorption has been investigated extensively by Knudsen (K2, K6), who has incorporated the effect into the reverberation theory: (using Eyring's form, which has proved most widely useful)

$$T=\frac{KV}{-S\ln(1-\alpha)+4mV}.$$

If V is in cu. ft., S in sq. ft., then $K=0.049$ and m is the attenuation coefficient for plane waves in air in (feet^{-1}), as used in $I=I_0e^{-mx}$. The coefficient m depends on frequency, humidity, and temperature (K3).

In order to apply these geometrical formulas in a reasonable manner, it is often necessary to follow the "rays" of sound about the room, as they reflect from the various wall surfaces. In this manner it is possible to discern the focusing effects of curved walls and to see how nearly each particular room satisfies the requirements of uniformity of sound distribution, necessary for the application of the geometrical formulas. Much work has been done with ripple tanks and spark photography in this field (A). Ray-tracing analysis has also been used to determine the ratio of reflected to direct sound reaching the listener at different places in an auditorium (A, K3).

8. Reverberation Measurements

A brief summary of the experimental methods of room acoustics appears desirable in this report to indicate the role that measuring techniques have played in uncovering the inadequacies of the geometrical theory. Full experimental details are given in numerous papers (A, A1, C1, H5, H6, H7, O1, S13, W5, W6, W7) and are presented concisely in several books (A).

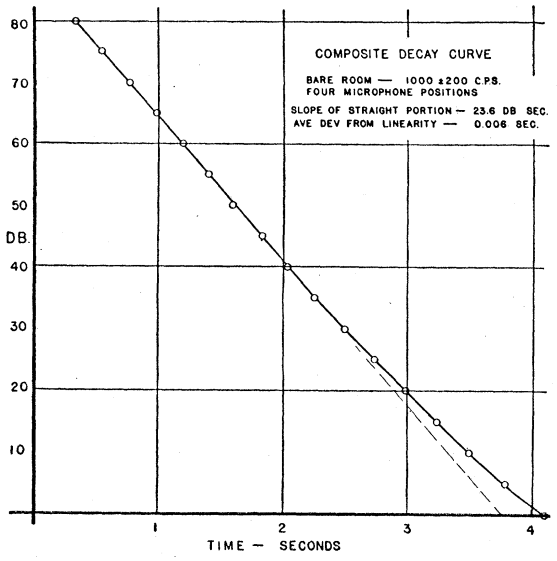

FIG. 5. Decay curve as average time for given drop in level. From reference H9.

Broadly speaking, measurements of room acoustics serve two purposes: (a) the evaluation of absorptive properties of materials and (b) the measurement of the properties of rooms; in many cases the same method is used for both.

The earliest measurements were those of Sabine, as already discussed (S1). These involved the use of a stop watch and the ear to detect and measure the time of decay. This procedure was improved successively by many investigators, leading to the automatic apparatus of Hunt (H5) which incorporates several refinements. The sound source is an oscillator with a warble-tone (a periodic variation of frequency over a small band) which excites a band of frequencies in the room, thus smoothing out the decay. Fluctuations are further reduced by (a) turning off the loudspeaker at the same phase of the sound wave for every decay, (b) rectifying the microphone output and filtering the envelope against the rapid fluctuations about the mean decay, (c) making observations at several microphone positions, and (d) averaging a large (40 or more) number of decays for each condition. Hunt's method employs an automatic timer which turns off the source after the sound level in the room has attained a predetermined level, turns it on again when the level drops to a predetermined level, and records the time of decay. This cycle of operations may be repeated automatically a number of times, and the average decay time to any preset level is obtained directly. A sample decay curve taken in this way is shown in Fig. 5.

An entirely different method of observing the decay of sound is by means of oscillographic recording, as used by Knudsen and others (K3). In this case the complete wave motion is reproduced, and the decay is evidenced by a diminishing envelope of the fluctuating curve. In these records, see Fig. 25 for example, the detailed variations of intensity and frequency show up, and if an "average" value of decay is desired, it must be obtained graphically. Both mechanical oscillographs and cathode ray types have been used, and considerable speed of recording can be attained.

A third type of instrument developed by Wente, Bedell, and others (S13, W6, W7), is the high speed level recorder. In its most refined form a light-weight arm carries a stylus which makes a trace on a moving strip of waxed paper, the position of the arm and stylus being governed by the amplitude of an input signal. Decay rates up to 600 db per sec. can be recorded. While this apparatus, operating at its highest speed, records rapid fluctuations in intensity, it does not generally reproduce the details of vibration of the sound as does the oscillograph. By varying the writing speed of the instrument, any desired degree of fluctuation may be retained; or, in other words, any desired degree of smoothing over can be achieved (W7). In this way a decay curve which was very tortuous as recorded by an oscillograph may be recorded as a fairly smooth curve, exhibiting only the major fluctuations. (See Fig. 6.)

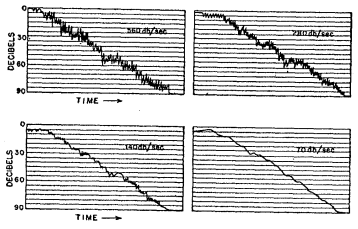

FIG. 6. Decay curve for 500 cycle sound traced by high speed level recorder at four different writing speeds, with the same average decay rate. From reference W6.

These methods of measuring reverberation in rooms can also be used to measure absorption coefficients of acoustic materials, by use of Eq. (2.4). This procedure has been standardized in several laboratories by using the same area of material (72 sq. ft.) in all cases and placing it always in the same position in a given room. Diffusing agencies such as large rotating paddles are used in an effort to achieve the "random distribution" of the geometrical theory.

Not all experimental techniques of the geometrical era have been based on transient behavior of sound. The measurement of steady-state intensity has been explored by Knudsen (K4) for determining absorption coefficients. This method (the "intensity method") is based on the steady-state term of Eq. (2.1). One sees that the mean-squared pressure in the steady state is

$$(p^2)_{Av} = (4\rho c/\alpha S)\Pi, \tag{2.6}$$

where ρ is the density of air, Π the power output (in ergs per second) of the source, and it is assumed that the energy density of sound in the room is $[(p^2)_{Av}]/\rho c^2$. This equation is subject to the same restrictions as Eq. (2.3).

In the experimental utilization of Eq. (2.6), a comparison procedure is employed: the total absorption of the bare room or of a "standard sample" must first be known, and the absorption of any other sample is obtained simply from a ratio of sound intensities. Though the method has not been used widely, it has experimental advantages in that considerable precision is readily attainable and that all measurements can be made at a high sound level to over-ride background sounds.[5] However the method has the same inherent limitations as any method based on the geometrical picture. This will be discussed more fully in Chapter V.

Another steady state type of measurement has been made by Wente (W8, H7). He considered the room to be an acoustic "transmission line," and measured the transmission as a function of frequency by means of a loudspeaker at one point, and at another point a microphone which fed a graphic level recorder. Only a qualitative interpretation of the transmission irregularities was possible on the geometrical basis, but the results are instructive from the wave point of view, as will be pointed out in Chapter V.

Absorption coefficients have also been measured by a variety of "tube methods," employing standing waves incident on a small sample (D3, L5, P3, T1, T2, M9, P1). These require only a simple measurement of the ratio of maximum to minimum pressure in the wave pattern. Laboratory control and repeatability are comparatively easy to achieve. But the coefficients measured in this way have not been in good agreement with reverberation results, except in special cases, for reasons which are now obvious. In subsequent chapters we will see that wave analysis applied to tube methods leads to very useful procedures for measuring acoustic impedance; and that impedance, in turn, can be used to calculate various kinds of absorption coefficients which are applicable to full-scale room acoustic design.

9. Critique of Geometrical Theory

The widespread use of reverberation theory for the acoustical correction of auditoriums and lecture halls and the growing demand for acoustically designed buildings give ample evidence of the importance of the field so ably initiated by Sabine. Using reverberation theory with due consideration of a few simple stipulations which have been fully verified by wide experience, one can at present predict accurately the acoustic behavior of *large* auditoriums, music and speech rooms, theaters, and studios. Subject to a greater number of restrictions and empirically derived rules, one can also design *small* speech and music rooms, broadcasting studios, etc., though these cases require a degree of "good guessing" which is possible only after one has had considerable experience in following through the design, construction, and testing of rooms.

For the reduction of noise in rooms the reverberation theory is adequate for analyzing most cases, at least in large offices, industrial plants, and in any room in which the dimensions are fairly conventional: provided the absorbing material is distributed "properly."

[5] It is difficult in the reverberation method to achieve adequate exclusion of background, especially if a wide range of decay is to be measured. This leads to elaborate and expensive sound isolation construction of reverberation chambers.

There have been observed, however, numerous discrepancies between reverberation theory and measurements. Precalculated reverberation times are sometimes from 20 to 50 percent in error, regardless of the formula used, and in extreme cases, such as in very small rooms and at low frequencies, the discrepancy may be several hundred percent (H8, P9, S14, W10). In a room of complicated shape, such as an auditorium with a reverberant back-stage, or a large rotunda with a dome ceiling, the reverberation may consist of two portions having widely different decay rates. The reverberation in coupled spaces has been studied (D1), but it is not fully understood.

Most of the difficulties in applying reverberation theory to rooms arise when the simple geometric assumptions are not fulfilled. Sound is often not random in its propagation nor is it uniformly diffuse throughout the room. As a result, in these cases, the decay is not logarithmic, is modulated by small irregularities, has major breaks in the curve, and is not the same everywhere in the room. Even more serious from the geometrical point of view is the observation that in many cases the effective absorption of an absorbing material is *not* independent of area nor of position in the room. Extensive measurements have been made on this "area effect" and "pattern effect" (A2, C2, D4, E4, P7, R2, S3), but a calculation of these effects has had to await the development of wave acoustics.

Probably the most serious defect of the geometrical approach has been its inability to yield consistent, reliable, standard measurements of absorption coefficients of materials. In a recent symposium on this problem, Hunt discussed the "absorption coefficient problem" (H8) and summarized the replies to questionnaires sent to a large number of groups of acousticians with the following statements: (1) Coefficients of the same material measured in different laboratories are not usually in agreement. (2) Field measurements yield smaller coefficients than laboratory measurements. (3) Increasing the sample size leads to smaller coefficients, but this effect will not explain the preceding discrepancies.

In the same symposium P. E. Sabine (S7), C. F. Eyring (E5), and others (S14) discussed the absorption measurement problem from various viewpoints. Provided standardized test procedures, arbitrarily specified, are followed by different laboratories, the variations in measured coefficients may be reduced considerably, particularly at higher frequencies. But even with due precautions, different laboratories continue to yield coefficients which in some cases differ as much as 20 percent.

III. GENERAL ASPECTS OF WAVE ACOUSTICS

The previous discussion has made clear that certain aspects of the problem of room acoustics can be understood only by taking into account the wave nature of sound. That the wave aspect plays a role in acoustics has long been appreciated (S1, S10, S15): the importance of this role has, however, only recently been investigated. Knudsen (K5) first showed experimentally that the reverberant sound has the characteristic frequencies of the normal modes of vibration of the room, and not necessarily the frequency of the source which initiated the reverberation. In several cases which he measured, two or more characteristic frequencies were present, and the resulting beat notes made the sound decay curves deviate appreciably from the usual exponential form. Wente (W8) studied the steady state response of a room as a function of the frequency of the source and pointed out that sharp response peaks occurred at the resonance frequencies of sound waves in the room. Several other experimental and theoretical workers (B5, B6, B8, H9, M2, M11, M12, S3, M1, M6) studied other aspects of wave acoustics, and subsequent work has expanded the field sufficiently to make the present report worthwhile although many unsolved questions still exist.

Three aspects of the problem present themselves for study: the nature of the reaction between the sound wave and its boundaries, the walls of the room; the nature of the steady-state response of the room to a source of sound; and the nature of the transient response, in particular, the reverberation. Each of these aspects will be treated in some detail later in this report; at present we shall find that a general statement of results is useful.

10. Acoustic Impedance

It has become apparent that the absorption coefficient is not a unique measure of the acoustic properties of a wall surface. The experimental work of Hunt and others (B3, B5, B12, C7, H9) has indicated that a more fundamental quantity is the acoustic impedance Z of the surface. This impedance is defined as the complex ratio[6] between the sound pressure at the surface and the air velocity normal to the surface just outside the surface. This normal velocity is due to a motion of the wall itself or else to a motion of air into pores in the wall. In either case we can speak of a wall with low acoustic impedance as being "soft" and one with large impedance as being a "hard" wall. If the impedance has a real component, energy will be absorbed at the surface; a purely reactive impedance implies only a change of phase on reflection.

The natural unit for Z is the acoustic resistance of air for free plane waves, ρc, which equals about 42 grams per cm^2 sec. Expressed in terms of this unit the impedance will be denoted by $\zeta=(Z/\rho c)=(1/\rho c)(R-iX)$ and will be called the *specific impedance* of the material. The absorbing properties of the surface are measured in terms of the *specific admittance* $\beta=(\rho c/Z)=\gamma-i\sigma$, where γ is the specific conductance and σ the specific susceptance. In particular, the quantity which most closely corresponds to the absorption coefficient in certain cases is the *normal wall coefficient*, α_p, defined as eight times the specific conductance γ. If the phase angle for the impedance Z is φ, then the quantities defined here are related as follows:

$$\zeta=(|Z|/\rho c)e^{-i\varphi},\quad \beta=(\rho c/|Z|)e^{i\varphi},$$
$$\gamma=(\rho c/|Z|)\cos\varphi,\quad \sigma=-(\rho c/|Z|)\sin\varphi; \quad (3.1)$$
$$\alpha_p=8\gamma.$$

[6] In this report we shall consider the dependence on time for simple harmonic motion to be $e^{-i\omega t}$, following the usual procedure for the discussion of wave motion. To make the concept of impedance correspond with electrical engineering, we must consider the quantity i in the present paper to correspond to *minus* the j of electrical engineering. Therefore we set $Z=R-iX=|Z|e^{-i\varphi}$ where the reactance X and phase angle φ correspond to the electrical engineering convention, X and φ being negative for a stiffness (capacitative) reactance and positive for a mass (inductive) reactance. This general convention will be followed except in Chapters V and VI, where the transient behavior is discussed by means of operational analysis, for in such a case both signs of i are needed.

As will be shown later, the acoustic impedance usually depends on the frequency of the incident sound. Sometimes it also depends on the angle of incidence of the sound wave. These matters will be discussed in Chapter IV. Since the normal velocity of the air at the wall is proportional to the normal gradient of the pressure at the wall, the boundary condition on the waves in the room will be that the pressure is proportional to its normal gradient at the wall. This requirement is less simple than that for a room with rigid walls although it is still linear and homogeneous. However, the ratio between the pressure and its normal gradient will in general depend on the frequency of the wave, so that the boundary conditions will be different for each different standing wave in the room. The normal modes of free vibration of sound will, therefore, not form an orthogonal set of characteristic functions, and the usual methods of attack by use of an ortho-normal set of functions cannot be used. The difficulty cannot be side-stepped, for the absorption of sound at the boundaries is an essential part of the problem; and it is not usually accurate enough to consider the actual room as a slight alteration from a room with rigid walls, so that perturbation methods are not usually adequate.

11. Steady-State and Transient Behavior

The difficulties mentioned above disappear if we consider the steady state case, where a source of sound is driving the air in the room with simple harmonic motion. This motion can be expanded in an ortho-normal set of characteristic functions since every normal mode has the frequency of the source, and hence the boundary conditions are the same for all modes. The transient case is then obtained by means of the methods of operational calculus, in a manner very similar to that used in electrical circuit analysis. This question will be treated in Chapter VI.

The transient state will in general consist of a number of "standing" waves, each with its own characteristic frequency which will be complex, corresponding to an exponential damping out of the wave. In the general case each wave will have a different decay rate, though we shall see

later that in some cases whole groups of waves will have nearly the same decay rate, and in many cases all the rates are nearly equal. In a simple rectangular room, however, we shall see in Chapter V that a number of different decay rates exist.

This brings us to the consideration of an important difference between the results of geometrical acoustics and those of wave acoustics. In the geometrical analysis all the sound in the room is considered to act together as one simple oscillator, and the resulting logarithmic decay curve turns out to be a straight line. In the wave picture it is clear that if some standing waves have decay rates different from the rest of the waves constituting the transient, the decay curve *cannot* be a straight line. Moreover, since many waves of nearly equal "natural frequencies" are usually excited together, the resulting beat notes and interference effects would lead to still further deviations from the simple straight line decay. Knudsen's pioneer work (K5) showed these effects actually to be present in certain cases, and more recently many workers (B5, H9, M3, W8) have verified and extended his findings.

As we shall show in Chapter VII, rooms having smooth, regularly shaped walls show the greatest divergence of values of decay rates for different standing waves. Those waves which move parallel to the most absorbent wall will in most cases damp out less rapidly than the waves which reflect normally from this wall. This is true if the wall is a plane or is a smooth convex surface; if the wall is a smooth concave surface, the reverse is true. If the surface is concave, the tangential waves, which cling to the wall, usually damp out much more rapidly than the normal ones, which are focused away from such a wall. In either case the logarithmic decay plot will be steepest at the beginning of the reverberation, and the magnitude of the slope will diminish later on when only the normal modes with small decay rate are left. In both cases some of the waves damp out more rapidly than the geometrical formulas would predict, and a few damp out much more slowly. Such rooms seem to have unsatisfactory acoustic qualities (B11, M5, V1).

12. Ergodic Wave Motion

One might expect, by a correspondence principle argument, that for high enough frequencies the behavior of sound in a regularly shaped room would go over to the smooth behavior predicted by geometrical theory. This is not so. At high frequencies, in rooms with *smooth, regularly shaped boundaries* the differences in decay rate between the various modes of vibration are more pronounced than with lower frequencies, and the decay plots are still more curved. Such a result seems in flat contradiction to the correspondence principle which usually holds in such cases, until we notice the words which are italicized in the statement. Standing waves in *regularly shaped* rooms have corresponding regularities and symmetries which are responsible for the differences in decay rates. Normal modes in *irregularly shaped* rooms have no such symmetries; no standing wave moves "parallel" to an irregular wall (if it is irregular enough!), and none is everywhere perpendicular. We shall see later that the introduction of irregularities in the walls of a room reduces the decay rate for the most rapidly damped waves and increases the rate for the slower ones, so that both rates approach the one predicted by geometrical acoustics.

The ideas involved here are closely related to those underlying statistical mechanics. A system can be treated by statistical mechanics *only* when its complexity is great enough so that symmetry has disappeared, i.e., so that no constants of the motion exist other than the energy. It is almost impossible to find a system which can be analyzed fully by both dynamical and statistical mechanical methods. If the motion is simple enough for dynamical methods to give an exact solution, then the motion is usually not ergodic; and, vice versa, most systems having ergodic motion are too complicated for successful analysis except by statistical methods. The formulas of geometrical acoustics are *statistical* formulas and apply only to rooms where "ergodic" wave motion takes place. From this point of view the practical value of wave acoustics would lie in its ability to tell us how to design rooms for which geometrical acoustics is valid and wave acoustics is not needed!

However in this respect also, room acoustics finds itself in the difficult intermediate region. There are many rooms which are regular enough so that the statistical formulas are invalid over most of the useful range of sound frequency, although one encounters many others so irregular in shape that the formulas of geometrical acoustics are satisfactory over the useful range. In general, wave acoustics will have to be used for small, regularly shaped rooms, and geometrical acoustics will be sufficient for the analysis of most large auditoriums. This, of course, is the reason for the annoying fact that the "absorption coefficient" measured in laboratory reverberation chambers differs from the value obtained by field measurements in large auditoriums (S13, S14, W10).

13. Effect of Irregularities

It is most important, both from the theoretical and from the practical viewpoints, that the intermediate cases be studied in detail, in order to find out *how much* irregularity must be introduced to obtain ergodic wave motion. The meager results obtained so far indicate that the tilting of one wall at an oblique angle to the rest is *not sufficient* as long as the wall remains smooth (M6). They also indicate that irregularities about the size of the wave-length are most effective in setting up ergodic motion and that the irregular placing of patches of absorbing material on smooth walls will sometimes produce enough diffraction and scattering to make the geometrical formulas valid, although this method is not as effective as the introduction of irregularities in wall shape (M5).

We also see that the correspondence principle does hold for most of these intermediate cases. For wave-lengths longer than about one-fifth of the length of the room, the scattering from relatively small irregularities in wall shape is insufficient to set up ergodic wave motion, and the curved decay plot typical of wave acoustics is in evidence. But for shorter wave-lengths, the same irregularities are more effective and the decay plot changes over to the straight line typical of the statistical results of geometrical acoustics.

For large auditoriums geometrical acoustics is usually sufficient for the study of sound reverberation; but even here wave acoustics is necessary for the accurate calculation of the acoustic properties of patches of absorbing material, and for the calculation of the ratio between the amount of sound coming directly from the speaker and the amount which has suffered one reflection. For these calculations the sound can be considered to consist of free, traveling waves since the results are going to be interpreted in terms of the geometrical picture. Such cases will be discussed in Chapter VIII. For regularly shaped rooms wave acoustics must be used, and an exact solution of the boundary value problem must be carried through if possible. The steady-state case for a rectangular room will be discussed in Chapter V and the transient case in Chapter VI.

Although the perturbation method is usually not sufficiently accurate for acoustical problems, it is the only method available at present for the study of the cases intermediate between simple wave acoustics and simple geometrical acoustics, where the walls are somewhat irregular. It will prove to be quite valuable in determining how much irregularity must be present before geometrical acoustics becomes valid. The results of the perturbation method will also serve to bring out more clearly the fundamental reasons for the differences in decay rates of waves in a regularly shaped room, even though the accurate values of these rates must be obtained by more exact methods. The perturbation method will be discussed in Chapter VII.

14. Classification of Waves in a Room

But before any of these questions can be taken up, we must obtain formulas which tell us how many waves of each different kind (if there are different kinds) are excited by a given source, and we must discuss in detail the nature of the boundary conditions on the sound at the walls of the room. The boundary conditions will be studied in Chapter IV, and the remainder of the present chapter will be devoted to one aspect of the problem first mentioned, a determination of the number of different waves having "natural frequencies" within any specified frequency range, in a given room.

This number can be computed once it is known how many different waves there are which have frequencies less than a given value ν. The number $n(\nu)$ of waves with frequency less than ν has been investigated by Rayleigh, Weyl, and others (J2, L1, M11, R3, S15, W9), and the first term in the asymptotic series for $n(\nu)$ has been computed. In room acoustics, however, the wave-length is long enough compared to the room dimensions so that the first term in the series for $n(\nu)$ is not sufficient, and further terms must be obtained.[7] This has been done by Maa, Bolt, Husimi, and Roe (B6, H10, M1, R8) for the rectangular room, and the solution will be outlined here.

First it is necessary to classify the various types of waves which can occur in a rectangular room. If the walls are rigid and the lengths of sides are L_x, L_y, L_z, then the expressions for the velocity potential ψ, pressure p, and air velocity $\mathbf{u}$ for a normal mode of vibration are

$$\psi = A\cos(\pi n_x x/L_x)\cos(\pi n_y y/L_y) \times\cos(\pi n_z z/L_z)e^{-2\pi i\nu t},$$
$$p=\rho(\partial\psi/\partial t),\quad \mathbf{u}=-\text{grad}\,(\psi), \qquad (3.2)$$
$$\nu^2=(c/2)^2[(n_x/L_x)^2+(n_y/L_y)^2+(n_z/L_z)^2].$$

These expressions are accurate enough for our present purpose, even if a certain amount of absorption does take place at the walls.

The standing waves described by this formula can be divided into three classes: those for which none of the n's are zero will be called *oblique waves*, those for which one n is zero will be called *tangential waves* (those for which n_x is zero are called the yz-tangential waves, etc.) and those for which two n's are zero will be called *axial waves* (those for which n_y and n_z are zero are called *x-axial* waves, etc.). The reason for this terminology is clear. Axial waves are made up of two traveling waves propagated parallel to one axis and striking only two walls. Tangential waves are built up of four traveling waves, reflecting from four walls and moving parallel to two walls. Oblique waves are built up of eight traveling waves reflecting from all six walls.

[7] For instance, for a room $10'\times15'\times30'$ the first term for n is about 50 percent below the correct value at 100 cycles/sec., about 10 percent low at 1000 cycles/sec., and about 1 percent low at 10,000 cycles/sec. See Fig. 7.

Each of these three types of waves has different properties. We will show in Chapter VI that they have different decay rates. There is also a difference in energy content, the total sound energy in the room for one of the waves being

$$E=\frac{\rho}{2}\int\int\int\left[(\text{grad}\,\psi)^2+\frac{1}{c^2}\left(\frac{\partial\psi}{\partial t}\right)^2\right]dv = \left(\frac{2\pi^2\nu^2\rho}{c^2}\right)L_xL_yL_zA^2\epsilon, \qquad (3.3)$$

where the factor ϵ has the value $\frac{1}{8}$ for oblique waves, $\frac{1}{4}$ for tangential waves, and $\frac{1}{2}$ for axial waves. Thus, for a given pressure amplitude an axial wave has four times the energy of an oblique wave. The consequences of this fact will become apparent later in this article.

The fact that in this simple case the traveling waves are plane waves should not lead one to expect that rooms with curved walls do not have tangential or axial waves. It will be shown in Chapter VII that there are axial waves in cylindrical rooms; some which move parallel to the cylindrical sides and reflect back and forth from the flat ends; some which reflect normally from the curved walls and focus at the center; and some which circle around the room parallel to the ends and to the curved wall. These can be called z-, r-, and φ-axial waves respectively. The waves moving parallel to the curved walls, which reflect from the flat ends, are the φ-tangential waves, and so on. We shall see later that each of these wave types has different rates of decay (K8).

Both the cylindrical and rectangular rooms have walls corresponding to coordinate systems for which the wave equation is separable; and it might be assumed that the classification above would only hold for such cases, for only in separable coordinates can standing waves be set up which move parallel to one coordinate system. It seems, however, that in any room which has a smooth wall which is several wavelengths in extent, there will be classes of waves which move parallel to this wall and others which reflect from the wall; and these classes will have different decay characteristics with

respect to the absorbing material on the smooth wall. This is true in the case of the triangular room (one of the few non-separable cases which has been solved) as will be shown in Chapter VII. It is to be hoped that other non-separable cases will be investigated, so that the limitations of the above classification can be found.

15. Frequency Distribution of Normal Modes

Equation (3.2) indicates that the characteristic frequencies in a rectangular room have the behavior of a vector, with components $cn_x/2L_x$ etc. (M11). Each natural frequency can therefore be represented by one point in a rectangular lattice in frequency space, having a lattice spacing in the x direction of $c/2L_x$ and so on. The "volume occupied in frequency space" by one point is therefore a rectangular parallelopiped of volume $c^3/8V$ with the point at the center, where $V=L_xL_yL_z$ is the volume of the room. The points fill all of the first octant in frequency space, which means that the space occupied is *more* than the first octant, since the parallelopipeds extend $c/4L_y$ beyond the (xz) plane, and so on. The total volume occupied by points with frequency less than ν is therefore

$$\frac{\pi}{6}\nu^3+\left(\frac{c}{4L_x}+\frac{c}{4L_y}+\frac{c}{4L_z}\right)\frac{\pi\nu^2}{4}+\left(\frac{c^2}{16L_xL_y}+\frac{c^2}{16L_xL_z}+\frac{c^2}{16L_yL_z}\right)\nu+\cdots.$$

To obtain the number of frequencies less than ν we divide by the volume occupied by one point, obtaining (M1, B6, R8)

$$n(\nu)=\frac{4\pi V}{3c^3}\nu^3+\frac{\pi S}{4c^2}\nu^2+\frac{L}{8c}\nu+0(\nu), \qquad (3.4)$$

where

$$V=L_xL_yL_z, \quad S=2(L_xL_y+L_xL_z+L_yL_z),$$
$$L=4(L_x+L_y+L_z),$$

and $0(\nu)$ is an irregular step function whose magnitude is of the order of unity. The quantity S is the area of the wall surfaces and L is the length of all the edges of the room shape. The first term in the expansion comes chiefly from the oblique waves, the second term mainly from the tangential waves, and the third term comes from the axial waves. The term $0(\nu)$ expresses the fact that n is actually a step function, increasing by unity whenever the sphere of radius ν encloses one more allowed frequency point. Figure 7 shows the calculated function $n(\nu)$ (stepped curve), the smooth curve for $n(\nu)$ without the function $0(\nu)$, and the first term only, which is well below the actual curve (B6).

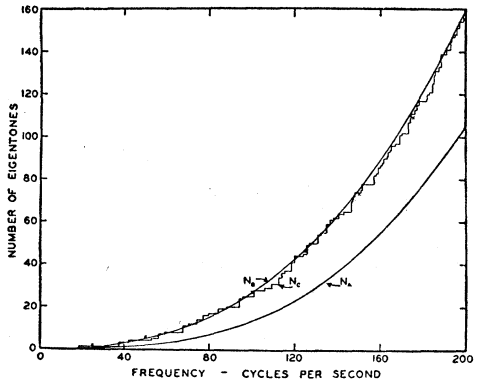

FIG. 7. Distribution of normal frequencies in a room $10\times15\times30$ ft. Actual function $n(\nu)$ compared with continuous part of Eq. (3.4), and with first term only. From reference B6.

It has been shown by Weyl (W9) that the first term in this asymptotic expansion for $n(\varphi)$ has the same form for a room of volume V, no matter what its shape is. So far the generality of the second term has not been demonstrated. However, for triangular and cylindrical rooms (R8) the second term has the same form as in Eq. (3.4), with S again the area of the room walls; so that it appears likely that this term also is of general validity. In an attempt to study this point for more complicated shapes, experimental measurements of normal frequencies have been made in a few small models (B8). The main limitation is that one cannot count very far up the frequency scale without encountering uncertainty as to the discreteness of peaks, due to overlapping of the increasingly crowded resonances by damping. The limited results indicate that corrections to the asymptotic term are always present, and that the following rule gives a reasonable estimate of their magnitude: (a)

use the actual volume of the room for V in the first term of Eq. (3.4); (b) for S in the second term, use the area of a smoothed-out "average" surface around the room such that the total volume contained is equal to V. This would indicate that the "effective" surface area S is often *smaller* in value than the actual wall area in irregular rooms.

The third term is still more uncertain. Apparently for rooms enclosed by plane walls L is the sum of the edge lengths (at any rate, this is true for the rectangular and triangular room). For a cylindrical room, however, $L=4\pi R+4L_z$, where R is the radius of the cylinder and L_z is the distance between flat ends; and this has the term $4L_z$ in addition to the $4\pi R$ for the two curved edges. Luckily most of our discussions will be for rectangular rooms, where we are sure of the validity of Eq. (3.4).

The number of waves, of one of the three types discussed above, having frequencies less than ν can be found by a similar argument. For instance, in the rectangular room, the number of oblique waves having frequencies less than ν is

$$n_p(\nu)=\frac{4\pi V}{3c^3}\nu^3-\frac{\pi S}{4c^2}\nu^2+\frac{L}{8c}\nu+O_p(\nu). \quad (3.5)$$

The number of yz-tangential waves with frequencies less than ν is

$$n_{tyz}(\nu)=\frac{\pi}{c^2}L_yL_z\nu^2-\frac{1}{c}(L_y+L_z)\nu+O_{tyz}(\nu), \quad (3.6)$$

and there are similar expressions for the xz- and xy-tangential waves. The number of x-axial waves with frequencies less than ν is

$$n_{ax}(\nu)=\frac{2}{c}L_x\nu+O_{ax}(\nu), \quad (3.7)$$

with similar equation for y- and z-axial waves. The last four equations with the terms $O(\nu)$ omitted are fairly accurate expressions for the n's whenever the wave-length (c/ν) is smaller than twice the smallest dimension in the room.

IV. ACOUSTIC IMPEDANCE

16. Impedance and Absorption

It has been demonstrated in a number of ways (A2, B3, B12, H9, M2, P1, S4, W10) that the absorption coefficient entering into the geometrical acoustical formulas is not a fundamental property of the wall surface. The measured value of the coefficient changes when the material is placed in different rooms (H8, P5, S14, W10), and for some materials it changes with angle of incidence of the sound (B9, W10). It is an average property, averaged for the particular distribution of sound which we have called "ergodic" in the previous section, and *has no meaning* in cases where the sound distribution is not ergodic (H8, B3).

It is well to emphasize this limitation on the use of the term absorption coefficient, for an over-optimistic use of the term may lead to erroneous results. In the present paper we shall use the term "absorption coefficient" *only* when conditions in the room under discussion are such that the Sabine formula for reverberation holds; i.e., when the logarithmic decay curve is a straight line, with a decay rate for the root mean square pressure equal to

$$k=(c/8V)\sum_n \alpha_n S_n, \quad (4.1)$$

where V is the volume of the room and S_n the area of one sort of wall material. This equation constitutes our definition of the coefficient α_n. The quantity thus loses all meaning in cases where the decay curves are not straight lines.

Recently there has been an increasing tendency (B2, B12, N9, M11, M12, S8) to consider that the acoustic impedance of the wall material, the complex ratio between sound pressure and normal air velocity at the wall, is a more useful measure of the absorbing properties of the wall material than is the absorption coefficient. It is true that the impedance is not a much more "fundamental" physical property than the absorption coefficient; its advantage lies in the fact that its measurement can be specified concisely and uniquely and that its value for a given material has a definite meaning no matter what the distribution of sound inside the room. The acoustic impedance of a material varies with the

frequency (B2, B3, S8), and in certain cases (B9, S8, W10) changes with the angle of incidence of the sound wave; nevertheless it can be used to determine the decay rate in rooms where the Sabine formula is not valid, where the absorption coefficient has no meaning.

There has been reluctance on the part of some acoustical engineers to adopt impedance as the primary acoustic property of a material. This is partly caused by an understandable hesitation at changing concepts, and also by an impression that the relationship between impedance and absorption coefficient is a rather vague one. Actually this impression has arisen because the fact has been lost sight of that the absorption coefficient is a vague and non-general quantity. It will be shown later in this paper that the relationship between the impedance of the walls and the decay rate of sound in the room is not a unique one, but depends on the distribution of the sound in the room. When the room, source, etc., are arranged so that ergodic sound motion is set up, there is one definite and unique relationship between the slope of the resulting straight line decay curve and the impedance of the walls. Since this is the *only* case where the term absorption coefficient should be used, we can thus say that there is a definite and unique relationship between impedance and absorption coefficient. This relationship will be discussed in Chapters VII and VIII. However, in cases where ergodic wave motion does not hold and wave acoustics must be used, the theory to be outlined in Chapter VI indicates that there is a *different* relationship between impedance and decay rate. The vagueness, therefore, only arises when the concept of absorption coefficient is pushed beyond its legitimate scope. The resulting failure in correlation must be ascribed to the inherent limitations of geometrical acoustics and recognized as another argument against considering absorption coefficient as a fundamental property of a material.

The pioneer experimental work of Hunt and his co-workers (B3, H7, H9, M2) has shown that the statements made in the above paragraph are true in general. Much detailed work remains to be done, however, before we can understand fully the interrelationships between the acoustic impedance of a material and its physical characteristics, on the one hand, and between the impedance of the walls and the reverberation of the room on the other. This section will outline the present status of our knowledge of the first relationship, that between the mechanical properties of a material and its acoustic impedance. The various experimental methods of measuring impedance will also be outlined, together with the conclusions which can be drawn from the few available data, in the light of the theory.

17. Mechanical Properties of Porous Materials

The relation between the density, porosity, and various other mechanical properties of a material, and its acoustic properties, has been studied for some time. Rayleigh (R4) calculated the absorption of sound at the face of a rigid porous material by considering the dissipation of sound energy into heat through viscous actions in capillary channels. If the channels are assumed to be small (less than 0.01 cm diam.), cylindrical, perpendicular to the surface, and long enough so that no sound is reflected from the back surface, yet short compared with a wave-length, the absorption coefficient as calculated by Rayleigh is:

$$\alpha = 4M/(2M^2+2M+1),$$

where

$$M = [2(1+g)(\nu\gamma)^{\frac{1}{2}}]/[r\omega^{\frac{1}{2}}],$$

g = ratio of unperforated to perforated area of surface, ν = kinematic viscosity of the gas, γ = ratio of the specific heats of the gas, r = radius of the pores (uniform, cylindrical), and $\omega = 2\pi \times$ frequency. While the term g is thus defined as a *surface* porosity, it is analogous, in the special case treated here, to the *volume* porosity which we shall use later. This equation predicts that α may go through a maximum at a frequency lying in the audible range. Rayleigh also considered sound striking the material at all angles of incidence and showed that in a certain case the absorption may be complete at a particular angle.

Paris (P2, P6) derived a formula giving the absorption coefficient at any angle of incidence if the "acoustical admittance" of the surface is known. He made no special assumptions as to the physical nature of the absorbing material, except

to specify that sound could not be propagated parallel to the surface inside the material. Expressed in terms of the acoustic impedance, which is the reciprocal of the admittance, the equation of Paris is:

$$\alpha(\theta)=1-\left|\frac{Z\cos\theta-\rho c}{Z\cos\theta+\rho c}\right|^2,$$

where Z = acoustic impedance of the surface, in general a complex quantity, ρ = density of air, and c = velocity of sound in air. ($\rho c \simeq 42$ c.g.s. units.) This equation, giving the absorption coefficient at a particular angle θ, has assumed considerable importance in recent discussions and correlations between impedance and absorption coefficients (H7, M11, S8, W4).

Crandall (C4) worked out a formula for the variation of absorbing power with the thickness of material having rigid backing, for normally incident sound. His treatment was the first to allow for reflections from the back of the material, which may give rise to interference maxima and minima in the curves for α as a function of frequency or thickness of material. Crandall also showed that the absorption approaches a constant value when the material becomes thick, and his various predictions were checked by measurements using the standing wave method in a tube. Further work on sound absorbents has been done by Davis and Evans (D3), who investigated the effect of an air cavity backing the porous material; Meyer (M6), who has studied flexible panel types of material extensively; and many others.

In the present analysis we shall distinguish between two different types (R7) of wall material: the *panel* type, where the reaction of the wall to the pressure fluctuations is due to the stiffness of the wall, and the normal velocity next to the wall is due to a motion of the panel as a whole; and the more usual *porous* type, where the normal velocity is due to the penetration of air into the pores of the material, and the reaction is due to the interaction of the penetrating air with the material of the pores. Of course there are intermediate cases, where the panel is backed by porous material, or where the porous material also acts as a panel; but these cases can be understood when the two limiting cases have been analyzed.

In studying the porous type, we shall follow the work of Wintergerst, Gemant, and Rettinger (G1, R6, R7, W11, M8) to some extent. A porous material allows elastic waves to be transmitted through it in various directions. In some cases the wave velocity normal to the surface is different from that parallel to the surface (W11), because of the layer-like construction, or the orientation of the pores in the material. In such cases the "index of refraction" of the material for waves traveling normal to the surface differs from that for waves parallel to the surface; and the material is acoustically bi-refringent.

First we must define the relevant mechanical properties of the porous material. The *porosity*, P, of the substance is the ratio of the volume of air in its pores to the total volume of the material. Therefore the volume flow of air through the material, $\mathbf{u}$, in cc per cm^2 per sec., is related to the average velocity $\mathbf{v}$ (in cm per sec.) of the air in the pores by the relation $\mathbf{u}=P\mathbf{v}$. The equation of continuity then can be used to obtain the equation

$$\operatorname{div}(\mathbf{u})=-(P/\rho c^2)(\partial p/\partial t), \qquad (4.2)$$

relating pressure and average flow. This equation indicates that the porosity can also be defined as the ratio between the stiffness of air alone and the stiffness (bulk modulus of elasticity) of the same volume of material: air, pores, and all. It suggests that the *effective porosity* (which we might call the dynamic porosity) which enters into our equations here, may differ from the geometrical value because the material surrounding the pores may not be incompressible. There is another reason why the effective porosity, which we shall use in our discussions to follow, may differ from the geometrical porosity: the stiffness of the air in the pores is assumed in Eq. (4.2) to be expressed by the quantity ρc^2, which assumes that the air in the pores expands adiabatically. Some work of Beranek(B4) indicates that the expansion may be more nearly isothermal. The difference in the stiffness, a factor equal to the ratio of the specific heats, will be absorbed in the effective porosity P.

The equation of motion of the air in the pores

is a more complicated one. In the first place there is a resistive reaction as well as an inertial one, and in the second place the motion of the air is not necessarily in the same direction as the driving force. This means that the effective density of the air in the pores, and its effective resistivity, are both dyadics, transforming a force vector into a velocity or acceleration vector. In the equation

$$\rho\mathbf{m}(\partial\mathbf{u}/\partial t)+\mathbf{r}\mathbf{u}=-\text{grad}\,(p),$$

both $\mathbf{m}$ and $\mathbf{r}$ are dyadics, and $\mathbf{u}$ is a vector. In the isotropic case, $\mathbf{m}$ and $\mathbf{r}$ reduce to scalars, when r is the *effective resistivity* of the material per unit volume, and m is the ratio of the *effective density* of the air in the pores to its density in the open. Since there is some motion of the porous material along with the air, m is often considerably larger than unity.

These effective values are supposed to include the possible effects of the motion of the porous material itself if it is a yielding structure. Therefore we should not expect the effective resistivity r used here necessarily to equal the d.c. flow resistivity measured (B13) by steady flow of air through the material, for the d.c. measurements would not include the resistivity due to motion of the structure. As we shall see later, measurements show that for porous materials with stiff structure, the r obtained from dynamical measurements equals the d.c. flow resistivity, whereas this check is not obtained for materials with yielding structure.

In the cases where m and r are not scalars, it is usually the case that the principal axis for both is normal to the wall surface. The matrices for m and r then reduce to diagonal ones, and the equations of motion become

$$\rho m_n(\partial u_x/\partial t)+r_n u_x=-(\partial p/\partial x),$$
$$\rho m_t(\partial u_y/\partial t)+r_t u_y=-(\partial p/\partial y),$$
$$\rho m_t(\partial u_z/\partial t)+r_t u_z=-(\partial p/\partial z),$$

where x is normal to the surface and y and z are tangential to it. When the dependence on time is simple harmonic, the time factor being $e^{-i\omega t}$, the equations can be combined with Eq. (4.2) to obtain the wave equation for sound in the porous material

$$(1/\epsilon_n)\frac{\partial^2 p}{\partial x^2}+(1/\epsilon_t)\left(\frac{\partial^2 p}{\partial y^2}+\frac{\partial^2 p}{\partial z^2}\right)+(\omega/c)^2 p=0; \quad (4.3)$$
$$\epsilon_n=(n_n+iq_n)^2=P[m_n+i(r_n/\rho\omega)],$$
$$\epsilon_t=(n_t+iq_t)^2=P[m_t+i(r_t/\rho\omega)].$$

The quantities n_n and q_n are the real and imaginary parts of the *index of refraction* of the material for sound waves traveling normal to the surface; n_t and q_t are the corresponding values for tangential waves.

Once the pressure is determined, the air flow can be obtained from the equations of motion given above. For simple harmonic waves this gives

$$u_x=\frac{P}{i\rho\omega\epsilon_n}\frac{\partial p}{\partial x}, \quad u_y=\frac{P}{i\rho\omega\epsilon_t}\frac{\partial p}{\partial y}, \quad u_z=\frac{P}{i\rho\omega\epsilon_t}\frac{\partial p}{\partial z}. \quad (4.4)$$

With the above equations it is possible to obtain a formula for the acoustic impedance of the material in terms of the "fundamental constants" m, P and r. If we know the dependence of these quantities on the frequency, we can predict the dependence of the impedance on frequency and on angle of incidence of the sound wave.

Suppose that the region occupied by the air of the room corresponds to negative values of x, the front surface of the porous material being the plane $x=0$, and the back surface being at $x=L$. In addition suppose that the sound pressure in front of the wall has the following properties:

$$(\partial^2 p/\partial x^2)=-\mu_n^2 p,$$
$$\nabla_t^2 p=(\partial^2 p/\partial y^2)+(\partial^2 p/\partial z^2)=-\mu_t^2 p; \quad (4.5)$$
$$(\partial p/\partial t)=-i\mu c p,$$
$$\mu_n^2+\mu_t^2=\mu^2, \quad \mu=(\omega/c)=(2\pi/\lambda).$$

We can then define the angle of incidence φ_i of the wave by

$$\sin\varphi_i=(\mu_t/\mu), \quad \cos\varphi_i=(\mu_n/\mu). \quad (4.6)$$

The sound pressure in the porous material will show the same dependence on y and z as does the pressure just outside the wall, but the factor depending on x will have the form

$$\sinh[\psi+i\mu(n_n+iq_n)x\cos\varphi_r], \quad 0<x<L,$$

where ψ is a phase angle determined by the boundary conditions at the back of the wall, and φ_r is the angle of refraction, defined by Snell's law

$$\sin \varphi_r = (n_t + iq_t)^{-1} \sin \varphi_i, \qquad \cos^2 \varphi_r = 1 - \epsilon_t^{-1} \sin^2 \varphi_i. \tag{4.7}$$

Unless q_t is zero, this angle is complex, but if the magnitude of n_t+iq_t is considerably larger than unity (as it often is) cos φ_r has a small imaginary part, and its real part never differs appreciably from unity. In the discussion following, this will be assumed to be the case unless it is specifically stated to be otherwise.

The ratio between the pressure at any point inside the material and the x component of the volume flow at the same point is then

$$\frac{p}{u_x} = Z_x = \frac{\rho c(n_n + iq_n)}{P \cos \varphi_r} \times \tanh \pi[\alpha + (2q_n/\lambda)(L-x) \cos \varphi_r + i\beta - i(2n_n/\lambda)(L-x) \cos \varphi_r], \tag{4.8}$$

$$\psi = \pi(\alpha + i\beta) = \tanh^{-1}[PZ_L \cos \varphi_r / \rho c(n_n + iq_n)],$$

where Z_L is the acoustic impedance of the material just back of the wall, at $x=L$. The acoustic impedance of the wall is then the value of Z_x at $x=0$. The behavior of this must now be studied for long wave-lengths and for a few typical cases of backing impedance Z_L, for any wave-length.

18. An Equivalent Circuit for Long Waves

The most instructive case is that for long wave-lengths; more accurately, for frequencies such that $(2\pi\nu L/c)(n_n+iq_n)$ is small compared to unity. In this case the behavior of the porous material is analogous to an electric circuit with lumped elements, the mass ρmL per unit area being analogous to the inductance, the flow resistance rL analogous to a resistance, and the reciprocal of the stiffness $\rho c^2/PL$ corresponding to a capacitance. We expand the expression in Eq. (4.8) in a power series in $(2\pi\nu L/c)(n_n+iq_n)$. To the third order, the equation becomes

$$Z_x \backsimeq \frac{Z_L + [(1/Z) - \frac{1}{3}i\omega C]^{-1}}{1 + Z_L[(1/-i\omega C) + \frac{1}{3}Z]^{-1}},$$

where Z_L is the backing impedance, $C=PL/\rho c^2$, and $Z=-i\omega\rho m_n L + r_n L$. This formula cannot be represented by a simple circuit, any more than a transmission line can be represented by a simple circuit. Nevertheless, several limiting cases can be represented by simple circuits. Usually the reactance $1/\omega C$ is larger than Z at low frequencies.

If the impedance Z_L of the backing material is of the same order of magnitude as Z, a fair approximation corresponds to having Z in series with Z_L, and C shunted across both. If Z_L is very small, $\frac{1}{3}C$ is shunted across Z alone, in the approximate equivalent circuit. If the backing material is very stiff and Z_L is large, the equivalent capacitance is shunted around Z_L, with $\frac{1}{3}Z$ in series with it. These circuits are shown in Fig. 8.

If the porous material also acts as a panel, having total mass M_s per unit area, effective stiffness constant for bending K_s, then another branch containing inductance, capacitance, and resistance in series must be shunted around the part corresponding to the air motion in the pores. The resistance R_s in this branch would be due to the internal friction in the panel as it bends.

The general equivalent circuits for long wave-lengths are shown in Fig. 8. The acoustic impedance at the front of the material is equal to that measured at Z_0 in the equivalent circuit, as long as the thickness L is small compared to a wave-length inside the material. Laminated material is thus analogous to a filter network, and it is possible to design the porous structure so as to absorb any required band of frequencies. An air space of thickness L' (small compared to a wave-length) in back of the porous panel, which is subdivided by partitions perpendicular to the panel to discourage transverse standing waves (B9), corresponds to a capacitance $L'/\rho c^2$ shunted across Z_L, with Z_L then being the acoustic impedance of the material behind the air space.

Transmission properties of acoustic materials

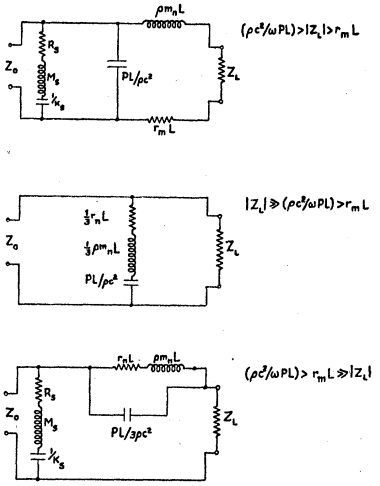

FIG. 8. Equivalent circuits for porous panel of thickness L backed by impedance Z_L, for long wave-lengths. R_s, M_s, and K_s are the equivalent constants corresponding to the bending of the panel and are infinite if the panel does not bend. The quantities r_n, m_n, and P are the constants corresponding to the porousness of the panel.

are also represented by the circuit of Fig. 8 since the current through Z_L corresponds to the normal air velocity just back of the panel. A series of panels separated by air spaces therefore corresponds to a low pass filter network.

When the wave-length is no longer large compared to the panel thickness, the acoustic behavior is analogous to the electric behavior of a leaky transmission line, and Eq. (4.8) must be solved exactly. Several cases merit discussion.

19. Results for Shorter Waves

The simplest case is when the backing material is rigid, when Z_L is infinite, and $\alpha+i\beta=\frac{1}{2}i$. The specific acoustic impedance of the wall surface $(Z_0/\rho c)$ is then

$$\zeta_p=\frac{n_n+iq_n}{P\cos\varphi_r}\tanh\left[(2\pi L/\lambda)(q_n-in_n)\cos\varphi_r+\tfrac{1}{2}\pi i\right] \quad \text{(for rigid backing)}.$$

The subscript p indicates that this impedance is due to motion of air in the pores of the material. A subscript s will be used when we discuss the impedance due to the panel motion.

A study of the quantities involved in this equation shows that a one-parameter family of curves can be drawn to show the dependence of the wall impedance ζ on frequency and on wall characteristics. The dependent variable is Γ, the independent variable is σ and the parameter is γ, where

$$\begin{aligned}\Gamma&=2\zeta(P/m_n)^{\frac{1}{2}}\cos\varphi_r,\\ \sigma&=(L/\lambda)(m_nP)^{\frac{1}{2}}\cos\varphi_r,\\ \gamma&=(r_nL/2\pi\rho c)\cdot(P/m_n)^{\frac{1}{2}}\cos\varphi_r.\end{aligned} \tag{4.9}$$

The equation for Γ then becomes

$$\begin{aligned}\Gamma&=(a+ib)\tanh\pi[-i\sigma(a+ib)+\tfrac{1}{2}i]\\ &=(2/\rho c)(P/m_n)^{\frac{1}{2}}(\cos\varphi_r)(R_p-iX_p),\\ a&=2n_n(Pm_n)^{-\frac{1}{2}}=\{2[1+(\gamma/\sigma)^2]^{\frac{1}{2}}+2\}^{\frac{1}{2}},\\ b&=2q_n(Pm_n)^{-\frac{1}{2}}=\{2[1+(\gamma/\sigma)^2]^{\frac{1}{2}}-2\}^{\frac{1}{2}}.\end{aligned} \tag{4.10}$$

The variable σ is proportional to the frequency, and the parameter γ is proportional to the flow resistance r_nL of the material. If the quantities m_n, r_n, and P are independent of the frequency, σ will be linearly proportional to the frequency, and γ will be independent of the frequency.

Curves of real and imaginary parts of the quantity Γ are plotted as functions of σ for four different values of γ in Fig. 9. In computing these curves it has been assumed that the imaginary part of $\cos\varphi_r$ is negligible. We see from these curves that for low frequencies (small values of σ) the reactive part of the impedance is very large, the stiffness of the air in the pores being the controlling factor. At these low frequencies the real and imaginary parts of the acoustic impedance Z of the wall approximate the following simple values:

$$R_p\simeq\tfrac{1}{3}r_nL,\quad X_p\simeq-(\rho c^2/\omega PL\cos^2\varphi_r) \tag{4.11}$$

(when $\sigma\ll\gamma<1$, for rigid backing) (see Fig. 8).

In this limiting case the effective resistance is one-third of the static flow resistance r_nL, the factor $\frac{1}{3}$ being due to the fact that the rigid backing prevents the air in the pores from moving enough to take full advantage of the resistivity. (See Eq. (4.15) for the corresponding case when the backing is soft.) The reactance is due to the stiffness of the air in the pores. This is the result for the equivalent circuit of Fig. 8 for infinite impedance Z_L.

At higher frequencies interference effects occur

with the wave reflected from the back of the material, and resonance peaks occur, which are sharper and higher for smaller values of γ, as the curves show. For very large values of γ the waves never reach the back of the material, the wall impedance shows no resonance effects, and the following approximate formulas are valid:

$$R_p \simeq (\rho c/P) n_n \sec \varphi_r, \qquad X_p \simeq -(\rho c/P) q_n \sec \varphi_r \tag{4.12}$$

(when $\gamma > 1$, $\gamma\sigma > 1$, for any sort of backing).

This is the characteristic impedance of the electric transmission line equivalent to the material. For high frequencies R_p approaches $\rho c(m_n/P)^{\frac{1}{2}} \times \sec\varphi_r$, and the reactive term reduces to $-(r_n c/2\omega)(m_n P)^{-\frac{1}{2}} \sec\varphi_r$. For very low frequencies (σ considerably smaller than $1/\gamma$) Eq. (4.12) is not valid, and Eq. (4.11) must be used.

We shall see in the next section that the sound absorbing quality of a wall is usually approximately proportional to the real part of the acoustic admittance ($1/Z$). Hence a large value of acoustic reactance for a wall at a given frequency will prevent the wall from absorbing much sound at that frequency. Eq. (4.11) shows that in order to have a material be a good absorber at low frequencies it must be thick (L large), porous (P close to unity), and have a tangential index of refraction much larger than unity (in order that $\cos^2 \varphi_r$ be as near unity as possible for any angle of incidence). This last specification insures that the acoustic impedance does not vary to a marked degree with the angle of incidence of the sound.

In the next section we shall see that the material absorbs somewhat better when it is not a pure resistance but has a small amount of negative (stiffness) reactance.

20. Effect of Air Backing

It is possible to provide negative reactance for a wall material for low frequencies by providing an air space behind it (B4, B9). In this case the constants α and β are fixed by setting Z_L equal to the impedance of the air space. Suppose the thickness of this space is L_a and that it is small compared to the wave-length of the sound in free space. Then Z_L is a stiffness reactance approximately equal to $(i\rho c^2/\omega L \cos^2 \varphi_i)$ (notice that the angle of *incidence* occurs in this formula). This approximation is valid whenever sound waves parallel to the wall can be set up in this air space, i.e., whenever the framework which holds the porous material away from the rigid wall is spaced more than a wave-length apart.

When this boundary condition is satisfied, it turns out that the only effect of the air space is to increase the effective thickness of the material. Equation (4.10) is still valid, and in Eq. (4.10) the values of σ and γ are changed by inserting the effective thickness

$$L_e = L + (L_a/P)(\cos \varphi_i/\cos \varphi_r) \tag{4.13}$$

(air backing, $L_a < \lambda/4$, transverse waves allowed),

instead of the actual thickness L in the equations. When the thickness L_a of the air space is larger than a quarter wave-length, a more accurate expression must be used for Z_L, and Eq. (4.10) must be revised.

In general therefore the presence of the air space increases the effective thickness of the material and reduces the height of the resonance peaks in the curve of impedance *vs.* frequency. The reason for this is that the presence of the air space behind the material moves the surface of zero normal velocity out back of the material,

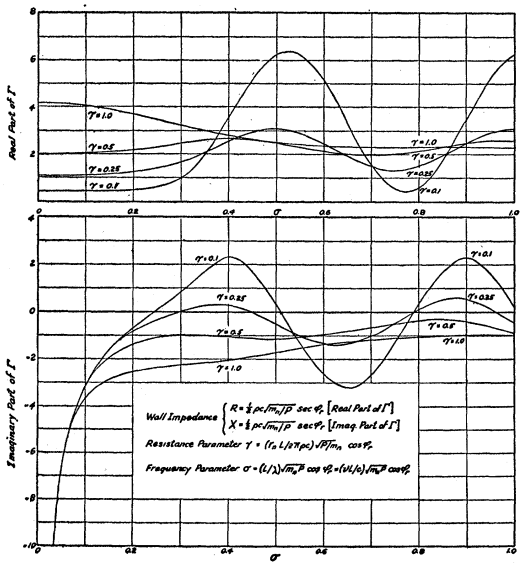

FIG. 9. Curves giving acoustic impedance of porous material of thickness L, with rigid backing.

allowing a greater flow of air through the pores, and therefore allowing a greater absorption of energy (B4).

However, an air space which allows waves to be set up in it which are tangential to the surface makes the impedance depend more strongly on the angle of incidence φ_i of the wave because of the factor cos φ_i in the formula for the effective thickness. This means that waves at near-grazing incidence are not absorbed any better with the air space than they are without it. In order to reduce the dependence on φ_i, it is necessary to break up the backing space by a honeycomb structure whose cells are small in dimensions compared to a half wave-length (B9). In this case the effective thickness of the material, to be substituted for L in Eqs. (4.10) and (4.11), is

$$L_e = L + (L_a/P \cos \varphi_r) \qquad (4.14)$$

(narrow air backing, transverse waves suppressed).

This expression is less dependent on φ_i than is L_e when no cell structure hinders the waves parallel to the wall surface; and thus even for waves striking at near-grazing incidence the effective thickness of the material is increased.

When the thickness of the air space becomes larger than a quarter wave-length, or when the material is made up of several layers having different properties, the analysis becomes more complicated. By using Eq. (4.8) several times, however, it is possible to compute the wall impedance for even these complicated forms. Of course, for the low frequencies the equivalent electrical circuit analysis can be used, as we have noted, according to Fig. 8.

21. Panel Vibration

The previous analysis in this section has taken into account that particular part of the normal velocity of air near the wall which is due to the penetration of the air into the porous material. In many cases, however, the surface of the wall yields to the pressure by moving as a whole, as a stiff panel (R7). This panel action must also be discussed. Its effects can be studied separately because, for any wall which is porous and also moves as a panel, the normal air velocity at the wall is simply the sum of the velocity of the material as a whole plus the velocity of the air into the pores. Therefore the impedances of the two separate effects can be considered to be in parallel. In this case the smaller impedance is the more important one. On the other hand, when the wall consists of a stiff impervious layer (as of paint) mounted on a porous backing material, the impedances of the two materials will act in series, and here the larger of the two impedances is the more important.

As with air space backing, when the supporting framework (assumed rigid) is spaced more than a wave-length apart, the effect of the panel action is markedly different from what it is when the spacing of the supporting network is less than a half wave-length. In the former case transverse waves are set up in the panel (M11), and we must use the theory of the wave motion of plates to obtain the impedance.

Let ρ_s be the density of the panel material, s its Poisson's ratio, Q its Young's modulus, and L its thickness. Then the equation for the normal displacement of the panel at a point (y, z) on its surface, owing to a pressure distribution over the wall, is

$$\rho_s L \frac{\partial^2 \xi}{\partial t^2} + [QL^3/12(1-s^2)]\nabla_t^4 \xi = p_0(y, z) - p_L(y, z), \qquad (4.16)$$

where p_0 is the pressure in front of the panel and p_L that in back.

The pressure in front, p_0, can be assumed to have the properties assumed earlier, in Eq. (4.5), with an angle of incidence given in Eq. (4.6). Inserting these expressions into Eq. (4.16), we obtain an equation for the acoustic impedance of the wall panel,

$$Z_s = Z_L - i\omega\rho_s L + \frac{iQL^3\omega^3}{192c^4(1-s^2)} \sin^4 \varphi_i \qquad (4.17)$$

(spacing between supports much greater than wave-length),

where Z_L is the impedance of the material (or air space) behind the panel.

The second term in this expression is the usual mass reactance of the panel. The third term is due to the stiffness of the panel as it tries to accommodate itself to alternations of pressure from point to point along its surface when the

wave is striking it obliquely. It has a positive sign indicative of a stiffness reactance (X negative), but it *increases* rapidly with frequency because of the fact that the panel finds it difficult to bend itself into the form of a short wave-length wave. Since the wave-length along the wall depends on the angle of incidence of the wave as well as its frequency, this part of the impedance depends very markedly on the angle of incidence, being small for small angles and having its maximum value, for a given frequency, for grazing incidence. Therefore a wall having a fairly stiff outer coating has a very large impedance for near-grazing waves and is, therefore, a poor absorber for such waves, particularly at higher frequencies.

When the frequency is small enough, the wave-length becomes larger than the spacing between supports, and Eq. (4.17) is no longer valid. In this case each portion of the panel which is between the supporting network acts as a stiff diaphragm having an effective mass per unit area $M_s \simeq \rho_s L$, an effective stiffness constant K_s, and an effective resistance R_s (as in the equivalent circuit), the values of these constants depending on the distribution of the supporting network. In this case the impedance of the wall is

$$Z_s = Z_L - i\omega M_s + (iK_s/\omega) + R_s \qquad (4.18)$$

(wave-length longer than four times support spacing).

This impedance is independent of the angle of incidence, which is an advantage; but the impedance becomes quite large in the low frequency range, so that the panel is a poor absorber in that range.

22. Types of Absorbing Materials

We can now classify the various sorts of wall materials and note again the equations giving the total acoustic impedance for each type:

1. Thin porous material, hard backing. Impedance from equivalent circuit of Fig. 8.
2. Thin porous material, air space in back, with supports spaced more than a wave-length apart. Impedances given in Eqs. (4.15) and (4.17) in parallel, with
$$Z_L = i\rho c^2/\omega L \cos^2 \varphi_i.$$
3. Thin porous material, air backing, with supports spaced less than a half-wave-length apart. Impedances given in Eqs. (4.15) and (4.18) in parallel with $Z_L = i\rho c^2/\omega L$.
4. Thick material, hard backing. Impedance from Eqs. (4.9) and (4.10).
5. Thick material, air backing, supports more than a wave-length apart. Impedances given in Eqs. (4.10), (4.13), and (4.17) in parallel, $Z_L = i\rho c^2/\omega L \cos^2 \varphi_i$.
6. Thick material, air backing, supports closer than a half-wave-length apart. Impedances given in Eqs. (4.10), (4.14), and (4.18) in parallel, $Z_L = (i\rho c^2/\omega L)$.
7. Very thick porous material, any sort of backing. Impedance from Eq. (4.12).
8. Thick porous material, hard backing, outer surface covered with thin stiff impervious layer (such as paint). Impedance given by Eq. (4.17) with Z_L given by Eqs. (4.9) and (4.10).

Impedances for other, more complicated structures can be built up in a similar manner.

It is interesting to notice that in four of these cases (which include the materials most generally in use), the acoustic impedance is nearly independent of the angle of incidence of the sound wave; since in most cases $\cos \varphi_r$ is nearly independent of φ_i. Only in the cases where thin porous material ($L < \lambda$) has an air backing with supports spaced widely apart, or where the surface is impervious enough so that the impedance because of panel action preponderates, does the impedance depend markedly on φ_i. Probably the most usual cases, which will be most useful to investigate later, are the case of ζ independent of φ_i and the case of ζ equal to a term independent of φ_i plus a pure reactive term ($i\rho c^2/\omega L \cos^2 \varphi_i$), typical of the behavior of an air space backing at low frequencies.

Enough measurements of impedance of acoustic materials have now been made to indicate that the above theoretical analysis provides a satisfactory picture of the sound absorption process. Moreover, the experimental data discussed later in this chapter indicate that the quantities P, m, and r for many commercial materials are *independent* of frequency over the range of frequency from 100 to 6000 cycles per

second. This indicates that these quantities can be considered as meaningful physical constants and that a measurement of the three constants for a material will enable one to predict its entire acoustical behavior. The theory greatly clarifies our understanding of the behavior of absorbing materials; and, for the lower frequencies where the equivalent circuit analysis is valid, it enables us to design materials to satisfy any specified acoustical requirements.

23. Measurement of Acoustic Impedance

We turn next to a brief review of the experimental methods of measuring acoustic impedance. The most straightforward way would be, of course, to measure the pressure, the air velocity, and their phase difference at the surface of the material. This is, however, exceedingly difficult experimentally. It is particularly difficult to build a small but sensitive *velocity* microphone, and the air particle velocity is usually much smaller than the pressure amplitude at the surface of a wall.

Attempts have been made to instrument this approach. Clapp and Firestone (C3) have developed an "acoustic wattmeter" consisting of miniature pressure and ribbon velocity microphones mounted closely together. Sound pressure, particle velocity, and their relative phase can be measured separately, and impedance is computed from these. It was found difficult to establish and maintain the calibration of the microphones, especially because of sensitivity to small wind currents and temperature changes. The device has been used for measuring impedance in a tube terminated by acoustic material; this is essentially the "hyperbolic tangent method" described below, except that p, $\mathbf{u}$, and φ are measured directly at one point in the standing wave, and then extrapolated to the position of the sample.

Another approach to the direct method has been explored by Bolt and Petrauskas (B7). Pressure and pressure gradient are measured by means of two small pressure microphones, separated by a distance d, placed close to the sample and along a line normal to it. A steady train of plane waves (from a loudspeaker) of length λ falls normally on the sample. The outputs from the two microphones, at which the sound pressures are p_1 and p_2 respectively, are combined in a circuit which yields voltages proportional to the sum (p_1+p_2) and the difference (p_1-p_2), and indicates the phase angle φ between the sum and difference terms. The acoustic impedance is then given by:

$$\frac{Z}{\rho c}=\frac{\pi d}{\lambda}\left|\frac{p_1+p_2}{p_1-p_2}\right|e^{i(\varphi-\pi/2)}.$$

Several approximations are involved: the finite difference $(p_1-p_2)/d$ is used for the pressure gradient; the midway point between the microphones is not "at" the absorbing surface but a distance h in front of it; the microphones have finite size. Also plane waves are assumed, and diffraction effects as would obtain for a small sample are neglected. With use of appropriate experimental control and correction factors, impedance values have been obtained in the range 100 to 700 c.p.s., for impedance magnitudes less than 5, which agree within a few percent with values obtained by the hyperbolic tangent method. These direct methods have the potential advantage that they can be applied to large samples of acoustic materials installed for use.

The next most direct procedure consists in setting up and exploring an interference pattern in front of the material (T1). In its simplest form this method makes use of a long straight tube of uniform cross section, with the material terminating one end. If a plane wave of a given frequency travels down the tube with partial reflection at the termination, the magnitudes and positions of the pressure maxima and minima in the resulting "standing wave" [8] pattern are determined uniquely by the complex impedance of the material at the end, except for dissipation along the tube and other effects for which corrections can be applied. The impedance Z of the material is then given by the equations (M11):

$$Z/\rho c=R/\rho c-iX/\rho c=\tanh\pi(\alpha-i\beta),$$

$$p_{\min}/p_{\max}=\tanh(\pi\alpha),$$

[8] Strictly speaking, this is a pseudo-standing wave since energy is being continuously absorbed and resupplied. This usage is common in acoustics for referring to normal modes of vibration of an enclosure, even when absorption is present.

and

$$d_{\min}=\frac{\lambda}{2}(\beta+n), \quad \text{where } n=0, 1, 2, 3, \cdots.$$

In these equations $p_{\min}$ and $p_{\max}$ are the sound pressures at the minima and maxima respectively, and $d_{\min}$ is the distance from the face of the material to the first, second, third, etc., minima.

This "hyperbolic tangent method," using a straight tube, possesses certain difficulties which limit its usefulness. In order to work with low frequencies a long tube must be used. Thus at 100 c.p.s. the tube should be longer than three meters. The high frequency limit is set by the transverse modes of vibration of the tube which break up the simple standing wave required by this method. In a tube of 10-cm diameter the lowest transverse vibration appears at about 2000 c.p.s. A further difficulty arises from the diffraction effects due to the presence of the microphone in the standing wave. In spite of these difficulties the method has proved useful for measurements on samples of moderate size (B9, P2, P3, P4, S9, D3, L5, P1, W10, P8).

Some of the objections of the straight tube have been overcome in an ingenious modification due to Hall (H1). The "tube" is an annular groove of square cross section machined in a heavy circular casting. The top of this groove is closed by a smooth surface of another circular casting, mounted so as to rotate with respect to the lower. A miniature condenser microphone, mounted with its diaphragm flush in the smooth surface, moves along the groove as the top casting is rotated. The acoustic transmission line is completed by two straight portions of square cross section milled into the castings so as to join the annular groove at opposite ends of a diameter. These tubes are terminated, respectively, by a loudspeaker unit and the sample to be measured. This method eliminates microphone diffraction and reduces the space required for low frequency measurements.

Impedance can also be measured by its influence on the acoustic resonance of a closed tube or chamber. A tube having a given length and a particular value of terminating impedance possesses discrete normal frequencies at which a resonant condition exists. The "sharpness of resonance" may be detected in three different ways: by measuring the pressure as a function of (*a*) the frequency of the sound, (*b*) the length of the tube, or (*c*) the position of the microphone. In any case a unique determination of the terminating impedance is achieved after appropriate analyses and various corrections have been applied.

The most precise impedance measurements to date are those of Beranek (B2, B3), who has developed a pressure *vs.* length resonance method. This method possesses a number of advantages in addition to the high degree of precision which has been obtained. Measurements have been made over a wide range of frequencies, from 100 to 8000 c.p.s. The method is absolute in that no comparison with a "standard' impedance is needed. All possible sources of error, such as temperature variation, dissipation along the tube, etc., are considered in the analysis. The experimental observables are pressure ratios, length, and frequency, and all of these are measured very accurately.

The resonance chamber in Beranek's apparatus is a length of steel tubing; two tubes, of different diameter, are used to cover the whole frequency range desired. Into one end of the tube is fitted a solid brass plug about one inch thick. The sound source is a loudspeaker unit to which is attached a high impedance multiple capillary tube to lead the sound into the resonance chamber, through a hole in the brass plug. This high impedance source is essentially independent of impedance variations in the resonance tube (H7). The sound detector is a small diameter brass tube which conducts sound from a point near the source out to a crystal microphone. The material to be measured is cut into a circular disk and fitted into a thin cylindrical shell. This shell is backed with a solid brass plug about three inches thick which slides into the resonance tube at the end opposite the source. The assembly holding the acoustical material is moved by means of a precision screw which can be read with an accuracy of 0.0005 cm. Sound is generated by an oscillator, the frequency of which is held constant to one part in 100,000 by comparison with a primary frequency standard. The output from the microphone is amplified and filtered, then passed into a calibrated at-

tenuator and meter with which to measure changes in sound pressure. In order to evaluate the acoustic impedance of a material, it is necessary to plot pressure-length resonance curves with and without the material at one end of the resonance tube, to determine the frequency, to hold the temperature constant, and to know the velocity of sound in the tube. In fact, variations in temperature during the measurements can be included in the formula.

Typical results of this impedance method are illustrated by Fig. 10. These and other data obtained by Beranek are used elsewhere in the present report for correlating experimental results with theoretically predicted curves. The over-all accuracy of these measurements is indicated by repeatability to ± 2 percent obtained over most of the frequency range. This is very satisfactory since variations of the same order are inherent in commercial acoustical materials.

The methods discussed here are proving useful for the measurement of acoustic impedance of small samples, mounted in a simple manner as with a rigid backing. In practice, however, materials are used in large areas and are mounted in a variety of ways. It is indicated (by the theoretical considerations earlier in this section and by preliminary experimental results) that for certain types of mounting the impedance will vary with angle of incidence of the sound. So it will eventually be necessary to measure impedance on large-scale samples, at least large enough to represent typical mounting conditions. We should also be able to study the possible variation of impedance with angle of incidence. Both of these problems are being attacked by extensions of the resonance chamber methods and the direct method mentioned above.

24. Determination of Effective Porosity, Density, and Flow Resistivity

The results obtained by the experimental techniques outlined above now make it possible to check the adequacy of the impedance theory outlined earlier in this chapter. The measurements of Beranek were all made on samples with a rigid backing, so Eq. (4.10) and the corresponding family of curves in Fig. 9 should be applicable. If we compare a particular experimental curve

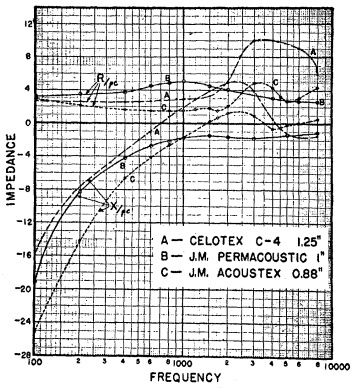

FIG. 10. Acoustic impedance of materials as function of frequency, as measured by Beranek. From reference B3.

with the impedance curves in this figure, an approximate value of the parameter γ may be chosen by inspection. The frequency scale is adjusted to fit the lower end of the reactive curve, after which a readjustment of γ may be necessary. This fitting process then indicates probable values for r, m, and P, and from these a complete impedance curve can be plotted.

It is hardly to be expected that a curve plotted in this way from a single set of *constant* parameter values should check experiment over the entire frequency range. Most acoustic materials are not perfectly isotropic and uniform as assumed in the derivation of Eq. (4.10). Also there is no *a priori* reason why r, m, and P should be constant with frequency; as in electrical circuits, inductance and capacity may vary with frequency. Consequently, it is gratifying to find that more than half of Beranek's impedance curves can be reproduced reasonably well by Eq. (4.10) with constant values of r, m, and P (B12, B4). More recent measurements, using various experimental methods, indicate that r, m, and P are reasonably constant for most commercial acoustic materials over the frequency range 100 to 6000 c.p.s.

These results lead to the hope that a direct measurement of r, m, and P and a subsequent calculation of impedance will eventually take the place of the more difficult procedure of measuring the impedance directly for all frequencies and for different mounting conditions. In order to explore this possibility for porous materials, measurements have been made of the d.c.

resistivity (B12, B13). This bears the same relation to the r used in the impedance equation as d.c. resistance does to a.c. resistance in electrical circuits; the two are not necessarily the same. The d.c. resistivity of porous acoustic materials has been discussed and measured by Gemant (G1), Rettinger (R6), and others (B4). A steady flow of air is maintained through a sample of the material, and the pressure drop across the sample is measured. The resistivity or flow resistance per unit cube is given by:

$$r=\frac{\delta p}{(V/t)}\frac{A}{L}\ \text{grams cm}^{-1}\ \text{sec.}^{-1},$$

where δp is the pressure drop in dynes, V is the volume of air in cubic centimeters which flows through the material in t seconds, A is the area and L the thickness of the sample. Measurements have been made on a number of materials ranging from a very porous hair felt with $r=10$ to building boards with $r=2\times10^4$ g/cm^3 sec. (B13). The majority of acoustic materials in general use appear to lie in the range from 50 to 500, with a few notable exceptions. About twelve of the fifteen materials reported by Beranek (B3) lie in this range.

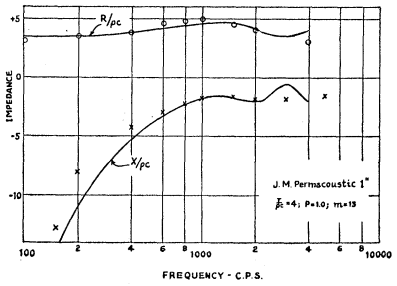

FIG. 11. Comparison of measured and computed values for acoustic impedance. Measured values of resistance are circles, of reactance are crosses, theoretical values for constant r, P, and m shown by curves.

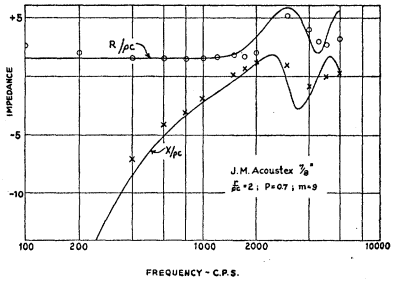

FIG. 12. Comparison of measured and computed values for acoustic impedance.

Returning now to the correlation of impedance data, we examine two cases in which the agreement between experiment and theory is very close when we use values of m, r, and P independent of frequency. These are Permacoustic and Acoustex, in Figs. 11 and 12. These two materials are physically similar in that they are comparatively rigid, and their surfaces are fissured, allowing easy flow of air into their interior. The d.c. resistivity measured for these materials is in fairly good agreement with the "effective" values of r chosen to fit the data. The agreement is particularly good for Permacoustic, and the other material shows a deviation of about 30 percent between static and effective values of r. The above considerations seem to indicate that most of the sound energy enters these materials by air penetration, and the absorption is due simply to viscosity in the pores, as postulated by the simple model.

Other materials have physical parameters which are not constant. For Temcoustic 0.5", Fig. 13, the experimental points gradually depart from the theoretical curves indicating a gradually decreasing γ with increasing frequency. This material is much more "fine-grained" than the two discussed above, and does not have fissures. Also it is somewhat compressible or "spongy." The static flow measurements on Temcoustic 0.5" indicate a probable value of d.c. resistivity about twice the effective value of $(r/\rho c)$ used in plotting Fig. 13. In this case it appears that sound energy enters the material by compressional vibration and is absorbed by internal damping, in addition to the viscous damping in the pores. There are indications that in some such cases the d.c. resistivity may be as much as a hundred times the effective dynamic resistivity.

The data quoted here are preliminary in nature and may be subject to revision. Further data are accumulating rapidly, however, and the indications are at present that for homogeneous materials the more accurate the measurements the more closely do the results correspond to the analysis given in this section.

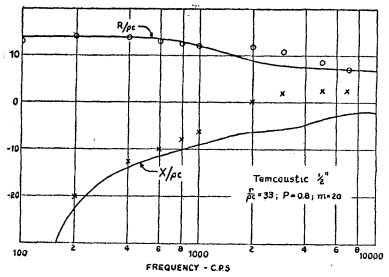

FIG. 13. Comparison of measured and computed values for acoustic impedance.

The material Celotex C-4, with its holes punched almost through the panel, and with the porosity in the hole lining considerably greater than that of the outer painted surface, presents a case which obviously cannot be represented by as simple a theory as that which gives Eq. (4.10). Since the conductivity of holes is greater the lower the frequency, presumably the effective porosity of the material should be that for the hole linings at low frequencies. The porosity for high frequencies should be that for the front perforated surface, a value which would decrease continuously as the frequency increases. To show this, Fig. 14 has two sets of theoretical curves drawn for two different (constant) values of the porosity and effective mass. Presumably a curve drawn with the parameters changing monotonically with frequency will fit the data reasonably well.

In conclusion, we see that the agreement between impedance theory and measurements for rigidly backed uniform materials is fairly satisfactory. Many materials are represented by physical parameters which are fairly constant with frequency. Also the effective value of resistivity is equal to the steady flow value for the more rigid porous materials and is less than the static value for some compressible materials.

V. STEADY-STATE SOUND IN RECTANGULAR ROOMS

In rooms of regular shape, with smooth walls, the sound is not statistically diffuse, and wave acoustics must be used. The wave equations must be separated and solutions found satisfying the boundary conditions. Theoretical analysis is thus restricted to room shapes corresponding to the eleven coordinate systems which allow separation of the wave equation (E2). It is fortunate that the most usual room shape, the rectangular parallelopiped, is also the easiest to calculate. Even for this case the analysis is complex enough so that the general physical picture is often lost among the obtruding details. Nevertheless the details must be studied before the picture can be made clear.

25. The Boundary Conditions

Let us study (M12) the acoustical behavior of such a room, having the dimensions L_x, L_y, L_z, with each wall uniformly covered with acoustic material. We first discuss the steady-state behavior of the room, with a source driving the room at frequency $\nu=(\omega/2\pi)$. The methods of operational calculus will be used later to obtain the transient behavior in terms of the steady-state performance. We will soon perceive that the steady-state solutions depend on the sign of the frequency constant ω in the ubiquitous exponential $e^{i\omega t}$. As has been already explained (Sec. 10, Footnote 6), we shall choose the negative sign for ω when discussing the steady state. But both signs for ω are needed in applying the operational calculus, so that our analysis here will be extended to cover both signs. It will appear that the characteristic functions and constants for negative values of ω are the complex conjugates of the quantities for the corresponding positive values of ω. For ease in discussion we shall adopt the convention of regarding the characteristic functions, constants, etc. (which are complex quantities), to be functions of the variable ω, which will be allowed to take on both positive and negative values, whereas the real and imaginary parts of these quantities will be considered to be functions of positive values of ω alone. For instance the complex impedance $Z(\omega)$ of a wall is defined for positive and negative values of ω, whereas $R(\omega)$ and $X(\omega)$, the resistance and reactance, are defined only for positive values of ω. Therefore $Z(\omega)=R+iX$, but $Z(-\omega)=R-iX$. A mass reactance is therefore always positive, a stiffness reactance always negative.

Returning to the rectangular room, we denote the specific acoustic impedance $(Z/\rho c)$ of the wall $(x=0)$ as ζ_{x1}, that of the wall at $(x=L_x)$ as

ζ_{x2}, and so on. The velocity potential for a standing wave in the room has the general form $\psi(\omega; x, y, z) = D(x) \cdot E(y) \cdot F(z) \cdot e^{i\omega t}$, where

$$D(x) = \cosh\left[(\pi i x/L_x)\chi_x(\omega) - \Phi_x\right], \quad (5.1)$$

with similar expressions for E and F. The characteristic value χ_x has a real part which will be denoted as μ_x and will be called the *wave number parameter*, and an imaginary part, denoted as κ_x, which will be called the *attenuation parameter*. In accordance with the convention discussed above, $\chi(\omega) = \mu + i\kappa$, $\chi(-\omega) = \mu - i\kappa$.

From the velocity potential can be obtained the pressure p and the air velocity $\mathbf{u}$ by the equations

$$p = \rho(\partial\psi/\partial t), \quad \mathbf{u} = -\text{grad}\,(\psi). \quad (5.2)$$

The boundary conditions, which fix the values of the constants κ, μ, and Φ, are that the ratio of pressure to normal velocity into the surface at each surface equals the impedance of the surface. Thus, for a driving frequency $(\omega/2\pi)$ (ω positive), at $x = 0$,

$$i\omega\rho\psi = \rho c\zeta_{x1}(\partial\psi/\partial x), \quad \text{or} \quad \coth(\Phi_x) = -(\zeta_{x1}/\eta_x)\chi_x.$$

The parameters $\eta_x = (\omega L_x/\pi c) = (2L_x/\lambda)$, and the corresponding ones η_y and η_z will be called the *frequency parameters*. They give the dimensions of the room in half wave-lengths. When we fit the boundary conditions at $x = L_x$, we obtain the basic equation for χ_x,

$$\pi i\chi_x + \coth^{-1}\left[(\zeta_{x1}/\eta_x)\chi_x\right] + \coth^{-1}\left[(\zeta_{x2}/\eta_x)\chi_x\right] = 0, \quad (5.3)$$

with two other equations for χ_y and χ_z.

26. Characteristic Values

The simplest case is when none of the impedances ζ depends on the angle of incidence of the sound wave. Then the three basic equations separate, and χ_x depends only on (ζ_{x1}/η_x) and (ζ_{x2}/η_x), and not on (ζ_{y2}/η_y) and the other constants for the other two wall pairs. Referring to Eq. (3.1) (and recalling that ω is positive here), we utilize the expression for the *specific acoustic admittance* of the walls, $\beta = (1/\zeta) = (\rho c/|Z|)e^{-i\varphi}$. We can then express the basic equations in the standard form,

$$\pi i\chi + \coth^{-1}(\chi/\beta_1\eta) + \coth^{-1}(\chi/\beta_2\eta) = 0. \quad (5.4)$$

When we insert the subscripts x, y, or z, we obtain the three basic equations.

There are an infinity of roots of this equation. As long as β_1 and β_2 have positive real parts there is at least one value (and not more than two values) of $\chi = \mu + i\kappa$, for μ between zero and unity. There is one root with μ between 1 and 2, another with μ between 2 and 3, and so on. The different roots, and their corresponding characteristic functions, will be distinguished, when necessary, by giving them different values of the subscript n, with $n = 0$ for the value of χ with the smallest value of μ, $n = 1$ for the next smallest value of μ, and so on.

In a good many cases the quantities $(\beta_1\eta)$ and $(\beta_2\eta)$ are much smaller than unity, so that it is possible to use the first terms of the series solution of Eq. (5.4):

$$\chi_0 = (i\eta/\pi)^{\frac{1}{2}}(\beta_1+\beta_2)^{\frac{1}{2}}\left[1 - \frac{i\pi}{6}\eta\frac{\beta_1^3+\beta_2^3}{(\beta_1+\beta_2)^2} + \cdots\right] \quad (n=0;\ \beta_1\eta,\ \beta_2\eta < 1); \quad (5.5)$$

$$\chi_n = n + (i\eta/\pi n)(\beta_1+\beta_2) + (\eta^2/\pi^2 n^3)(\beta_1+\beta_2)^2 + \cdots \quad (n>0;\ \beta_1\eta,\ \beta_2\eta < n).$$

These formulas are adequate except for the case where one or both of the walls are quite soft.

In reverberation chambers, however, where acoustical materials are measured, data are sometimes taken with absorbing material spread over one wall (or over the floor). Therefore, it is important to obtain a solution of Eq. (5.4) when

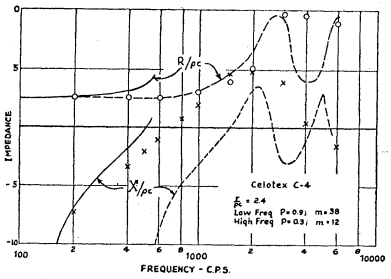

FIG. 14. Comparison of measured and computed values for acoustic impedance. Lack of agreement may be explained by variation of P and m with frequency.

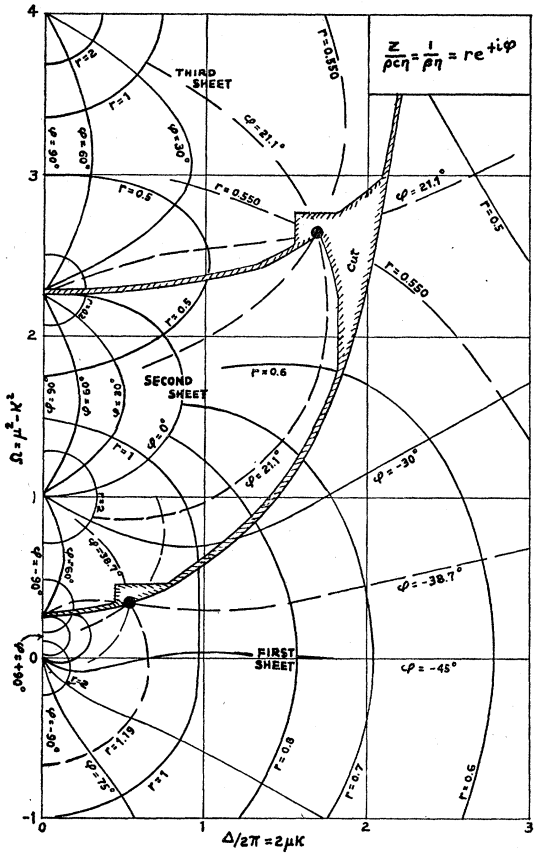

FIG. 15. Conformal transformation from wall impedance parameter $re^{i\varphi}$ to square of characteristic value $\chi^2=(\mu+i\kappa)^2$. Branch points are shown as black circles and cuts as shaded bands.

one of the β's (suppose it is β_1) is small, but the other β is not small. In this case χ can be split into two terms:

$$\chi\simeq\chi_2+(i\beta_1\eta/\pi\chi_2)\left[1+\frac{i\beta_2\eta/\pi}{\chi_2^2-\beta_2^2\eta^2}\right]^{-1}(\beta_1\eta<\chi_2), \tag{5.6}$$

where the quantity χ_2 is one of the roots of the transcendental equation,

$$(1/\chi_2)\coth(-\pi i\chi_2)=(1/\beta_2\eta)=(2Z_2L/\rho c\lambda), \tag{5.7}$$

where Z_2 is the impedance of the softer wall. The χ's for the other four walls of the reverberation chamber, which are fairly hard, can be obtained from Eqs. (5.5).

Plots of real and imaginary parts of the roots of Eq. (5.7) as functions of the magnitude and phase angle of β_2 have been published (H9, M13). The plots correspond to the conformal transformation from $\ln(\beta_2\eta)$ to χ_2, defined by Eq. (5.7). The transformation is multivalued, with an infinite number of sheets, corresponding to the infinite number of roots for χ_2, as can be seen from Fig. 15, which gives the transformation from $\ln(\beta\eta)$ to χ^2. The details of the transformation from χ_2^2 to $\ln(1/\beta_2\eta)$ will be discussed later, and plots of some of the sheets are given in Figs. 16–19.

27. Resonance Frequencies and Damping Constants

Solution of the three basic Eqs. (5.4) makes it possible to compute the characteristic values and thus the characteristic functions of our boundary value problem. These functions, for positive ω, have the form $\psi_N(\omega;x,y,z)=D(x)E(y)F(z)$, where

$$D_{n_x}(x)=\cosh\left[(\pi ix/L_x)\chi_{x,n_x}+\coth^{-1}(\chi_{x,n_x}/\beta_{x1}\eta_x)\right], \tag{5.8}$$

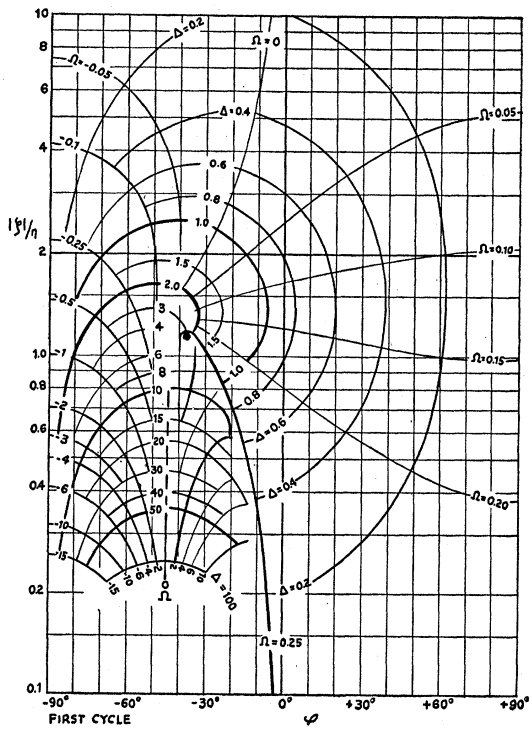

FIG. 16. Conformal transformation from $\chi^2=\Omega+i\Delta/2\pi$ to $\ln(\zeta/\eta)$ for first sheet shown in Fig. 15. Branch point is at $(|\zeta|/\eta)=1.19$, $\varphi=-38.7°$.

where $\chi_{x,nx}(\omega)$ is the n_xth root of Eq. (5.4) for the x-walls, and where the letter N stands for the trio of numbers n_x, n_y, n_z. These functions satisfy the differential equation

$$\nabla^2\psi_N(\omega)+(1/c^2)[\omega_N(\omega)+ik_N(\omega)]^2\psi_N(\omega)=0,$$

corresponding to the characteristic value

$$[\xi_N(\omega)]^2=[\omega_N+ik_N]^2=(\pi c)^2\{[\chi_{xn_x}(\omega)/L_x]^2 +[\chi_{yn_y}(\omega)/L_y]^2+[\chi_{zn_z}(\omega)/L_z]^2\}. \quad (5.9)$$

The quantity ω_N, which we shall call the *resonance frequency* of the standing wave ψ_N, and k_N, which we shall call its *damping constant*, are defined only for positive values of ω in accordance with our convention.

In most cases of practical interest the damping constant k_N is much smaller than the resonance frequency ω_N, so that the approximate equations

$$\omega_N(\omega)\simeq\pi c\left[\frac{\mu_x^2-\kappa_x^2}{L_x^2}+\frac{\mu_y^2-\kappa_y^2}{L_y^2}+\frac{\mu_z^2-\kappa_z^2}{L_z^2}\right]^{\frac{1}{2}} \quad (5.10)$$

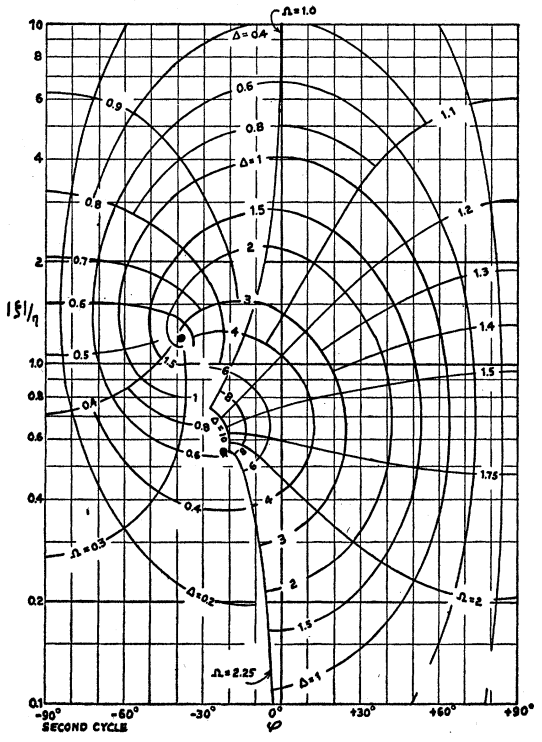

FIG. 17. Conformal transformation from χ^2 to ln (ζ/η) for second sheet. Additional branch point is at $(|\zeta|/\eta)=0.550$, $\varphi=-21.1°$.

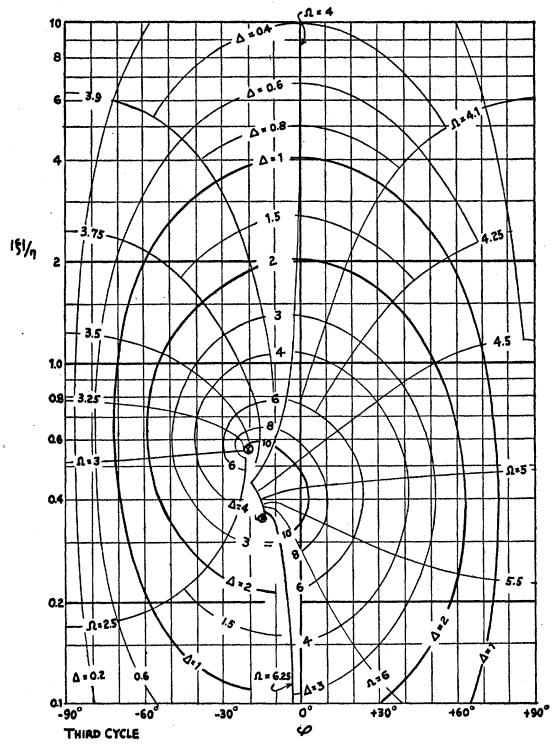

FIG. 18. Conformal transformation from χ^2 to ln (ζ/η) for third sheet. Additional branch point is at $(|\zeta|/\eta)=0.355$, $\varphi=-15.0°$.

and

$$k_N(\omega)\simeq(c/4)\left[\frac{4\pi\mu_x\kappa_x}{\eta_xL_x}+\frac{4\pi\mu_y\kappa_y}{\eta_yL_y}+\frac{4\pi\mu_z\kappa_z}{\eta_zL_z}\right]$$

are valid. It will be shown shortly that ω and k are usually the quantities determined experimentally, rather than the wave number and attenuation parameters μ and κ. Therefore, in our computations, it will be more suitable to obtain values of the quantities $\mu^2-\kappa^2$ and $2\mu\kappa$, rather than μ and κ themselves. These quantities are the real and imaginary parts of χ^2, so that the most useful conformal transformation is that between χ^2 and ln $(1/\beta\eta)$, corresponding to Eq. (5.4) or Eq. (5.7).

The series expressions in Eqs. (5.5) enable us to compute ω_N and k_N when all the walls are fairly hard. The results can be expressed most easily in terms of the real and imaginary parts of the specific admittance β: the *specific acoustic conductivity* being denoted as γ, and the *specific acoustic susceptance* as σ; so that $\beta(\omega)=\gamma+i\sigma$ and $\beta(-\omega)=\gamma-i\sigma$, according to our convention.

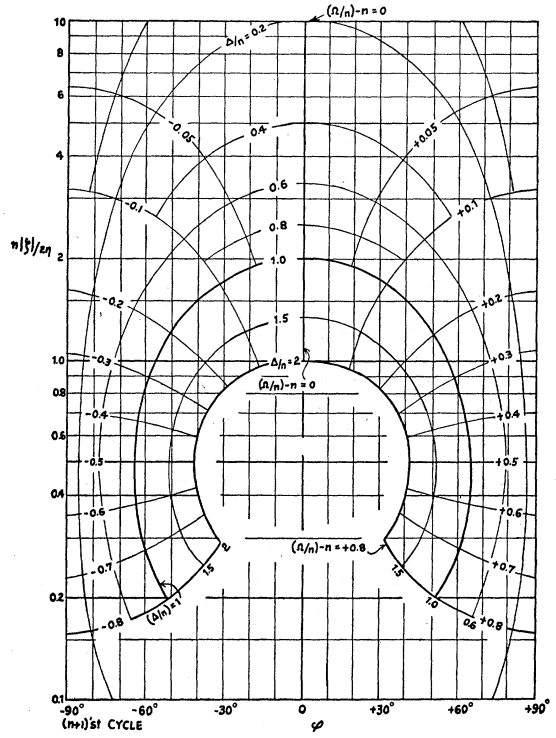

FIG. 19. Approximate transformation from χ^2 to ln (ζ/η) for $(n+1)$st sheet. Contours close to the branch points omitted because the approximation is not valid there.

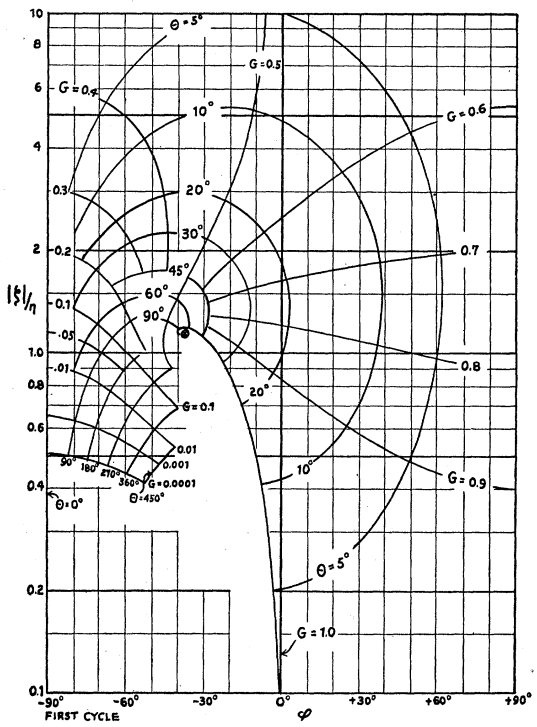

FIG. 20. Conformal transformation from normalizing function $Ge^{i\theta}$ to wall impedance function ln (ζ/η), for first sheet.

From Eqs. (5.5) we obtain

$$\mu_n{}^2-\kappa_n{}^2\simeq\begin{cases}-(\eta/\pi)(\sigma_1+\sigma_2), & n=0\\ n^2-(2\eta/\pi)(\sigma_1+\sigma_2), & n>0\end{cases}$$
$$4\pi\mu_n\kappa_n/\eta\simeq\begin{cases}2(\gamma_1+\gamma_2), & n=0\\ 4(\gamma_1+\gamma_2), & n>0\end{cases} \qquad (5.11)$$
$$\gamma=(\rho c/|Z|)\cos\varphi,\quad \sigma=-(\rho c/|Z|)\sin\varphi$$
$$\text{for } |\zeta|\gg\eta/(n+1).$$

The approximate expression for the damping constant when all walls are fairly hard is, therefore,

$$k_N\simeq(c/8V)[8e_{nx}(\gamma_{x1}+\gamma_{x2})S_x+8e_{ny}(\gamma_{y1}+\gamma_{y2})S_y+8e_{nz}(\gamma_{z1}+\gamma_{z2})S_z], \qquad (5.12)$$

where V is the volume of the room, S_x the areas of the walls at $x=0$ and $x=L_x$, etc., and the quantity e_n is unity when $n>0$, and $\frac{1}{2}$ when $n=0$. Since e_n is the factor which depends on the standing wave and not on the wall, we can call it the *wave type factor*.

In this case the effect of each wall is additive, and the formula for the damping constant bears a close resemblance to the formula of Sabine, Eq. (2.2), for the ergodic distribution. The similarity is not complete, however, for the Sabine formula assumes that *all* waves have the same value of k, whereas Eq. (5.12) differentiates between the oblique, tangential and axial waves through the wave type factors e_n. An axial wave, with two e's equal to $\frac{1}{2}$, is damped much less rapidly than the oblique waves, with all three e's equal to unity.

For the case of a reverberation chamber having one wall which is soft, we can use Eq. (5.6) to obtain approximate formulas for the resonance frequency and the damping constant. We first define the quantities G and θ by the equation

$$G_2\exp(i\theta_2)=\left\{1+\frac{i\beta_2\eta/\pi}{\chi_2{}^2-\beta_2{}^2\eta^2}\right\}^{-1}, \qquad (5.13)$$

where χ_2 is defined by Eq. (5.7). For small values of β_2, θ_2 is small and G_2 is unity if $n>0$,

and is $\frac{1}{2}$ when $n=0$ (in other words, it approaches the quantity e_n used in Eq. (5.12). Values of G and θ for larger values of β/n can be read off the charts given in Figs. 20 and 21 for the first two cycles of the transformation from $\beta_2\eta$ to χ_2. Then the contributions to ω and k due to the soft wall and the wall opposite the soft one are

$$\mu^2-\kappa^2=\Omega_2+(2\rho c\eta G_2/\pi|Z_1|)\sin(\varphi_1-\theta_2), \quad (5.14)$$

and

$$4\pi\mu\kappa/\eta=\Delta_2/\eta+(4\rho cG_2/|Z_1|)\cos(\varphi_1-\theta_2),$$

where $\chi_2^2=\Omega_2+(i\Delta_2/2\pi)$. The quantities Ω and Δ can be read from the plots of Figs. 16–19, in terms of the impedance and phase angle for the soft wall; whereas G and θ can be read from the plots of Figs. 20 and 21. For the further cycles and for larger values of $(Z_2/\rho c\eta)$ than those shown in the plots, it is sufficiently accurate to let $G=1$ and $\theta=0$, (except for the initial cycle, for which $G=\frac{1}{2}$ is the limiting value).

The quantities Ω and $\Delta/2\pi$ are the real and imaginary parts of the quantity χ^2, which is related to $\beta\eta$ by the relation

$$(1/\chi)\coth(-\pi i\chi)=(1/\beta\eta),$$

as given in Eq. (5.7). Therefore the transformation from the real and imaginary parts of $\ln(1/\beta\eta)$ to Ω and $(\Delta/2\pi)$ is a conformal one. The transformation is multi-valued, any given value of $\beta\eta$ corresponding to an infinity of allowed values of Ω and Δ. Each sheet has its branch points and connecting cuts, which link it with the next sheets above and below. The branch points are shown by heavy circles on the charts of Figs. 16 to 19, and the cuts by blank spaces. Figure 15 shows the inverse transformation, with the cuts shown as double lines, shaded. Other representations of this transformation have previously been given (H9, M13).

Equations (5.14) show that the absorption of opposite walls is *not* additive whenever one wall of the pair is soft. The contributions to ω and k due to the wall opposite the soft wall (wall No. 1 in Eqs. (5.14)) are modified by the factor G_2 and the phase angle θ_2, which depend on the value of the impedance of the soft wall. This is because of the fact that the presence of a soft wall appreciably distorts the form of the standing wave in the room. In some cases ($n=0$, or φ_2 positive for $n>0$) the pressure near the soft wall has a larger amplitude than it does near the opposite harder wall, so that the relative effect of the harder wall is reduced. In other cases (for $n>0$ and for negative values of φ for the soft wall) the pressure amplitude is reduced near the soft wall compared to that near the hard wall, so that G_2 is larger than unity. The most extreme case is for $n=0$, for $(|\zeta_2|/\eta)$ less than unity and for φ_2 negative; where G_2 becomes extremely small, so that the harder wall has practically no absorbing effect. In these cases the pressure amplitude falls off exponentially away from the soft wall, and the amplitude near the harder wall is practically negligible, so that very little energy is present to be absorbed by wall No. 1.

28. Characteristic Functions

The above discussion covers the behavior of the characteristic values defined in Eq. (5.9). We must now complete our discussion of the

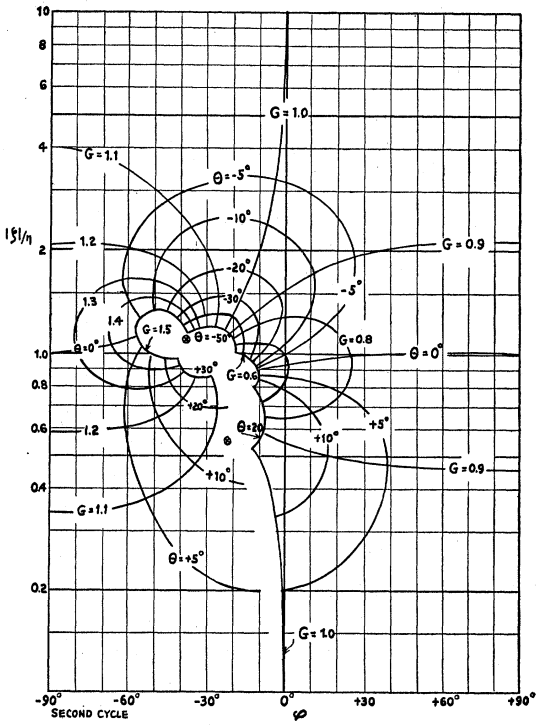

FIG. 21. Conformal transformation from $Ge^{i\theta}$ to $\ln(\zeta/\eta)$ for second sheet.

characteristic functions ψ_N. The functions are orthogonal, in that the integral of the product $\psi_N(\omega)\psi_{N'}(\omega)$ over the room volume is zero unless the trio of numbers represented by N is identical with the trio represented by N'. (Note that we do not multiply ψ_N by the complex conjugate of $\psi_{N'}$, for the conjugate would be the characteristic function for $-\omega$). The normalization factors for the functions are

$$\Lambda_N(\omega)=\int\int\int\psi_N^2(\omega)dV=\Lambda_{n_x}\Lambda_{n_y}\Lambda_{n_z} \tag{5.15}$$

and

$$\Lambda_n(\omega)=\frac{L}{2}\left\{1+\frac{i\beta_1\eta/\pi}{\chi_n^2(\omega)-\beta_1^2\eta^2}+\frac{i\beta_2\eta/\pi}{\chi_n^2(\omega)-\beta_2^2\eta^2}\right\},$$

where the subscripts x, y, and z are to be inserted in the second equation to obtain the three factors of Λ_N. When both walls of a parallel pair are hard, the corresponding normalization factors can be computed from the series formulas

$$\Lambda_n\simeq\begin{cases}L[1-(\pi i\eta/3)(\beta_1^3+\beta_2^3)(\beta_1+\beta_2)^{-2}], \\ \qquad (n=0;\ \beta_1\eta,\ \beta_2\eta<1) \\ (L/2)[1+(i\eta/\pi n^2)(\beta_1+\beta_2)], \\ \qquad (n>0;\ \beta_1\eta,\ \beta_2\eta<n).\end{cases} \tag{5.16}$$

When all the walls are rigid, the normalizing factor has the more familiar value

$$\Lambda_N\rightarrow(V\epsilon_N),$$

$$\epsilon_N=\frac{\frac{1}{8}}{e_{n_x}e_{n_y}e_{n_z}}=\begin{cases}1, & n_x=n_y=n_z=0\\ \frac{1}{2}, & \text{only two } n\text{'s zero}\\ \frac{1}{4}, & \text{only one } n \text{ zero}\\ \frac{1}{8}, & \text{not any } n \text{ equal to zero}\end{cases} \tag{5.17}$$

where $V=L_xL_yL_z$ is the room volume.

In the case when one wall of a pair (wall No. 2, for instance) is soft and the other is hard, we can use Eqs. (5.13) and (5.14) to obtain the corresponding factor in the normalizing constant,

$$\Lambda_n\simeq(L/2)[(1/G_2)\exp(-i\theta_2)+(i\beta_1\eta/\pi\chi_2^2)].$$

As for the characteristic functions themselves, if the wall at $x=0$ is hard ($\beta_{x1}\eta_x$ small), the x-factor for ψ_N takes on a form simpler than that given in Eq. (5.8),

$$D_{n_x}\simeq\cosh[(\pi ix/L_x)\chi_x+(\eta_x\beta_{x1}/\chi_x)]. \tag{5.18}$$

If the opposite wall is also hard, then the following approximate formulas are valid,

$$D_{n_x}\simeq\begin{cases}\cosh\left\{\left[\frac{\pi\eta_x}{i(\beta_{x1}+\beta_{x2})}\right]^{\frac{1}{2}}\cdot\frac{1}{L_x}\cdot\right. \\ \qquad \left.\cdot[\beta_{x1}(x-L_x)+\beta_{x2}x]\right\}, \quad (n_x=0) \\ \cosh\{(\pi inx/L_x)-(\eta_x/nL_x)\cdot \\ \qquad \cdot[\beta_{x1}(x-L_x)+\beta_{x2}x]\}, \quad (n_x>0).\end{cases} \tag{5.19}$$

This completes our discussion of the standing waves in a rectangular room, with uniform coverage of material whose impedance is independent of angle of incidence φ_i. An exact solution for the case when the impedance depends on φ_i is beyond the scope of this article. When the walls are hard, the angle of incidence against the x-walls, for instance, is approximately

$$\cos^{-1}\{(n_x/L_x)[(n_x/L_x)^2+(n_y/L_y)^2+(n_z/L_z)^2]^{-\frac{1}{2}}\}.$$

For this approximate value of angle the impedance for the x-walls can be computed, and values of μ_x, κ_x, etc., can be obtained. If this result is not accurate enough, a more exact value of angle of incidence can be obtained by setting the computed values of μ_x, κ_x in the equation

$$\cos\varphi_i\backsimeq(\pi c/\omega_N L_x)(\mu_x^2-\kappa^2)^{\frac{1}{2}},$$

and recomputing the values of impedance and corresponding resonance frequency and damping constants.

29. Steady-State Response

Now that the characteristic values and functions have been discussed, and methods have been outlined whereby their values can be computed in the various cases of practical importance, we must apply the results to the study of the steady-state response of a rectangular room. We assume that a distribution of sound source is present in the room, so that in the cm cube around the point (x, y, z) there is an air outflow $q(x, y, z, t)$ cc per sec. of air at the time t. In the present section we shall study the behavior due

to simple point sources, but it is possible to study the effect of any sort of source by building up a space distribution of sources of various intensities. The equation for the velocity potential in the presence of a distribution of sources turns out to be

$$\nabla^2\Psi-(1/c^2)(\partial^2\Psi/\partial t^2)=-q(x, y, z, t).$$

When the source is simple harmonic,

$$q=Q(x, y, z)e^{-i\omega t},$$

and we can expand Ψ and Q in series of the characteristic functions discussed above. These series will satisfy the boundary conditions for the frequency $(-\omega/2\pi)$. Substituting the series into the equation for Ψ and using the equation relating the characteristic functions $\psi_N(-\omega)$ with the characteristic values ω_N-ik_N, we finally obtain the series

$$\Psi=-c^2\sum_N\frac{B_N\psi_N(-\omega; x, y, z)}{\omega^2-(\omega_N-ik_N)^2}e^{-i\omega t},$$
$$B_N=\frac{1}{\Lambda_N(-\omega)}\iiint Q\psi_N(-\omega)dv. \tag{5.20}$$

The steady-state pressure at point (x, y, z) is then $-i\rho\omega\Psi$.

If the loudspeaker is considered to be a simple point source of strength Q_0 at point (x_0, y_0, z_0), then

$$B_N=Q_0\psi_N(-\omega; x_0, y_0, z_0)/\Lambda_N(-\omega). \tag{5.21}$$

This indicates that the relative amount of the Nth wave in the series excited by a point source is proportional to the amplitude of the wave at the position of the source. To eliminate a wave from the steady-state sound, one can place the source where the amplitude of the unwanted standing wave is zero.

A more important factor in each term, however, is the resonance denominator, which is small when the driving frequency is equal to the resonance frequency $(\omega_N/2\pi)$, making the corresponding term in the series quite large. The resonance peak for each standing wave is fairly narrow; the half-breadth (the amount the driving frequency must differ from the resonance frequency in order that the mean square pressure be half its resonance value) being $(k_N/2\pi)$. For low frequencies, such that the wave-length is not small compared to the room dimensions, the separation between successive resonance frequencies is, on the average, larger than this half-width. The response at these frequencies is quite irregular; it is small when the driving frequency is not equal to one of the resonance frequencies, and quite large at resonance. In this case it is possible to study each standing wave separately, by driving the room at the corresponding resonance frequency.

The limiting frequency, below which individual standing waves can be excited separately, can be obtained from Eq. (3.4), which gives the average number of resonance frequencies less than ν. If we differentiate Eq. (3.4) and set dn equal to unity, we find the corresponding value of $d\nu$ is the average frequency spacing between resonance frequencies. Neglecting all but the first term in the series, we see that an approximate value for this spacing is $(c^3/4\pi V\nu^2)$. In order to separate individual resonance peaks, this spacing must be larger than $(k_N/2\pi)$. Therefore individual standing waves can be excited separately in a room for driving frequencies ν such that

$$\nu<(c^3/2Vk_N)^{\frac{1}{2}}, \tag{5.22}$$

where V is the volume of the room, and k_N is given by Eq. (5.10).

30. Phenomena at Low Frequencies

So far we have been tacitly assuming that our problem was to compute the acoustic behavior of the room when the impedances of the walls are given. A problem of equal importance, however, is the reverse one, of finding the impedance of a material from measurements of the acoustic behavior of a reverberation chamber having the material on one wall. The discussion immediately above suggests two different methods of solving this problem.

Both methods require the use of small scale chambers in order that the resonance frequencies be spaced far enough apart in the useful frequency range so that individual standing waves can be excited separately. Chambers about 3 feet in largest dimension, and with sides approximately in the ratio 1.5:2.5:3.5 have been found

suitable (B5, B9, H7). The source can be a tube transmitting the sound into a chamber through a hole in one side, so that it acts as a point source. In this case the coefficients B_N in Eq. (5.20) are given in Eq. (5.21). If we suitably arrange the position in the wall of the end of the tube, it is sometimes possible to separate the response of two standing waves which have overlapping resonance peaks. The chamber should be made of very heavy, rigid, impervious material in order that the contribution to k_N from all the walls not coated with absorbing material be negligibly small.

The first of the two methods mentioned above involves the measurement of the dependence of the pressure in the chamber on the driving *frequency* (B5, H7). By measuring the response of the room near one of its resonance frequencies one can obtain values of ω_N and k_N for the room. A comparison of the measured values of these quantities for the untreated chamber with those obtained when the absorbing material is placed on one wall may enable one to find values of Ω and Δ corresponding to the absorbing wall (see Eq. (5.14)). From these, by using the charts in Figs. 16 to 19, it is possible to obtain the specific impedance for the absorbing material at the various resonance frequencies.

In practice, however, it seems to be much more difficult to measure Ω, which involves a measurement of the change in the resonance frequency[9] caused by placing the absorbing material on one wall, than it is to measure Δ, which involves only a comparison of half-widths of resonance peaks for the room with and without the absorbing material. If Ω cannot be measured, and only one value of Δ is measured, the value of ζ cannot be determined; but if the values of Δ for two or more different standing waves, of nearly the same frequency but having different values of n_x, can be measured, it is sometimes possible to obtain the value of ζ. For instance, if we know values of Δ for a wave which grazes the material ($n_x=0$) and for a wave with nearly normal incidence ($n_n \gtrsim 1$), we can compare Figs. 16 and 17 to find what value of ζ gives this pair of values. This method, however, does not always give unique answers (B5, H7), and slight errors in measured values of k_N may lead to very large errors in the resulting values of ζ. On the whole, the frequency variation method is more reliable when both Ω and Δ can be measured.

A second method of working backward from steady-state measurements on standing waves to acoustic impedance involves the measurement of the dependence of the pressure on *position* in space. A moving microphone is used to obtain the dependence of the pressure amplitude of a resonating standing wave on the distance from the absorbing wall. If the absorbing material to be measured is placed on the wall $x=L_x$, and the wall at $x=0$ is rigid, the dependence of the mean-square pressure on x will correspond to the factor

$$(p^2)_{\text{Av}} = \tfrac{1}{2}\cosh(2\pi\kappa_x x/L_x) + \tfrac{1}{2}\cos(2\pi\mu_x x/L_x). \quad (5.23)$$

A family of curves of ten times the logarithm of this factor (p^2 in db as function of $(\mu x/L)$, for different values of (κ/μ), is shown in Fig. 22. By fitting the horizontal scale of the experimental curves to those of the figure, one can obtain a value of μ_x; and by correlating the shape of the experimental curve with one of the family of theoretical curves, a value of κ_x can be obtained. Once these two parameters have been determined, values of $\Omega_x=\mu_x^2-\kappa_x^2$ and $\Delta_x=4\pi\mu_x\kappa_x$ can be computed and Figs. 16 to 19 can be used to find the specific impedance ζ_{x2}. If the wall at $x=0$ is not perfectly rigid, the origin for Eq. (5.23) will not coincide exactly with the hard wall, but will be displaced by an amount which can be determined by Eq. (5.18). Also, according to Eq. (5.14), correction terms must be subtracted from $\mu_x^2-\kappa_x^2$ and $4\pi\mu_x\kappa_x$ in order to obtain the values of Ω_x and Δ_x to use in obtaining ζ_{x2}. Values of these correction terms can be determined by measuring the pressure distribution in the chamber before the absorbing material is placed on one wall.

Few applications of these methods have been reported to date, but these have been sufficient to furnish some enlightening results and to indicate that this approach can be useful for obtaining certain kinds of information which are difficult to get by other methods. In particular, the

[9] Shifts in resonance frequencies have been observed experimentally (B8, K5), but quantitative correlations with wall impedance have not been reported.

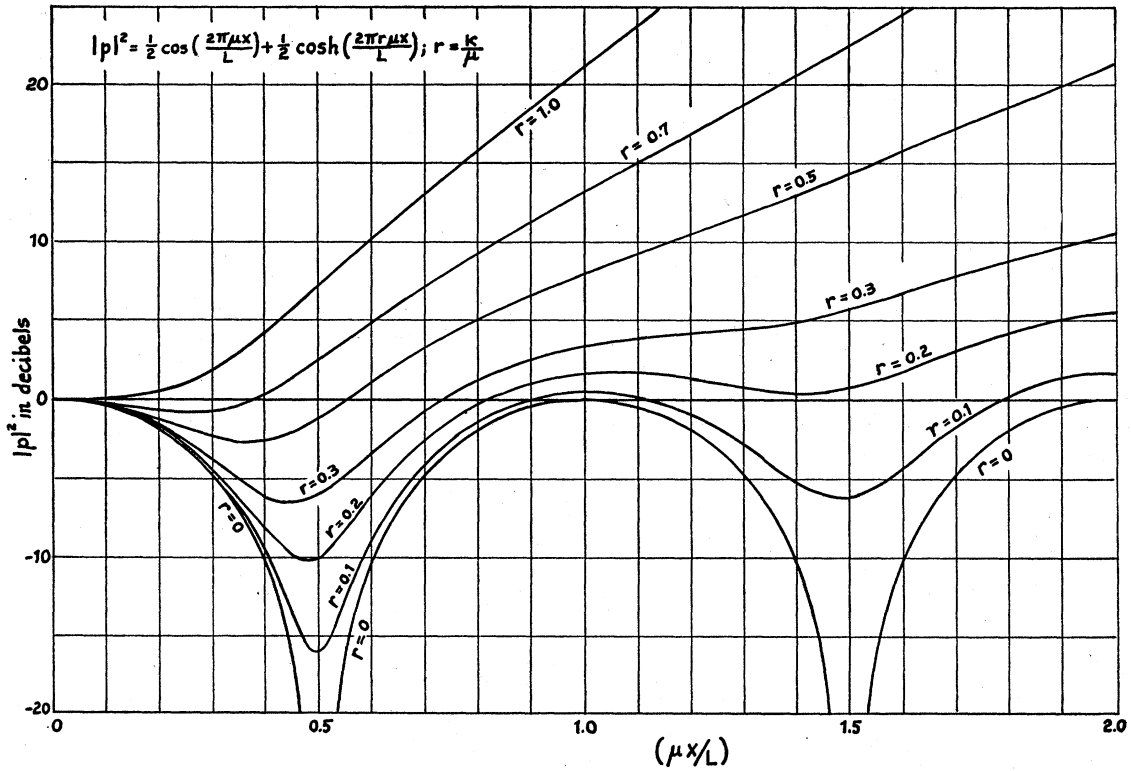

FIG. 22. Mean-square pressure in decibels; dependence on one coordinate.

study of isolated modes of vibration in rectangular chambers can yield values of impedance as a function of angle of incidence and of mounting conditions, on samples large enough to simulate full scale applications.

Hunt (H7) made a study along the lines of the first method outlined above, measuring resonance peaks to determine absorptive properties of acoustic materials for different kinds of waves. However, this work was done before the measurements of Beranek (B3) and others had demonstrated the importance of the imaginary part of the impedance; no attempt was made to obtain a reactive term, so only the quantity corresponding to Δ was measured, and Ω was ignored. Transite slabs, 2″ thick, were used to form model chambers of variable dimensions such as to give isolated peaks from 250 to 1500 c.p.s. A high impedance sound source was used to minimize reaction of the standing wave which, as Eq. (5.20) shows, undergoes wide variations in impedance in the neighborhood of a normal frequency. A resonance peak width is measured between points on each side at which p^2 is one half the maximum peak value, and this width in c.p.s. is just twice k_N, the damping constant of Eq. (5.12).

Measuring a given mode with and without a wall covered with material makes it possible to determine the γ for the material since all other γ's in Eq. (5.12) are equal, and have the value for bare walls. Since the wave analyses reported here were not fully developed at that time, the results were interpreted along the lines of free wave propagation as discussed in Chapter VIII. Hunt computed $\alpha(\vartheta)$ from an equation similar to Eq. (8.5), on the assumption that the acoustic impedance was independent of angle of incidence and by fitting to an impedance measurement at one point. It was then found that values of $\alpha(\vartheta)$ measured for waves of various angles of incidence on the sample, by the peak width method, fitted this curve well with one exception; values for grazing incidence were not zero as predicted by

the free wave theory. This is now understood in terms of the analysis in the present chapter; in an enclosure, waves which "graze" a wall (one or two n's equal to zero) are somewhat damped by material on that wall.

Bhatt (B5) used a variation of the first method described above. He determined the equivalent of Δ for two or more modes having about the same frequency but different angles of incidence. As mentioned above, this does not always give a unique answer. But Bhatt showed that if a large number of "probable" values are determined by pairs of modes, and plotted against frequency and smoothed, the correct impedance curve can be inferred with reasonable certainty. Values measured in this way checked values obtained by the hyperbolic tangent method (Chapter IV) closely. Instead of measuring peak widths, he used two other methods for determining Δ: (a) decay rate measurement, and (b) pressure measurement, of individual normal modes. The decay method was fairly accurate, giving k_N to within a few percent. The measurement of peak pressure was much less accurate, and there were unexplained variations, related perhaps to minor changes in mounting conditions.

A start has been made on the application of the second method suggested above, that is measurement of the pressure distribution in space. A heavy walled chamber similar to that used by Bhatt, dimensions about $2'\times3'\times4'$, was fitted with a miniature microphone movable continuously in all directions by external controls. Pressure plots were obtained both with bare walls and with absorbing materials on different walls. The method of fitting these results to the curves in Fig. 22 was found to be straightforward and simple. An exploratory study was made of the problem of variation of impedance with angle of incidence, by using spaced porous felt materials. The impedance of this type of structure had been studied for normal incidence (B9) and is developed theoretically in Sec. 21 above. The difference between Eqs. (4.13) and (4.14) was strikingly demonstrated, i.e., a dependence of impedance on angle of incidence when waves could travel parallel to the material behind it and independence when the backing space was broken up with a cellular structure. This method should provide a useful tool for the study of new absorptive structures.

31. Phenomena at High Frequencies

Individual standing waves can be measured in small chambers at usual frequencies, or in larger rooms at very low frequencies. In conventionally sized rooms at "usual" frequencies (200 to 5000 c.p.s.) the resonance frequencies are so close together that a number of standing waves will be excited, by the source, with about equal amplitudes, so that no individual wave can be studied by itself. In this case it becomes quite difficult to work backward to find values of wall impedance from measurements of steady-state response of the room although it is possible to predict the behavior of the room when the wall impedances are known.

It is not possible to make any general statements about the room response when only a few standing waves are excited together. The pressure distribution must be obtained by detailed computation of Eq. (5.20). The room response is quite irregular in its dependence on frequency in this range, and the pressure distribution is still far from uniform. However when the natural frequencies are so closely spaced that a hundred or more different standing waves have frequencies within a half-breadth of the driving frequency, it is possible to study the room response by statistical means. By arguments similar to those used in deriving Eq. (5.22) we see that the statistical analysis may be used for ranges of driving frequency ν satisfying the following inequality

$$\nu > (50c^3/Vk_N)^{\frac{1}{2}}. \tag{5.24}$$

In this case there are enough standing waves resonating to make it possible to transform the summation in Eq. (5.20) into an integral. However, before the analysis of Chapter III can be used to effect this change, we must make certain approximations to simplify our calculations, and we must classify our standing waves into the oblique, tangential and axial waves discussed in the earlier chapter.

In the first place at these higher frequencies the wave number parameters μ are usually much larger than the attenuation parameters κ, so that Eq. (5.17) can be used for the normalizing

factor. This is a good approximation for the oblique waves (which comprise the majority of the waves) though it may not be valid for the tangential or the axial waves if one or more of the walls is soft. In the second place we can see that although the introduction of absorption has altered the resonance frequencies from the simple values used in Chapter III, nevertheless the average density of resonance frequencies at these higher frequencies is the same as that given by Eq. (3.5). Therefore the average number of the three different types of waves having resonance frequencies between ω and $\omega+d\omega$ is

$$\begin{aligned} dn_p &\simeq (V\omega^2/2\pi^2c^3)d\omega, && \text{oblique waves;} \\ dn_t &\simeq (L_yL_z\omega/2\pi c^2)d\omega, && y\text{–}z \text{ tangential waves;} \end{aligned} \tag{5.25}$$

and

$$dn_a \simeq (L_x/\pi c)d\omega, \qquad x \text{ axial waves,}$$

to the first approximation.

Therefore we can consider the quantity ω_N in Eq. (5.20) to be the magnitude of a vector in frequency space, which covers all the first octant in frequency space as the summation is carried out, and which has the "density" given in Eqs. (5.25). Instead of summing, we can then integrate over all directions and magnitudes in the first octant. First, however, we must find out how the damping constant k_N changes as a function of the frequency vector.

According to Eq. (5.12) the damping constants for a room with fairly hard walls depend on the magnitude of the vector ω_N, but are independent of the direction of ω_N (the relative magnitudes of n_x, n_y, and n_z) as long as the wave is an oblique one; that is, as long as the vector is not parallel to a wall or an edge. The x-y tangential waves, with vectors parallel[10] to the (x, y) plane, also all have the same value of damping constant, which is different from the value for the oblique waves, and so on. Even with one or more walls of the room soft, the majority of oblique waves usually have damping constants which are nearly equal. For instance when the wall at $x=L_x$ is moderately soft, Eq. (5.14) and Figs. 16 to 19 show that the value of Δ_2 for $n_x=0$ or 1 may differ markedly from the rest of the roots but that as n_x is increased the allowed values of Δ_2 rapidly approach the limiting value given by Eq. (5.11). In most cases of practical interest only the first two roots differ markedly from the limiting value, so that even here all the oblique waves, except those with vector ω_N most nearly parallel to the soft wall, have the same value of k_N. (One might call these exceptional oblique waves the "almost-tangential waves.")

[10] Actually the vector is not exactly parallel to the wall since for an absorbing room none of the three components of ω_N, $(\pi c/L_x)(\mu_x^2-\kappa_x^2)^{\frac{1}{2}}$, etc., is exactly zero. However for the purposes of our statistical discussion, we can refer to the vector ω_N for tangential waves as though it were parallel to the corresponding walls.

32. The Wall Coefficients

In view of the above discussion, we shall make one more change of notation in order to make our equations correspond as nearly as possible to the form of the Sabine equations. We shall define the *wall coefficients* (B12, H8) for the x-walls by the equation

$$\alpha_{n_xx1}+\alpha_{n_xx2}=(8\pi\mu_{n_x}\kappa_{n_x}/\eta_x),$$

with two other equations for the y and z wall coefficients. These quantities α play a role in wave acoustics similar to the absorption coefficients in geometrical acoustics. However they are *not* equal to the ratio between absorbed and incident energy, but are more nearly proportional to the ratio between absorbed and average energy in the room. In some cases the distribution of energy is far from uniform over the room, with the intensity at some walls larger than the average intensity; so that the wall coefficients may sometimes be larger than unity.

To each wall in a room, therefore, we can assign a set of coefficients α, which depend in general on the shape and size of the room, on the particular standing wave which is excited, on the acoustic impedance of the wall; and sometimes even on the impedance of the opposite wall. When the wall is hard ($|Z|/\eta$ larger than about ρc) and the frequency vector ω_N of the wave in question is not parallel to the wall ($n>0$), the coefficient has the value

$$\alpha_p=8\gamma=(8\rho c/|Z|)\cos\varphi, \tag{5.26}$$

where Z and φ are the acoustic impedance and phase angle for the wall in question. This quantity will be called the *normal coefficient.*

When the wall is hard and the frequency vector of the wave is parallel to the wall, the coefficient is

$$\alpha_s = (8\rho c G_2/|Z|)\cos(\varphi - \theta_2), \qquad (5.27)$$

where G_2 and θ_2 depend on the impedance of the wall opposite the one under consideration, their values being obtained from Figs. 20 and 21. This coefficient will be called the *supplementary coefficient*. When $(|Z|/\eta)$ is larger than about $4\rho c$, both α_s and α_t are approximately $\frac{1}{2}\alpha_p$.

When the wall is soft and the wave vector is parallel to it ($n=0$), the coefficient is

$$\alpha_t = 2\Delta/\eta, \qquad (5.28)$$

where the value of Δ is obtained from Fig. 16, the first sheet of the transformation. This will be called the *grazing* or *tangential coefficient*. The coefficient for $n=1$, where the frequency vector is nearly tangential, is $2\Delta/\eta$, with the value of Δ obtained from Fig. 17, the plot for the second sheet of the transformation. In most cases the coefficient for $n=2$, which can be obtained from Fig. 18, is almost equal to the normal coefficient given in Eq. (5.26); and in all but the most exceptional cases the coefficients for still higher values of n are quite accurately given by Eq. (5.26), or obtained from Fig. 13.

Therefore the damping constant (see Eqs. 4.1 and 5.10) for a particular standing wave is given by the formula

$$k_N = (ca_N/8V),$$
$$a_N = L_yL_z(\alpha_{x1}+\alpha_{x2}) + L_xL_z(\alpha_{y1}+\alpha_{y2}) + L_xL_y(\alpha_{z1}+\alpha_{z2}), \qquad (5.29)$$

where a_N is the *room absorption factor* for the wave specified by the trio of quantum numbers $N=(n_x, n_y, n_z)$. For a room with all its walls hard and when the wave is an oblique one, the α's are equal to the corresponding normal coefficients for each wall; when the wave is tangential or axial the coefficients for the walls perpendicular to the frequency vector are still the normal coefficients, those for the walls parallel to the frequency vector are equal to the corresponding grazing coefficients, which in this case are one-half the normal coefficients. When one wall of a pair is soft and when the frequency vector is parallel to this pair, the coefficient for the harder wall of the pair is the supplementary coefficient and that for the softer wall is the grazing coefficient, whose value in this case must be obtained from Fig. 16. For waves with frequency vectors almost parallel to this pair ($n=1$) the normal coefficient is used for the harder wall and the coefficient α_1, obtained from Fig. 17, is used for the softer wall. For waves with still smaller angles of incidence ($n>1$) in most cases the normal coefficients are used for both softer and harder walls. When both walls of a pair are soft, Eq. (5.3) must be solved to find μ and κ for the pair, and Eq. (5.26) used to find the sum of the coefficients, which in this case cannot be separated into two terms, each depending on one of the two walls separately.

Equation (5.29) is similar in form to the expression derived by Sabine (Eq. (4.1)) for the case of ergodic distribution. The difference lies in the fact that in the present case the coefficients not only depend on the nature of the walls, but also on the nature of the standing wave under consideration, and sometimes on the size and shape of the room. For the majority of the oblique waves the coefficients are the normal coefficients, which do not depend on the room size (though they may turn out to be larger than unity). The tangential and axial waves always have different values for some of the coefficients, and when one or more of the walls is soft, their grazing coefficients depend on the room size as well as on the wall impedance. If the wall is soft enough, the "almost tangential waves" also have special values of the coefficients.

33. Coherent and Incoherent Waves

Returning to our study of the room response, we can now say that the damping constants for the majority of the standing waves in the series of Eq. (5.20) are independent of the direction of the vector ω_N. In case the frequency of the source satisfies the inequality of Eq. (5.24) the summation may sometimes be replaced by an integration over all magnitudes of the vector ω_N, and over all directions inside the first octant of frequency space. When Eq. (5.21) is used, each term in the series has the product $\psi_N(-\omega; x_0, y_0, z_0)\psi_N(-\omega; x, y, z)$. When the hyperbolic cosines are expressed as exponentials

and the product multiplied out, there will be a sum of 64 different exponentials for each term in the series. One of these exponentials will be $\exp[(i/c)(\omega_N - ik_N)\cdot\mathbf{R}]$, where the direction of the vector $(\omega_N - ik_N)$ is determined by the ratio of the quantum numbers n_x, n_y, n_z, and $\mathbf{R}$ is the vector distance between the source (x_0, y_0, z_0) and the point P, (x, y, z). There are seven other exponentials of the same form, except that instead of the vector $(\omega_N - ik_N)$, its mirror image in one of the other seven octants of frequency space is used. Therefore instead of integrating the eight exponentials over the first octant, one of the exponentials can be integrated over all directions in frequency space. There are other exponentials in which the vector $\mathbf{R}$ is replaced by the vector distance between the point P and the mirror image of the source in one or more of the octants (mirror image of source in nearest walls).

When we attempt to integrate the eight exponentials first mentioned over all directions, we encounter a restriction on the size of the vector $\mathbf{R}$. The resonance denominator ensures that the integrand is only large when the magnitude of ω_N is between $\omega + k_N$ and $\omega - k_N$. As we sweep the vector ω_N over this important spherical shell in frequency space, it will not be possible to change from a summation over the allowed directions to an integration over all directions unless $\mathbf{R}$ is small enough so that $(1/c)\omega_N\cdot\mathbf{R}$ changes by an amount smaller than $(\pi/2)$ when we change ω_N from one allowed direction to a next nearest allowed direction. If we use Eqs. (5.25) and (5.29), this requirement can be reduced to the simple inequality

$$R < (a_p/64)^{\frac{1}{3}}, \tag{5.30}$$

where a_p is the value of a_N given in Eq. (5.29) when normal coefficients α_p are used for every wall. This usually means that the point P must be fairly close to the source in comparison to the size of the room, in order that integration be valid.

If R does satisfy the inequality of Eq. (5.30) the result of the integration of the eight exponentials is the simple expression

$$\psi_c = (Q_0/4\pi R)e^{(i\omega/c)(R-ct)}, \tag{5.31}$$

where we have utilized Eq. (5.25) for dn_p, as well as Eqs. (5.17) and (5.21). The expression on the right-hand side is the *velocity potential for radiation from a simple source in the open.* This part of the velocity potential can be called the *coherent part.* Unless the source is closer to a wall than the limit given in Eq. (5.30), none of the rest of the sixty-four exponentials can be arranged so that their sum changes to an integral. Therefore the remainder is an *incoherent part* with no definitely directed flow of energy or ordered wave motion, a quantity which will have to be studied by statistical methods later in this section.

If the source is near to one wall, the distance between the point P and the image of the source in this wall will be small enough to satisfy Eq. (5.30), so that another term must be added to the coherent part representing the reflection of the wave by the wall. This term is multiplied by a factor arising from the fact that energy is absorbed by the wall when reflection takes place. This extra term will be discussed in Sec. 53, where the coherent part will be dealt with by less fundamental but more straightforward methods.

As the point P moves away from the source, the coherent part of the sound diminishes in intensity, until when R equals the limit given in Eq. (5.30), it has the same average magnitude as the incoherent part. Beyond this limit there is still a coherent part, but it is quickly lost amid the incoherent part, and would be exceedingly difficult to measure experimentally (R1).

The incoherent part of the sound, when the frequency is high enough to satisfy Eq. (5.24), is distributed fairly uniformly throughout the room and is fairly isotropic, except near the walls. This does not mean, however, that the incoherent sound in a simple rectangular chamber is ergodic in distribution, for it is still possible to distinguish between oblique and tangential and axial waves. The difference is analogous to the difference between multiply periodic motion and ergodic motion in mechanics.

34. Mean-Square Pressure

In order to study the incoherent part, we must determine its mean square amplitude. Using Eqs. (5.17), (5.20), and (5.21), we find that the

general expression for the mean-square pressure at the point P owing to a point source at (x_0, y_0, z_0) is

$$(p^2)_{Av}=\frac{4c^4\rho^2\omega^2Q_0^2}{V^2}\left|\sum_N\left(\frac{1}{\epsilon_N}\right)\frac{\psi_N(-\omega;x_0,y_0,z_0)\psi_N(-\omega;x,y,z)}{\omega^2-(\omega_N-ik_N)^2}\right|^2. \tag{5.32}$$

In making reverberation chamber measurements there are two positions where the microphone and loudspeaker source are usually placed: either at a corner of the room, or on a rotating arm so that a space average is measured. For a corner of the room ψ_N is approximately unity (plus or minus), whereas the space average of ψ_N^2 is approximately ϵ_N. Therefore there are three special forms of Eq. (5.32) which will be useful to write down; one for the case where both source and microphone are at "average" positions in the room (far enough apart so that the coherent part is negligible); one for the case where one, either source or microphone, is in a corner of the room and the other is moved so that an average is measured; and the third for the case where one is at one corner and the other at one of the other corners of the room. In all three cases the terms involving two different values of N cancel out in the summation because of the orthogonality of the ψ's in the case of the space averages and the equal numbers of plus and minus signs in the case where source and microphone are at different corners; so that only the squared terms are summed. The results are

$$(p^2)_{Av}=\frac{c^4\rho^2\omega^2Q_0^2}{2V^2}\sum_N\frac{E_N}{(\omega^2-\omega_N^2+k_N^2)^2+4\omega_N^2k_N^2},$$

$$E_N=\begin{cases}1, \text{ (space average for both)}\\ (1/\epsilon_N), \text{ (average for one, other in corner)}\\ (1/\epsilon_N)^2, \text{ (both in corners)}\end{cases} \tag{5.33}$$

where ϵ_N is defined in Eq. (5.17).

This summation can be changed to an integration if the frequency of the source is large enough to satisfy Eq. (5.24). As indicated in Eq. (5.29) and the preceding discussion, in most cases the k's for all oblique waves in a given frequency band are equal since they are obtained by using all normal coefficients in the expression for a_N (the corresponding value of a_N will be called a_p). Similarly, the k's for the yz-tangential waves are all obtained by using grazing coefficients for the x-walls and normal coefficients for the other walls in the expression for a_N (which will be denoted by a_{tyz}). The damping constants for the other tangential waves and the axial waves can be obtained in an analogous manner, and the a_N's can be similarly denoted (for instance, a_{ax} involves grazing coefficients for the y and z walls and normal coefficients for the x walls, and is for the x-axial waves).

Referring to Eqs. (3.5)–(3.7), we see that when the summation is changed to an integration, it will be necessary to integrate $\omega_N^2d\omega_N$, $\omega_Nd\omega_N$, and $d\omega_N$ divided by the resonance denominator $[(\omega^2-\omega_N^2+k_N^2)^2+4\omega_N^2k_N^2]$, over ω_N from zero to infinity. When k_N is small compared to the driving frequency ω, approximate values of these integrals are $(\pi/4k_N)$, $(\pi/4\omega k_N)$, and $(\pi/4\omega^2k_N)$, respectively. When all the integration is performed and when the proper values of the k's, in terms of the a's discussed above, are written in, we obtain an approximate formula for the mean-square pressure of the incoherent sound.

$$(p^2)_{Av}=\frac{\rho^2\omega^2Q_0^2}{2\pi}\left[\frac{1}{a_p}\left(1-\frac{\pi Sc}{4V\omega}+\frac{\pi Lc^2}{8V\omega^2}\right)\right.$$
$$\left.+\sum_{xy}\frac{\pi L_xL_yc}{\omega Va_{txy}}\left(1-c\frac{L_x+L_y}{L_xL_y\omega}\right)+\sum_x\frac{2\pi L_xc^2}{\omega^2Va_{ax}}\right], \tag{5.34}$$

when both source and microphone are moved to obtain space averages. This is a rather complicated formula, but in many cases only the first term is important. This first term is the quantity which would be obtained by the simpler Sabine theory for a simple source in a room with walls having absorption coefficients equal to the normal coefficients given in Eq. (5.26). Therefore, most steady-state measurements in rectangular chambers give values of the *normal coefficients* of the walls, and *do not give values of the Sabine absorption coefficient.* In exceptional cases where one wall is much softer than the others, one of

the a's for tangential waves may be much smaller than a_0, and therefore one of the terms in the summation over (xy) may be larger than the first term in Eq. (5.34). In this case the quantity measured by the steady-state technique would correspond more nearly to the grazing coefficient for the soft wall than it would to the normal coefficient. This corresponds to the well-known fact that placing all the absorbing material on one wall of a rectangular room is not the most efficient arrangement of material, since there are some tangential and axial waves which move parallel to the material and are not readily absorbed.

When either source or microphone is in a corner of the room and the other is moved about to obtain a space average, then the quantity in the first parenthesis in Eq. (5.34) is multiplied by 8, the terms in the second parenthesis are multiplied by 4 and the last term by 2; whereas if both microphone and source are in corners, the extra factors are 64, 16, and 4 respectively.

35. An Approximate Formula

When none of the walls is especially soft (to be more precise, when the smallest of the a's for tangential waves is larger than a_p divided by the longest dimension of the room measured in half-wave-lengths), a somewhat simpler expression can be used instead of the one given in Eq. (5.34). Using the definitions of S and L given in Eq. (3.4), and recalling that $\eta_x=(2L_x/\lambda)$, etc., we can write the approximate equation

$$(p^2)_{\text{Av}}\simeq\frac{\rho^2\omega^2Q_0^2}{2\pi a_p}\left(1-\frac{1}{2\eta_x}+\frac{a_p}{\eta_x a_{tyz}}\right)\times\left(1-\frac{1}{2\eta_y}+\frac{a_p}{\eta_y a_{txz}}\right)\left(1-\frac{1}{2\eta_z}+\frac{a_p}{\eta_z a_{txy}}\right), \quad (5.35)$$

which is valid to the second order in the quantities $(a_p/\eta_x a_{tyz})$ etc.

However, $(\rho\omega^2Q_0^2/8\pi c)$ is the total power radiated from a simple source of strength Q_0, so that Eq. (5.35) can be generalized for any source of reasonably small dimensions (not considerably larger than a wave-length). If the source is emitting sound energy at a rate of Π ergs per second, then an approximate formula for the mean-square incoherent pressure in the rectangular room (with space average for both source and microphone) is

$$(p^2)_{\text{Av}}\simeq\left(\frac{4\rho c}{a_p}\Pi\right)B_xB_yB_z,$$

$$B_x=\left[1-\frac{1}{2\eta_x}+\frac{a_p}{\eta_x a_{tyz}}\right], \quad (5.36)$$

with similar equations for B_y and B_z. The factor in parentheses is the quantity obtained by the simple Sabine theory with normal coefficients for every wall; the correction factors B arise from the fact that sound in a rectangular room with uniform walls does not produce an ergodic sound distribution.

When either source or microphone is in a room corner and the other is moved about, the factor B_x equals $[2-(1/\eta_x)+(a_p/\eta_x a_{tyz})]$, etc. When both source and microphone are at corners, the factor B_x has the value $[4-(2/\eta_x)+(a_p/\eta_x a_{tyz})]$, with similar modifications for B_y and B_z.

When one of the walls (wall $x2$, for instance) is soft enough so that the "almost tangential" waves have a coefficient α_1 which is not equal to α_p, the expression for B_x is modified and becomes

$$B_x=1-\frac{3}{2\eta_x}+\frac{a_p}{\eta_x a_{1yz}}+\frac{a_p}{\eta_x a_{tyz}}, \quad (5.37)$$

where a_{1yz} is the value of a obtained when the "almost tangential" coefficient α_1 for the soft wall is used for κ_{x2} in Eq. (5.29). The further modifications for corner placing of source or microphone, or both, are that the first three terms are multiplied by 2 or 4, and the last term is unmodified.

Equation (5.36) indicates that the *Sabine absorption coefficient cannot be measured* by steady-state measurements in a simple rectangular chamber. If the chamber is large (η's large) or the frequency high and if none of the walls is particularly soft, the quantity which is measured is nearly equal to the *normal coefficient* which, we shall see later, is not exactly equal to the Sabine coefficient (and may sometimes differ from it widely). Otherwise an analysis of the measure-

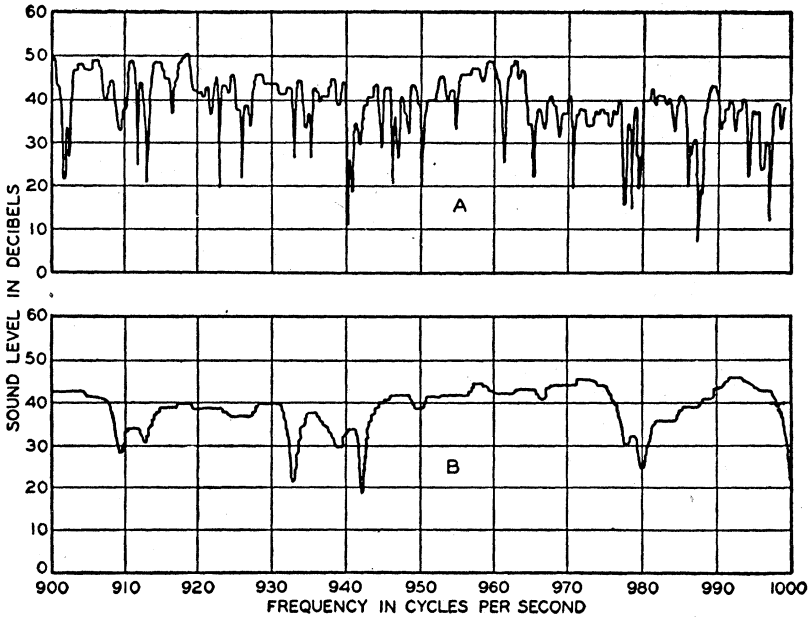

FIG. 23. Steady-state response characteristics of a room. Curve *A*, room live; curve *B*, room damped. From reference W8.

ments is further complicated by the fact that the B's are not equal to unity, and the quantity measured is a weighted average of normal coefficient and grazing coefficient, the weighting factors depending on the ratio between room size and wave-length.

36. Measurements of Steady-State Sound

Experimental studies of steady-state sound in rooms have not kept step with measurements involving the transient state. This is partly because music and speech sounds are predominantly transient in character, so it is natural to associate the hearing quality of a room with the properties of sound *decay*. Another reason is that Sabine and other pioneers, who lacked modern electronic techniques, recognized that the time of reverberation was something that could be observed by the ear, whereas it would be impossible for the ear to judge relative intensities of steady-state tones with sufficient accuracy to give significant absorption measurements. With the advent of modern instruments, however, this limitation has been overcome.

Some of the steady-state investigations to which we referred earlier in this report will be described a little more fully here. Wente (W8) in 1935 studied the transmission characteristics of rooms with a high speed level recorder. The loudspeaker was fed by an oscillator which was changed very slowly in frequency. The signal picked up at some other point in the room was thus indicative of the steady-state transmission properties of the room. This method is commonly used in studying electrical transmission systems. Figure 23 shows two of Wente's records; the upper one is for a live room, and the lower one for the same room (about 10,000 cubic feet in volume) with absorbing material added. In the damped room the resonance peaks are markedly broadened, as discussed in connection with Eq. (5.20), and the curve is consequently smoother. Wente carried this a step further and showed empirically that a simple functional relation existed between the "transmission irregularity" and the total amount of absorption in the room. Wente's work led to the investigations of Hunt (H7) and Bhatt (B5) discussed in the previous section.

Steady-state measurements were utilized by Knudsen (K4) in developing the "intensity method" for obtaining absorption coefficients.

In this case an averaging over a large number of standing waves is desired, and precautions are taken to eliminate individual resonances. The basic equation for this method, as given by the approximate Sabine theory, is

$$a \simeq \frac{4\rho c \Pi}{(p^2)_{Av}}, \quad \text{(see Eq. (5.36))},$$

where $a = \sum \alpha S$ is the total absorption at the walls of the room, and p is the sound pressure; $(p^2)_{Av}$ is proportional to the average intensity in the room. According to this equation the total absorption is inversely proportional to the steady-state intensity. If the absorption of the bare chamber walls is first evaluated by introducing a "standard" absorbent with a known coefficient, then the coefficient of any material may be measured by a straightforward comparison of steady-state intensities. This method has the advantage over reverberation methods that a moderate background noise is not a disturbing effect since all measurements can be made at high intensities. Decay measurements, on the other hand, must be carried on in very quiet surroundings which are not always easy to obtain.

Unfortunately, there are not sufficient data at present to make a very thorough correlation of the intensity method with the wave theory treatment outlined above. Only two materials were reported and impedance values for these are not available. However, if certain reasonable assumptions are made, it is possible to calculate the correction terms in the simplified Eq. (5.36) for the cases measured by Knudsen (K4). This calculation indicates that the difference between the geometrical theory and the wave theory is experimentally negligible for these cases, at least insofar as the correct *relative* values of absorbing coefficients are concerned. For a plaster of $\alpha = 0.083$ covering all surfaces in a room $18 \times 18 \times 16$ ft. high, the product of the correction factors $B_x B_y B_z$ in Eq. (5.36) is about 1.14. This means that the actual absorption is somewhat greater than the value inferred from the intensity measurement and the simple formula. However, the correction factors have almost the same values for the bare walls ($\alpha = 0.014$) as for the plastered walls, so that the *ratio* of absorption with and without the plaster is changed by less than 0.5 percent by the wave theory modifications. Nevertheless, the wave theory does bring out one new point of importance in this case: that the quantity which is actually measured is the normal coefficient and not the statistical coefficient. The good agreement with reverberation measurements is due to the fact that the reverberation method also gives normal coefficients for frequencies lower than about 500 c.p.s. The adequacy of the geometrical theory in giving the correct *relative* absorption in this instance is owing to the low value of α and to the completely uniform coverage of all surfaces. Most acoustic materials of interest are more absorptive than the plaster discussed, and it is usual to cover only one surface or a portion of one. In many such cases Eq. (5.36) would be significantly different from the simpler form.

VI. TRANSIENT SOUND IN RECTANGULAR ROOMS

The transient characteristics of the rectangular room are obtained from the steady-state characteristics by using the operational calculus. From Eqs. (5.20) and (5.17) we obtain an expression for the steady-state velocity potential at the point (x, y, z) in the room due to a simple source of unit strength and frequency $(+\omega)$ at (x_0, y_0, z_0):

$$\Psi_s(\omega) = -c^2 \sum_N \frac{1/\Lambda_N}{\omega^2 - \xi_N^2(\omega)} \psi_N(\omega; x, y, z) \times \psi_N(\omega; x_0, y_0, z_0) e^{i\omega t}, \quad (6.1)$$

where ψ_N is the characteristic function and ξ_N the characteristic value (see (Eq. 5.9)) corresponding to the Nth standing wave for the driving frequency $(+\omega)$. Their behavior has been discussed in the previous section. According to our convention

$$\xi_N(\omega) = \omega_N + ik_N, \quad \xi_N(-\omega) = \omega_N - ik_N.$$

37. The Operational Calculus

As we have seen in the previous section, close to the source the coherent wave preponderates, and from Eq. (5.31) the approximate formula

for the steady-state wave,

$$\Psi_s(\omega)\simeq\Psi_c(\omega)=(1/4\omega R)e^{i\omega[t-(R/c)]}, \quad (6.2)$$

holds for distances R from the source smaller than the limit given in Eq. (5.30). Outside this limit the incoherent wave is largest, and the full series of Eq. (6.1) must be used.

The operational calculus enables one to obtain expressions for the general transient phenomena of a system in terms of the *indicial admittance*, the transient response of the system to a single pulse driving force. In the present case it can be shown that the response of the room to a source at (x_0, y_0, z_0) having zero strength for $t<0$ and unit strength for $t>0$, can be given by the contour integral

$$A(t)=U(t)\Psi_s(0)$$
$$+(1/2\pi i)\int_{-\infty}^{\infty}[\Psi_s(\omega)-\Psi_s(0)](d\omega/\omega), \quad (6.3)$$
$$(\text{for } q=U(t))$$

where $U(t)$ is the Heaviside "unity function"

$$U(t)=\begin{cases}0 & t<0\\ 1 & t>0\end{cases}, \quad (6.4)$$

and the contour for the integration lies just below the real axis. The function $\Psi_s(0)$ is the velocity potential for a room with unit source of zero frequency. At zero frequency most walls have an infinite impedance, so that the corresponding characteristic values and functions have quite simple forms.

The presence of $\Psi_s(0)$ in the integrand of Eq. (6.3) removes the pole at $\omega=0$; the other poles are due to the resonance denominators of the terms in the series. There are two such poles for each term, one at $\omega=\xi_N(\omega_N+ik_N)$ and the other at $\omega=-\xi_N(-\omega_N+ik_N)$. These values of ω are the self-consistent solutions of Eq. (5.9) obtained by inserting the solution, instead of ω, back into the boundary conditions determining the χ's. In other words ξ_N must have such a value that when the quantities $(\xi_N L_x/\pi c)$ etc., are used instead of the quantities η_x etc., in Eqs. (5.4) to determine the χ's, then Eq. (5.9) will result in this same value of ξ_N. The real part of this self-consistent solution (for the positive case) is called the Nth *natural frequency* of the room and will de denoted as ω_{ON}; the imaginary part will be called the *natural damping constant*, and will be denoted as k_{ON}. We note that these quantities, for the transient decay of sound, are *not* the same as the resonance frequency $\omega_N(\omega_N)$ and damping constant $k_N(\omega_N)$ for the steady-state response. In certain special cases this difference turns out to be large enough to be apparent experimentally (K5).

With this notation, the two poles for the Nth term in the series are at $\omega_{ON}+ik_{ON}$ and $-\omega_{ON}+ik_{ON}$, and by evaluating the residues for each term, the indicial admittance for positive values of t can be shown to be

$$A(t)=U(t)\Psi_s(0)-c^2\sum_N\frac{1}{\omega_{ON}^2+k_{ON}^2}$$
$$\times W_N\exp(-k_{ON}t)\cos(\omega_{ON}t+\Gamma_N-2\Phi_N), \quad (6.6)$$

where

$$\xi_N(\omega_N+ik_N)=\omega_{ON}+ik_{ON}$$
$$=(\omega_{ON}^2+k_{ON}^2)^{\frac{1}{2}}\exp(i\Phi_N);$$
$$(1/\Lambda_N)\psi_N(\omega_{ON}+ik_{ON};x_0,y_0,z_0)$$
$$\times\psi_N(\omega_{ON}+ik_{ON};x,y,z)=W_n\exp(i\Gamma_N).$$

This general form is useful in studying the incoherent part of the wave. For the coherent part, the indicial admittance has the simple form

$$A_c(t)=(1/4\pi R)\,U[t-(R/c)]. \quad (6.7)$$

The velocity potential in the room at time t, due to a source of strength $q(t)\cdot U(t)$ at the point (x_0, y_0, z_0) is then

$$\Psi=A(t)q(0)+\int_0^t A(t-\lambda)q'(\lambda)d\lambda \quad (6.8)$$
$$(\text{for source } q(t)\,U(t)),$$

where $q'(t)=(d/dt)q(t)$. This formula is a general one, and from it we can obtain both the transient and steady-state behavior of the room. The pressure can be obtained from this by using the formula $p=\rho(\partial\Psi/\partial t)$.

If the source is a simple harmonic one, which has been turned on for an indefinitely long time, the corresponding response can be obtained from Eq. (6.7) by changing the zero of time back into the past. The response is then by definition the

steady-state response of the room, so that

$$\psi_s(\omega)=\int_{-\infty}^{t} A(t-\lambda)q'(\lambda)d\lambda \qquad (6.9)$$

(when $dq/dt=i\omega q$).

If the source had been started a long time before, and was stopped at $t=0$, the resulting velocity potential after the source is stopped can be obtained by subtracting Eq. (6.8) from (6.9):

$$\psi=\int_{0}^{\infty}[A(t+\lambda)q'(-\lambda)]d\lambda-[q(0)\cdot A(t)] \qquad (6.10)$$

(for source $q(t)[1-U(t)]$).

38. Pulse Wave

Before we discuss such problems, however, let us first study the transient velocity potential due to an explosive pulse

$$q_p=\lim_{\Delta t\to 0}\{(B/\Delta t)[U(t+\Delta t)-U(t)]\}, \qquad (6.11)$$

where a volume B of air is sent out from the source in a time Δt. We see from Eq. (6.7) that the coherent part of the wave is an outgoing spherical pulse

$$\Psi_{cp}=\lim_{\Delta t\to 0}\left\{(B/4\pi R\Delta t)\left[U\left(t+\Delta t-\frac{R}{c}\right)-U\left(t-\frac{R}{c}\right)\right]\right\}, \qquad (6.12)$$

which reaches point P a time (R/c) after the pulse originated at the source. This equation neglects the part of the coherent wave which has been reflected from the walls. With as sharp a pulse as this, the coherent wave will be apparent after several reflections. From physical considerations one would expect in this case to find some successive pulses of the coherent wave to be distinguishable above the background of the incoherent wave.

Maa has discussed the pulse wave for the one-dimensional case (M3). Here the sound waves are all plane waves, the natural frequencies are all harmonic (if the walls are hard), and the wave *stays coherent*. Consequently the exact solution is a sequence of pulses of form similar to Eq. (6.12), emanating from the sequence of images of the source plane in the two parallel walls, and the series solution is exactly equal to this sequence of pulses. Maa uses this solution to illustrate some of the properties of flutter echoes. The correspondence with actual flutter echoes is only approximate since most impulsive sound sources are more nearly points rather than planes and since it is rare that only two walls reflect the sound and the effect of the other four walls can be completely neglected. The formulas given in the present section would be better approximations, but their considerably greater complexity renders them less amenable for demonstrating the properties of flutter echoes.

The incoherent part must be obtained from the full series of Eq. (6.6), and it turns out to be

$$\Psi_p=c^2B\sum_N(\omega_{ON}^2+k_{ON}^2)^{-\frac{1}{2}}\times W_N\exp(-k_{ON}t)\sin(\omega_{ON}t+\Gamma_N-\Phi_N). \qquad (6.13)$$

The mean-square pressure corresponding to this velocity potential is

$$(p_p^2)_{Av}=\sum_N\frac{\rho^2c^4B^2}{2|\Lambda_N|^2}|\psi_N(\omega_{ON}+ik_{ON};x_0,y_0,z_0)\times\psi_N(\omega_{ON}+ik_{ON};x,y,z)|^2\exp(-2k_{ON}t). \qquad (6.14)$$

All frequencies are equally important in the incoherent wave due to an explosive pulse. A decay curve[11] of the mean-square pressure will not be a straight line, as would be the decay curve of a simple damped oscillator, but will be decidedly curved. The initial slope will be quite large, corresponding to the strongly damped, high frequency waves; and the final slope corresponding to the most slowly damped waves, usually the lowest frequency axial waves between the hardest wall-pair.

Individual experimental decay curves taken for this case, moreover, would not give the smooth curve predicted by Eq. (6.14), because of the pulse-like nature of the coherent part of the transient. The pulse is quite sharp and high before its first reflection, and though it will broaden and reduce in height at each reflection

[11] The term *decay curve* in this paper always denotes a curve of the logarithm of the mean-square pressure as a function of time in seconds. When plotted it is often expressed in decibels (ten times the logarithm to the base ten).

(especially if the wall is soft, as we shall see in Section 53) the irregularities due to its presence will be noticeable in the curve for some time after $t=0$. As a matter of fact, nothing will be heard at point P until a time $t=(R/c)$, when the first pulse arrives; and subsequently the coherent pulses diminish in importance compared to the smooth incoherent decay.

39. Reverberation

In measurements of room reverberation, however, curves are not measured for such a discontinuous sound. Usually the source emits a single frequency note, or else a warble note with a band of frequencies, for a long enough time so that a steady-state condition is reached; then the source is shut off. We shall first study the case for a simple harmonic source; if a warble tone is used, the answer can be computed by superposing the results for single frequencies. Using Eqs. (6.10) and (6.6) we can perform all the integrations and obtain for the transient velocity potential at point P at a time t $(t>0)$, due to a source $Q\sin(\omega t-\varphi)[1-U(t)]$ at point (x_0, y_0, z_0):

$$\Psi=-c^2Q\sin\varphi\sum_N\frac{W_N\exp(-k_{ON}t)}{\omega_{ON}^2+k_{ON}^2}\cos(\omega_{ON}t+\Gamma_N-2\Phi_N)$$

$$-\tfrac{1}{2}c^2\omega Q\sum_N\frac{W_N\exp(-k_{ON}t)}{\omega_{ON}^2+k_{ON}^2}\left\{\frac{\sin(\omega_{ON}t+\Gamma_N-2\Phi_N-\varphi-\Omega_{N-})}{[(\omega_{ON}-\omega)^2+k_{ON}^2]^{\frac{1}{2}}}+\frac{\sin(\omega_{ON}t+\Gamma_N-2\Phi_N+\varphi-\Omega_{N+})}{[(\omega_{ON}+\omega)^2+k_{ON}^2]^{\frac{1}{2}}}\right\},\quad(6.15)$$

where the phase angles Γ_N and Φ_N are defined in Eq. (6.6) and where we have set

$$(\omega_{ON}\pm\omega)+ik_{ON}=[(\omega_{ON}\pm\omega)^2+k_{ON}^2]^{\frac{1}{2}}\exp(i\Omega_{N\pm}).$$

The pressure corresponding to this velocity potential is then

$$p=+\rho c^2Q\sin\varphi\sum_N W_N(\omega_{ON}^2+k_{ON}^2)^{-\frac{1}{2}}\exp(-k_{ON}t)\sin(\omega_{ON}t+\Gamma_N-\Phi_N)$$

$$-\tfrac{1}{2}\rho c^2\omega Q\sum_N\frac{W_N\exp(-k_{ON}t)}{(\omega_{ON}^2+k_{ON}^2)^{\frac{1}{2}}}\left\{\frac{\cos(\omega_{ON}t+\Gamma_N-\Phi_N-\varphi-\Omega_{N-})}{[(\omega_{ON}-\omega)^2+k_{ON}^2]^{\frac{1}{2}}}+\frac{\cos(\omega_{ON}t+\Gamma_N-\Phi_N+\varphi-\Omega_{N+})}{[(\omega_{ON}+\omega)^2+k_{ON}^2]^{\frac{1}{2}}}\right\}.\quad(6.16)$$

The first series in this expression represents the pressure pulse set up by the sudden cessation of the source (which we might call the cut-off pulse). The size of this cut-off pulse depends on the phase φ of the source at the instant it is shut off. The origin of the pulse is more clearly shown in the expression for the coherent part of the wave. If we use Eqs. (6.7) and (6.10), the velocity potential for the coherent part is found to be

$$\Psi_c\simeq(Q/4\pi R)\cdot\sin\left[\omega\left(\frac{R}{c}-t\right)+\varphi\right]\cdot U\left(\frac{R}{c}-t\right).\quad(6.17)$$

The coherent part of the pressure is proportional to the time derivative of this. It is unaffected by the cessation of the source until a time $t=(R/c)$, after which it drops to zero. However, unless $\varphi=0$ or π there is a discontinuity in Ψ_c, which gives rise to a sharp pulse in the pressure just before it drops to zero. The pulse is present unless the loudspeaker source is stopped at an instant when the diaphragm velocity is zero (i.e., unless $\varphi=0$ or π). The nature of the pulse is indicated by the fact that the first series in Eq. (6.16) for the pressure is proportional to the series in Eq. (6.13) for the velocity potential for an explosive pulse. The pressure pulse from an explosion is a double one, a condensation followed by a rarefaction; whereas the pressure pulse caused by stopping the source is a single one, either just condensation or just rarefaction, depending on the value of the phase angle φ.

Of course in actual practice the source does not stop instantaneously. Unless $\varphi=0$ or π the diaphragm will have its transient motion before it comes to rest. If the loudspeaker is highly damped, the effect will be almost the same as if it came to rest instantaneously, and the cut-off

pulse will be a single one, though it will be broader and not so high as the one represented by the first series in Eq. (6.16). If the loudspeaker damping is not large, its transient will involve several oscillations at its own natural frequency, which will not usually be the same as the driving frequency. The series for the cut-off pulse for this case can be computed by the methods outlined above, once the transient motion of the loudspeaker is known, and it can be substituted in Eq. (6.16) instead of the first series. It will emphasize those natural frequencies of the room near the natural frequency of the speaker, whereas the second series in Eq. (6.16) emphasizes those near the driving frequency.

40. Details of the Decay Curve

It is now possible to make a few general remarks about the transient behavior of the sound at point P after a simple harmonic source at (x_0, y_0, z_0) has been shut off at $t=0$. At first there is little change from the steady-state condition, but at $t=(R/c)$ there is a pulse, the first arrival of the cut-off pulse, whose size depends on the phase at which the source was stopped and whose shape depends on the transient characteristics of the loudspeaker. After this the sound decays, each standing wave having its own natural frequency and decay rate. Several reflections of the pulse from the walls of the room may be apparent, producing characteristic irregularities in the individual decay curve. To obtain a smooth decay curve, it would be necessary to stop the source at an instant when its velocity is zero, or else to obtain an average curve from a number of decays involving different values of the phase φ. The resulting, smoother curve then corresponds to the second series in Eq. (6.16).

This question of source cut-off has been given some experimental consideration by Hunt (H6) and others. The automatic reverberation equipment of Hunt (see Sec. 8) incorporates a means for stopping the source always at the same phase of the frequency variation cycle of the warble tone. This could be carried a step further to cut off at a particular phase of the driving frequency. But it appears to be much simpler experimentally to allow random cut off and obtain an average curve from a large number of decays. In addition, detailed variations in decay are smoothed out by the timing method used by Hunt, so it is likely that variations due to the cut off pulse would also be smoothed out.

On the other hand, the fluctuating nature of sound decay is very evident from inspection of oscillograms or high speed level records. The detailed correlation of these fluctuations with physical properties of the room and source is a complicated problem, and one on which there remains much work to be done. Some study has been given to the problem by Jones (J3), who has studied the effect of the average decay rate on the magnitude of the fluctuations; and Watson (W3) has investigated fluctuations experimentally by means of a recording system which compensates for the exponential decay.

At low frequencies, corresponding to the requirement of Eq. (5.22), the natural frequencies ω_{ON} are spaced far enough apart so that usually a single term of the second series is much larger than all the rest (the one for which $(\omega_{ON}-\omega)$ is nearly zero). A single standing wave has been excited, and the average decay curve will be a straight line, with a slope corresponding to the wave's natural damping constant. (Note that even in this case the cut-off pulse will appear in the individual decay curves). In cases where the frequency is somewhat larger than that required by Eq. (5.22), or where two characteristic functions have natural frequencies closer than the average spacing, two standing waves may be excited strongly. As long as the source is radiating sound, these waves have the same frequency as the source, as is indicated by the steady-state solution of Eq. (5.20). When the source is turned off, however, the standing waves each oscillate with their own natural frequency; and if these differ somewhat, the decay curve will exhibit irregularities (K5) due to the resulting beat note, in addition to the irregularities due to the cut-off pulse. The exact nature of the best irregularities will depend on the relative amount of excitation of the two waves and on the phase angle of the source at the instant it was stopped, as can be seen from examination of Eq. (6.16).

Some of these effects have been strikingly demonstrated by Knudsen (K3, K5); a typical result is shown in Fig. 24. These are oscillograms

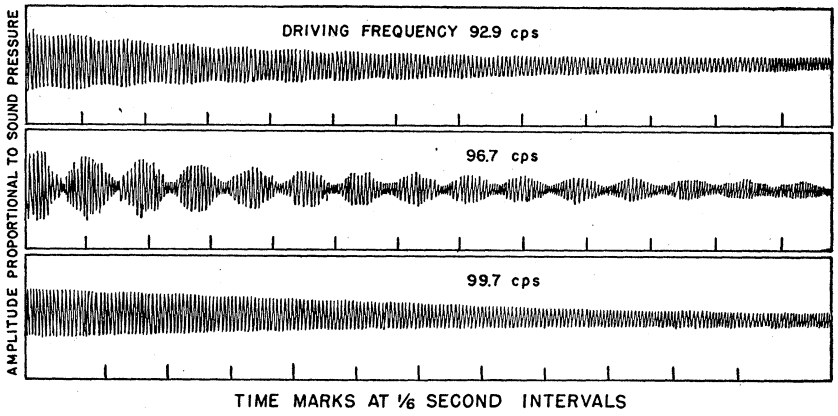

FIG. 24. Oscillograms illustrating beats in sound decay for different driving frequencies. Top and bottom curves are for driving frequency equal to a resonance frequency of the room, so only one mode is strongly excited. Middle curve is for an intermediate driving frequency, with two modes equally excited, showing the beats between the two natural frequencies as they damp out. Redrawn from reference K5.

of sound decay in a rectangular room $8' \times 8' \times 9.5'$. Each decay was obtained with a different driving frequency, the value of which is recorded on the curve. There are theoretical normal frequencies at 92.8 and 99.8 c.p.s. and no others closer than 70.3 and 115.9 c.p.s. It is seen that driving frequencies of 92.9 and 99.7 produce almost pure (exponential) decay curves; whereas an impressed frequency of 96.7, which lies about half way between, produces strong beats of about 7 c.p.s. as expected. At other driving frequencies, the two components are excited in varying amounts, yielding various degrees of cancellation in the beats. But all impressed frequencies in the range shown produce 7 c.p.s. beats (if any), which convincingly demonstrates that only the two normal frequencies noted partake in the decay of sound energy. At a frequency of 118 c.p.s. in this same room, Knudsen observed the coexistence of beats at 3.3 and 19.3 c.p.s. arising from simultaneous excitation of three normal frequencies 99.8, 116, and 119.2 c.p.s. At somewhat higher frequencies, when several waves are excited, the transient behavior of the room becomes still more complicated.

41. Approximate Formula for Decay Curve

When a large number of waves are excited, however, it becomes possible to analyze the reverberation by statistical methods analogous to those used in the previous section. This occurs for frequencies high enough to satisfy Eq. (5.24), or else for warble notes of band width $\Delta\nu$ and average frequency ν such that $\Delta\nu > (50c^3/V\nu^2)$. If we leave aside the series for the cut-off pulse, the second term in Eq. (6.16) can be used to obtain the mean-square incoherent pressure. By methods analogous to those used in obtaining Eq. (5.33) the results prove to be

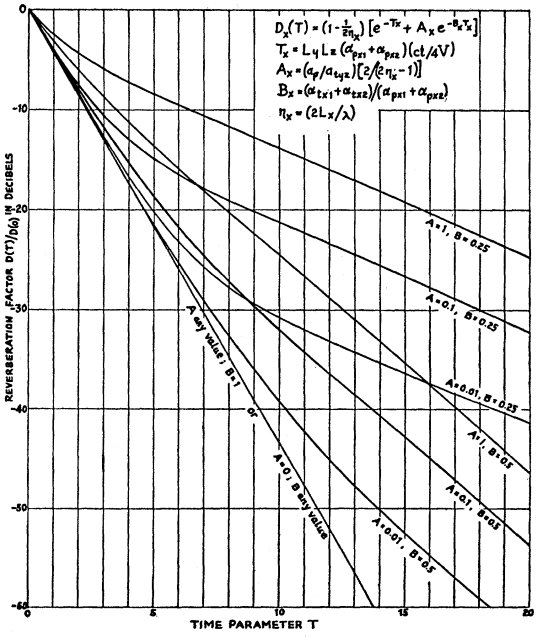

FIG. 25. Approximate decay factors for rectangular room.

$$(p^2)_{Av}=\frac{c^4\rho^2\omega^2Q^2}{8V^2}\sum_N\frac{E_N\exp(-2k_{ON}t)}{\omega_{ON}^2+k_{ON}^2}\left\{\frac{1}{(\omega_{ON}-\omega)^2+k_{ON}^2}+\frac{1}{(\omega_{ON}+\omega)^2+k_{ON}^2}\right\}, \tag{6.18}$$

and this can then be added over all oblique, tangential, and axial waves to obtain a formula corresponding to Eq. (5.34):

$$(p^2)_{Av}=\frac{\rho^2\omega^2Q^2}{2\pi}\left\{[\exp(-a_pct/4V)]\left(\frac{1}{a_p}\right)\left(1-\frac{\pi Sc}{4V\omega}+\frac{\pi Lc^2}{8V\omega^2}\right)\right.$$

$$\left.+\sum_{xy}[\exp(-a_{txy}ct/4V)]\left(\frac{\pi L_xL_yc}{\omega Va_{txy}}\right)\left(1-c\frac{L_x+L_y}{\omega L_xL_y}\right)+\sum_x[\exp(-a_{ax}ct/4V)]\left(\frac{2\pi L_xc^2}{\omega^2Va_{ax}}\right)\right\}, \tag{6.19}$$

where we have taken space averages for both source and microphone.

Finally when none of the walls is particularly soft, and if all the η's are larger than about 3, an approximate equation can be obtained analogous to Eq. (5.36):

$$(p^2)_{Av}\simeq(4\rho c\Pi/a_p)D_x(t)\cdot D_y(t)\cdot D_z(t),$$

$$D_x(t)=\left\{\left(1-\frac{1}{2\eta_x}\right)\exp[-L_yL_z(\alpha_{px1}+\alpha_{px2})ct/4V]+\left(\frac{a_pv}{\eta_xa_{tyz}}\right)\exp[-L_yL_z(\alpha_{tx1}+\alpha_{tx2})ct/4V]\right\}, \tag{6.20}$$

where α_{px1} is the *normal coefficient* for the $x1$ wall, α_{tx1} is the grazing coefficient for the same wall, and so on. The quantity v is unity if both source and microphone are moved about, $\frac{1}{2}$ when the source or microphone is moved about and the other is in a corner of the room, and $\frac{1}{4}$ when both are in different corners. Plots of decay curves corresponding to this formula are shown in Fig. 25.

A logarithmic plot of $(p^2)_{Av}$ is the decay curve. We see that to the approximation represented by the last equation, the decay curve is a sum of three curves, one for each wall-pair. Each individual curve starts with a slope corresponding to the normal coefficients for both walls of the pair, and ends with a slope corresponding to the grazing coefficients. The "break" in the curve, where the slope changes from initial to final value, comes at a time when both terms in D are equal, i.e., when

$$t_{bx}=(4L_x/c)(\alpha_{px1}+\alpha_{px2}-\alpha_{tx1}-\alpha t_{x2})^{-1}\times\ln[(a_{tyz}/va_p)(\eta_x-\tfrac{1}{2})]. \tag{6.21}$$

In general this time is long when the normal coefficients α_p are small and do not differ greatly from the grazing coefficients, and is short when one or both of the normal coefficients is large. The logarithmic curve for the D corresponding to the softest wall-pair therefore usually has its "break" sooner than the other two curves, and also has the largest slope of the three curves. In fact when only one wall of a rectangular room is soft (as in a reverberation chamber), the component of the decay curve which is due to the soft wall lowers the level of the decay curve so rapidly that the "breaks" in the components due to the harder pairs usually come at a level below the limits of measurement. In such cases only the normal coefficients for the harder walls can be measured, and the only break apparent in the measured decay curve is the one for the softest wall pair.

Suppose that the only soft wall is perpendicular to the x axis, and suppose that the frequency is large enough so that $\eta_x=(2L_x/\lambda)$ is larger than ten. In this case, by inserting Eq. (6.21) in Eq. (6.20), we can see that the first break in the decay curve for the room will occur at a level approximately

$$(10a_p/L_yL_z)(\alpha_{px1}+\alpha_{px2}-\alpha_{tx1}-\alpha_{tx2})^{-\frac{1}{2}}\times\log_{10}(\eta_xa_{tyz}/va_p)\ \text{db}$$

below the level for $t=0$. This break occurs at a time given by Eq. (6.21).

To recapitulate: the individual decay curve measured for high frequencies ($\nu>(400c^2/a_p)^{\frac{1}{3}}$) in a reverberation chamber with one soft wall will be more or less irregular because of the cut-off

pulse, and will not begin to drop until this pulse first reaches the microphone from the source. An average curve, made from a series of curves for different cut-off phases, will drop fairly smoothly after the first arrival of the pulse. Its initial slope will depend on the normal coefficients of the walls; it will usually have only one "break" during its measurable extent, and its slope after the break will correspond to the grazing coefficient for the soft wall, the complimentary coefficient for the opposite wall, and the normal coefficients for the other four walls. If the difference between grazing and normal coefficients for the soft wall is a large one, the break may be very near the beginning of the curve, and it may be hard to distinguish the initial steep slope from the first arrival of the cut-off pulse. In this case the majority of the decay curve depends on the waves which are parallel to the soft wall, which are less quickly damped but more strongly excited than the oblique waves.

On the other hand, as we shall see in the next chapter, any presence of irregularities in the shape of the walls or the distribution of absorbing material, or any use of diffusing vanes in the room, will tend to make the normal and grazing coefficients approach each other in value. Since it will turn out that the grazing coefficients increase more rapidly than the normal coefficients decrease, as irregularities are introduced, it is quite possible by this means to lengthen the initial part of the decay curve enough so that even the first "break" is outside the measured extent, and at the same time have the slope of this initial part correspond fairly closely to the normal coefficients given by Eq. (5.26) for non-diffused waves. Therefore in rooms where diffusion of sound is not complete enough to create an ergodic distribution, "absorption coefficients" obtained from decay curves which seem to be straight for the first thirty or forty db will be more closely equal to the normal coefficients discussed above than they will be to the true Sabine coefficient. Also, comparison with Eq. (5.36) indicates that the coefficients obtained by steady-state measurements in such rooms will usually be smaller than the normal coefficients obtained by measuring the initial slope of the decay curves. This is because of the fact that steady-state measurements give an average result for all waves excited, whereas the initial slope of the decay curve is concerned only with the oblique waves.

Decay curves of the sort shown in Fig. 25 are often encountered in practice, and presumably would provide an interesting series of correlations between the measured impedance of the walls and the usual decay curve measurements. Hunt, Beranek, and Maa (H9) used an equation similar to Eq. (6.20) for their analysis of decay curves and obtained fairly satisfactory checks with theory, as is shown in Fig. 26. The measurements were made in a room $20'\times14'\times8'$ with walls and ceiling of concrete and the whole floor covered with absorbing material. Circles are experimental points and solid line is the theoretical curve. The departures from straight line of the decay curves are quite apparent. A similar analysis (B12), in which a modification of Eq. (6.20) and other experimental conditions were used, also gave a satisfactory check between theory and measurement.

In using Eq. (6.20), one should note that it is an approximate expression, and not valid if any η is less than 2. One should also take care to use the approximate expression $\alpha_s=\alpha_t=(4\gamma)$ *only* when $(|Z|/\eta\rho c)$ is larger than about 4.

VII. PERTURBATION CALCULATIONS FOR ROOMS OF VARIOUS SHAPES

42. The Influence of Room Shape

In the past two sections we have studied the separable case of the rectangular room with uniform wall coverage in considerable detail. We have found the exact theory quite complicated, but have discovered that in the great majority of cases (at the higher frequencies, walls not too "soft," etc.) the normal modes can be divided into a few general classes with regard to their decay rates. The great majority of waves, most or all of the oblique waves, react with the material on the walls in a manner defined by the normal coefficient, α_p, equal approximately to eight times the specific conductance γ of the wall material. For those waves parallel to the wall in question, the effective coefficient is the tangential or supplementary coefficient, depending on whether the wall in question or the one

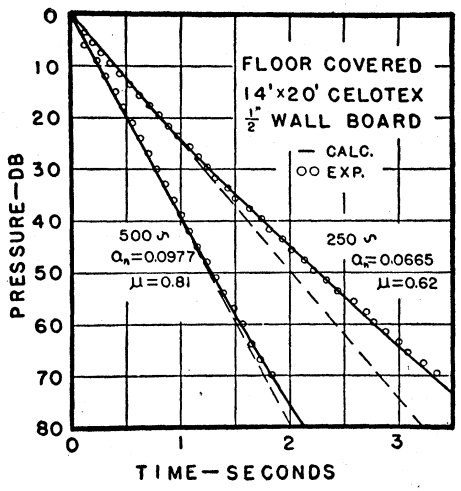

FIG. 26. Decay curves; check between theory (solid line) and experiment (circles). From reference H9.

opposite is softer. In the limiting case of fairly hard walls, both the tangential and supplementary coefficients turn out to be one-half the value of the normal coefficient.

Thus in most cases for the rectangular room with uniform walls, the Sabine assumptions are almost valid, but differ just enough from actuality so as to be inapplicable. The majority of the modes in a given frequency band (the oblique modes) have nearly the same decay rate, but the decay rates of some modes (the tangential and axial ones) are appreciably different, and the resulting decay curve for the combination is not a straight line. The normal coefficient turns out to be larger, and the grazing coefficients smaller than the Sabine coefficient.

In the present section, we shall investigate rooms of more complicated shape, with walls having non-uniform distribution of absorbing material. Exact solutions cannot be obtained for many of these cases, but a perturbation method will be developed which will be accurate enough most of the time (i.e., for hard enough walls). The results will show that many other room shapes are regular enough so that not all their standing waves have the same decay rate, and will indicate how irregular the shape must be in order to have the Sabine assumptions become valid.

From the time of Sabine, it has been widely recognized that room shape has a very important influence on acoustic behavior; and this aspect is about as well understood, from an empirical point of view, as could be expected within the limitations of the geometrical approach. General aspects of shape in auditorium design have been well summarized by Bagenal and Wood (A), Knudsen (K3), and others. Two fundamental principles are: (a) avoid shapes which give acoustical defects, such as sound foci from concave surfaces, distinct echoes, etc. and (b) design shapes to facilitate flow of sound energy to all listeners in the room. These considerations can be studied by geometrical ray constructions on drawings of sections through the room, by spark photography of pressure pulses in small models, and by surface waves of a liquid bounded by a small scale section of the room (ripple tank method) (A). Three-dimensional scale models have also been employed, with light rays reflected from small mirrors appropriately placed. In all of these methods (A) one can follow the course of a ray starting in a given direction from a position corresponding to the actual sound source in the room, through a large number of successive reflections, and in this way study how well the sound energy is spread over the seating area by multiple reflections and how well sound foci have been avoided.

Attempts to express the effects of shape analytically have, by the very nature of the problem, not been very fruitful by the geometrical approach. Knudsen (K3) has studied the influence of shape on reverberation time by measuring mean free paths, using the light ray method. He followed paths through some 25 successive reflections, for rays starting in a number of typical directions. The mean free path enters into the derivation of the reverberation equations (Sections 7 and 8), and has been assumed to be $4V/S$, which is exactly the asymptotic value in rectangular rooms. Knudsen measured this for some dozen shapes, including rectangular, fan shaped, octagonal with dome, cruciform, and others. The results are expressed as effective values of K, in Eqs. (2.3)–(2.5), the computed value being 0.049 assuming $4V/S$ as the mean free path. Values ranged from 0.046 to 0.053 in the shapes studied.

Knudsen's study revealed another effect of more importance than the small correction to the

reverberation time: it showed that some surfaces had a greater probability of reflection than others. This means that absorbing materials placed on these surfaces are more effective in absorbing energy since more energy on the average reaches them. The effect was particularly striking in a room with large horizontal dimensions and a low ceiling, a common shape for large offices. In a room approximately $50'\times40'\times10'$ with all of the acoustic treatment on the ceiling, the measured reverberation would be as much as 20 percent shorter than that given by Eq. (2.4). This result could now be computed by Eq. (6.19) or (6.20).

We see in this example a striking demonstration of the fundamental difference between geometrical and wave acoustics. By geometrical methods a certain result is predicted (reverberation Eqs. (2.3, 4.5)) on statistical assumptions (Sec. 5); a different result is observed in a special case; qualitative reasoning shows the basic assumptions are not valid; a geometrical ray method is used to find the actual (non-statistical) energy distribution; and this result is used to modify a factor in the reverberation equation, still *retaining the Sabine absorption coefficient.* By wave methods the component waves in a room are described analytically; the effective damping of each "kind" of wave is computed, by taking into account the room shape, the distribution of absorbing material, and the absorbing properties; the acoustic impedance is assumed to be the invariant quantity describing the behavior of the absorbing material; the component waves are combined according to type, and averaging processes are used to obtain approximate formulas applicable to various special cases of practical significance; and in this process there emerge *several coefficients of different kinds* in place of the single absorption coefficient of geometrical theory. The explicit result of the wave method is the modification of the absorption coefficient while the geometrical method can take account of the actual energy distribution only by an external, empirical correction factor.

43. Perturbation of Boundary Conditions

The most suitable perturbation method for the problems at hand is based on Green's theorem (F1, F2, M2). One starts with a room R_0 of simple shape and rigid walls, for which the wave equation can be solved exactly. The characteristic functions $\psi_n(x)$ satisfy the usual equation

$$\begin{gathered}\nabla_x^2\psi_N(x)+(\omega_{0N}/c)^2\psi_N(x)=0;\quad x=(x,y,z);\\ N=(n_x,n_y,n_z);\quad \omega_{0N}=2\pi\nu_N=(2\pi c/\lambda);\\ \iiint_{R_0}\psi_N(x)\psi_M(x)\,dV_x=V_0\epsilon_N{}^0\delta_{NM},\end{gathered}\tag{7.1}$$

where V_0 is the volume in the room R_0, and where $\epsilon_N{}^0$ is the average value of $\psi_N{}^2$ over R_0.

One also needs the solution G for the waves from a unit source at point $X=(X, Y, Z)$ in R_0, having frequency $\nu=(\omega/2\pi)$, satisfying the equations

$$\begin{aligned}\nabla_x^2G_\omega(x,X)+(\omega/c)^2G_\omega(x,X)&=\delta(x-X),\\ \nabla_X^2G_\omega(x,X)+(\omega/c)^2G_\omega(x,X)&=\delta(x-X),\end{aligned}\tag{7.2}$$

where $\delta(x-X)$ is the Dirac delta function for three dimensions. Since this Green's function satisfies the same boundary conditions as the ψ_N's $(\partial\psi/\partial n=0)$, it can be expanded in terms of the ψ_N's, in the usual series,

$$G_\omega(x,X)=\sum_N\frac{c^2}{V_0\epsilon_N{}^0}\frac{\psi_N(x)\psi_N(X)}{(\omega^2-\omega_N{}^2)},\tag{7.3}$$

which is the form reached by Eqs. (5.20) and (5.21) when no absorption is present.

We shall follow the work of Feshbach (F2) in studying the effect on the characteristic functions because of small changes in the boundary conditions and in the shape of the boundaries. We can imagine the shape of the room to be changed slightly to a new shape R, whose walls are *everywhere inside* the original room R_0. We also allow the new walls to be non-rigid, having an impedance, Z, which may change from point to point on the new walls. In order that the approximation converge, we must assume that R does not differ much from R_0 and that $|Z|$ is everywhere large compared to ρc. The new boundary condition on the walls of R is therefore

$$\frac{\partial\varphi}{\partial n}=i\omega(\rho/Z)\varphi=i(\omega/c)\beta\varphi=(\omega/c)(\sigma+i\gamma)\varphi,\tag{7.4}$$

where Z, β, σ, and γ are often functions of the position on the wall surface.

The use of Green's theorem, together with the equation for G, provides us with an integral equation of considerable generality:

$$\varphi(x)=\int\int_S\left[\varphi(X)\frac{\partial}{\partial n_X}G_\omega(x,X)-G_\omega(x,X)\frac{\partial}{\partial n_X}\varphi(X)\right]dS_X, \quad (7.5)$$

where the integration is over S, the surface of new room R. The solution of this integral equation, φ, is a solution of the wave equation $\nabla^2\varphi+(\omega/c)^2\varphi=0$ inside R, and is *zero outside* R (for instance, in the region outside of R but inside of R_0). The function Ψ_N defined by the equation

$$\Psi_N(x)=\int\int_S\left[\psi_N(X)\frac{\partial}{\partial n_X}G_{\omega_N}(x,X)-G_{\omega_N}(x,X)\frac{\partial}{\partial n_X}\psi_N(X)\right]dS_X \quad (7.6)$$

is equal to ψ_N inside R, but is zero outside R.

Remembering Eq. (7.4) for the new boundary conditions, we can show that the solution of the integral equation,

$$\varphi(x)=\int\int_S\varphi(X)\left[\frac{\partial}{\partial n_X}G_\omega(x,X)-i\left(\frac{\omega\beta}{c}\right)G_\omega(x,X)\right]dS_X, \quad (7.7)$$

is zero everywhere for most values of ω. However, for a discrete set of ω's, which we can call ξ_N, the solution φ is not zero inside R, but is a solution of the wave equation satisfying the new boundary conditions on S (it is still zero outside R). Therefore solutions of Eq. (7.7) are the required characteristic functions, and the ξ_N's are the characteristic values for the new room R and for the boundary conditions of Eq. (7.4).

Equation (7.7) can no more be solved exactly than can the original differential equation, if R has a complicated surface S and if the wall impedance varies over S in any complicated way. It is, however, set up in a form peculiarly adapted for perturbation calculations since the integrations are over the new surface and involve the new boundary conditions. One needs only to replace $\varphi(X)$ inside the integral by $\psi_N(X)$ and to substitute Eq. (7.3) for G to obtain a first approximation to φ. Moreover, one can re-use Green's theorem (F2) to obtain an equation

$$\xi_N{}^2=\omega_N{}^2+c^2\left[\int\int_S\varphi\left(\frac{\partial}{\partial n}\psi_N-i\left(\frac{\omega\beta}{c}\right)\psi_N\right)dS\right]\cdot\left[\int\int\int_R\varphi\psi_N dV\right]^{-1}, \quad (7.8)$$

from which an approximate value of ξ_n can be obtained.

The difficulty with substituting ψ_N for φ inside the integral in Eq. (7.7) is that the resulting series converges very poorly because of the discontinuity in φ at the surface S. This can be obviated by using Eq. (7.6) to subtract the discontinuity (or most of it):

$$\varphi(x)=\Psi_N(x)+\int\int_S\left\{\varphi(X)\frac{\partial}{\partial n_X}G_\omega(x,X)-\psi_N(X)\frac{\partial}{\partial n_X}G_{\omega_N}(x,X)-G_\omega(x,X)\left(i\frac{\omega\beta}{c}\right)\varphi(X)+G_{\omega_N}(x,X)\frac{\partial}{\partial n_X}\psi_N(X)\right\}dS_X, \quad (7.9)$$

where Ψ_N is equal to ψ_N inside R and is zero outside R.

A first approximation to φ can now be obtained which converges fairly satisfactorily. If we substitute ψ_N for φ inside the integral, we obtain:

$$\varphi(x)\simeq\Psi_N-\int\int_S G_{\omega_N}(x,X)\times\left[\frac{i\omega\beta}{c}\psi_N(X)-\frac{\partial}{\partial n_X}\psi_N(X)\right]dS_X, \quad (7.10)$$

and, using Eq. (7.3), we finally have

$$\varphi(x)\simeq\Psi_N(x)+c^2\sum_M{}' A_{MN}(\omega_N{}^2-\omega_M{}^2)^{-1}\psi_M(x),$$

$$A_{MN}=(1/V\epsilon_M)\int\int_S\psi_M\left(\frac{\partial}{\partial n}\psi_N-i\frac{\omega_N\beta}{c}\psi_N\right)dS, \tag{7.11}$$

$$\int\int\int_R\psi_N{}^2dV=V\epsilon_N,$$

where V is the volume of room R, ϵ_N is the mean squared value of ψ_N inside R (see Eq. (5.17)), and where the prime over the summation sign indicates that the term for $M=N$ is omitted.

The corresponding equation for the characteristic value is

$$\xi_N{}^2\simeq\omega_N{}^2+c^2A_{NN}+c^4\sum_M{}'(\epsilon_M/\epsilon_N)A_{MN}{}^2/(\omega_N{}^2-\omega_M{}^2), \tag{7.12}$$

where Eq. (7.11) has been substituted in Eq. (7.8).

44. Perturbation Due to Patches of Absorbing Material

Let us first consider the case where the room *shape* is still simple, and the boundary condition of Eq. (7.4) is the only perturbation. In this case R is identical with R_0 and the integral A_{MN} entering in Eqs. (7.11) and (7.12) becomes

$$A_{MN}=-i\omega_N(1/cV_0\epsilon_M{}^0)\int\int_{S_0}[\psi_M\beta\psi_N]dS.$$

This case has been studied by Maa (M2) and by Feshbach and Clogston (F1, F2).

The first approximation to the frequency parameter ξ_N is, in this case,

$$\xi_N(-\omega)\simeq\omega_N-\frac{1}{2}\frac{c}{V_0\epsilon_N{}^0}\int\int(\sigma+i\gamma)\psi_N{}^2dS, \tag{7.13}$$

which is to be compared with Eq. (5.9). The function φ will therefore have an exponential factor in it of the nature

$$\exp(-i\xi_Nt)\simeq\exp\left\{-i\left[\omega_N-\frac{c}{2V_0\epsilon_M{}^0}\int\int\sigma\psi_N{}^2dS\right]t-\frac{ct}{2V_0\epsilon_N{}^0}\int\int\gamma\psi_N{}^2dS\right\}. \tag{7.14}$$

The mean square of φ will therefore have an exponential decay factor of the usual form $\exp[-(ca_Nt/4V_0)]$ (see Eq. (6.19)). The effective wall coefficient for the room walls,

$$\alpha_N=(a_N/S)\simeq\frac{8}{2S\epsilon_N{}^0}\int\int\gamma\psi_N{}^2dS, \tag{7.15}$$

$$\gamma=\text{real part of }[\rho c/Z],$$

is given in terms of the wall area S; the mean square of the wave function ψ_N over the volume, $\epsilon_N{}^0$; and the integral of the absorbing factor (8γ), weighted by $\psi_N{}^2$, over the wall area. This is to be compared with Eqs. (5.26) and (5.29). The earlier equations were derived for a uniform wall, but the present one is as accurate (or inaccurate, as the case may be) for a non-uniform wall, with patches of absorbing material placed here and there, as it is for a uniform one. We see, from the earlier chapter, that the approximation is valid if $(|Z|/\rho c\eta)>2$, where η is the ratio between the room "dimension" and the half-wave-length.

Several interesting conclusions can be drawn from this first-order result. In the first place, a piece of absorbing material is most useful, in producing a large absorption coefficient, if it is placed in a position on the walls where most wave functions have their maxima. In a rectangular room, therefore, the most effective positions for absorbing material are at the corners; next best positions are along the edges. In the second case, if material is to be spread over a number of walls, it is better to place patches of material in a rather irregular manner over the walls rather than to space them in too regular a pattern. A regular pattern will almost inevitably place the absorbing material at the minima of ψ^2 for *some* modes, and these modes will be very poorly damped.

Equation (7.15) can be still further simplified if the absorbing material on each wall is uniform

over regions large compared to the wave-length. In this case the integral $\int\int \gamma\psi_N^2 dS$ is approximately equal to the area S times the constant value of β, multiplied by the mean square value of ψ_N on the wall in question. Therefore *to the first approximation* and *for samples of material large compared to the wave-length* the *wall coefficient of a material on a given wall is*

$$\left.\begin{aligned} &\alpha_N \simeq (8\gamma)e_N, \\ &e_N = \frac{1}{2}\left[\frac{\text{Av. value of } \psi_N^2 \text{ over wall in question}}{\text{Av. value of } \psi_N^2 \text{ over volume of room}}\right] \\ &\text{(Formula valid for } |Z|\lambda > 4\rho c L, \text{ where } L \text{ is the largest dimension of the room).} \end{aligned}\right\} \quad (7.16)$$

The factor e_N, which is the only place the wave-type enters in this first approximation, might be called the *wave type factor*. It is to be noted that α_N is *not usually equal* to the Sabine coefficient. The rooms we are discussing here are still too regular in shape to satisfy the Sabine conditions.

Therefore, even to the first approximation the absorption coefficient of a material depends not only on the acoustic impedance of the material, but also on the wall on which the material is placed and the particular normal mode considered. If we are interested in making the initial slope of the sound decay curve as steep as possible, we should place our material so that the wave type factor e_n is as large as possible for the majority of modes in a given frequency range. If we wish to make the final slope of the decay curve as large as possible, we should place our material so that no mode will find all the absorbing material on a wall of low e_n for that mode. This was shown in Chapter VI for rectangular rooms with uniform coverage; the present results show it to be true for any regular room, and even with non-uniform coverage (at least to the first approximation).

To make these rules capable of practical application, we should compute the values of e_N for various room shapes likely to be encountered. For instance, for rectangular rooms, by use of the known properties of the cosine factors in the normal modes, we obtain:

For all oblique modes
  $e_N = 1$ for all walls;
For all tangential modes
  $e_N = \frac{1}{2}$ for the two walls parallel to the wave motion,
  $e_N = 1$ for the other four walls;
For all axial modes
  $e_n = \frac{1}{2}$ for the four walls parallel to the wave motion,
  $e_n = 1$ for the two other walls.

Reference should be made to the discussion following Eq. (3.2), and to Eq. (5.12).

One can go further, and compute the value of some of the e's for any room having two walls plane, parallel, and opposite to each other, the remaining walls all being perpendicular to the plane-parallel pair. An example would be a room whose side-walls are all perpendicular, with any sort of complicated floor-plan, and with plane horizontal floor and ceiling (floor and ceiling are also called walls in the present paper). Suppose we set the x coordinate perpendicular to the plane-parallel walls. Then even though we cannot separate the wave equation in the two coordinates perpendicular to x (call them y and z), we can separate the x factor in the characteristic function for each mode.

$$\psi_N = \cos(\pi n_x x/L_x) F_{n_y n_z}(y; z).$$

The average value of ψ_N^2 over the volume will be $(K_{n_y n_z}/2e_{n_x})$ where $e_{n_x} = 1$ (if $n_x > 0$), $= \frac{1}{2}$ (if $n_x = 0$), and where K is the average value of F over y, z. Therefore for large patches of absorbing material placed on either of the plane-parallel walls

$$e_N = e_{n_x} = \begin{cases} 1 \text{ for waves striking these walls } (n_x > 0) \\ \frac{1}{2} \text{ for waves tangential to these walls } (n_x = 0), \end{cases} \quad (7.18)$$

to the first order of approximation. For a more

exact answer we should have to use the methods discussed in Chapter V.

We shall now compute the values of the e's for cylindrical and triangular rooms. These rooms have been discussed by Roe (R8).

45. Cylindrical Room

The characteristic functions for a cylindrical room of height L and radius R are

$$\psi_N = \begin{matrix}\cos\\ \sin\end{matrix} (n_\varphi \varphi) J_{n_\varphi}(\pi \tau_{n_\varphi, n_r} r/R) \cos(\pi n_z z/L), \quad (7.19)$$

where τ is any one of the numbers which satisfy the equation

$$\frac{d}{d\tau} J_{n_\varphi}(\pi\tau) = 0,$$

$\tau_{n_\varphi, 0}$ being the lowest value, $\tau_{n_\varphi, 1}$ being next, and so on. The limiting values of τ for n_r or n_φ large are

$$\tau_{n_\varphi, n_r} \simeq n_r + \tfrac{1}{2} n_\varphi + \tfrac{1}{4}; \quad n_r \gg 1, \ (n_r/n_\varphi) \gg 1$$

$$\tau_{n_\varphi, n_r} \simeq (n_\varphi/\pi) + \tfrac{1}{2}[9(n_r + \tfrac{1}{4})^2 n_\varphi/\pi]^{\frac{1}{3}}; \quad n_\varphi > 1, \ (n_\varphi/n_r) \gg 1$$

$$\tau_{n_\varphi, 0} \simeq (n_\varphi/\pi) + 0.2575 n_\varphi^{\frac{1}{3}}; \quad n_\varphi \gg 1, \ n_r = 0.$$

The average value of the square of the φ factor is 1 for $n_\varphi = 0$ and is $(\frac{1}{2})$ for $n_\varphi > 0$. This is also true for the z factor. The average value of the square of the r factor is

$$(2/R^2) \int_0^R J_{n_\varphi}^2(\pi\tau r/R) r dr = J_{n_\varphi}^2(\pi \tau_{n_\varphi, n_r})[1 - (n_\varphi/\pi\tau_{n_\varphi, n_r})^2].$$

Therefore, from Eq. (7.16), the ratio between the wall coefficient for a large sample of material and the normal coefficient (8γ) is:

For material on the two plane circular walls,

$$e_N = \begin{cases} \tfrac{1}{2} \text{ for waves tangential to these walls } (n_z = 0) \\ 1 \text{ for wave striking these walls } (n_z > 0); \end{cases} \quad (7.20)$$

For material on the cylindrical walls,

$$e_N = \tfrac{1}{2}[1 - (n_\varphi/\pi\tau_{n_\varphi, n_r})^2]^{-1}.$$

Values of e_N for the cylindrical walls for various values of n_r and n_φ are given in Table I and the following asymptotic formulas.

$$e_N \simeq \tfrac{1}{2}[1 + (n_\varphi/\pi n_r)^2], \quad n_r \gg 1; \ (n_r/n_\varphi) \gg 1,$$

$$e_N \simeq 0.309 n_\varphi^{\frac{2}{3}} + \tfrac{1}{8}, \quad n_\varphi \gg 1; \ n_r = 0,$$

$$e_N \simeq \frac{1}{2}\left[\frac{n_\varphi}{3\pi(n_r + \frac{1}{4})}\right]^{\frac{2}{3}} + \tfrac{1}{8}, \quad n_\varphi \gg 1; \ (n_\varphi/n_r) \gg 1.$$

The situation for the curved walls is obviously different from that for the flat walls. Here the waves which travel in a circle, "parallel" to the curved walls $(n_r = 0)$, have a coefficient $\alpha_N = (8\gamma) e_N$ which is (for $n_\varphi \gg 1$) larger than the normal coefficient (8γ). This is due to the fact that such waves cling closely to the outer walls, whereas the waves tangential to flat walls have less than the usual energy near the walls, and so have tangential coefficients one half of the normal. For cylindrical rooms large compared to the wave-length (c/ν), the particular mode with n_z and n_r both zero and n_φ large has the majority of its energy within a half-wave-length of the outer wall so that the energy is quickly absorbed. For instance, for $n_z = n_r = 0$ and $n_\varphi = 20$, the wall coefficient for material on the circular walls is 2.3 times the normal coefficient (8γ); and for $n_\varphi = 100$ it is 6.7 times the normal coefficient, whereas for the flat walls it is one-half of the normal coefficient.

However, these circular tangential waves are very special cases, which are hard to excite unless the source is close to the circular walls, and are hard to measure unless the microphone is close to these walls. One would expect that the decay curve for a cylindrical room would differ considerably when measured at different points. A curve taken from close to the circular walls would have a more pronounced steep initial part than would one taken from the center of the room.

In contradistinction to the (r, z) tangential

TABLE I. Values of e_N for cylindrical walls.

n_r \ n_φ =	0	1	2	3
0	0.50	0.70	0.86	1.00
1	0.50	0.52	0.55	0.57
2	0.50	0.51	0.52	0.54
3	0.50	0.51	0.52	0.53

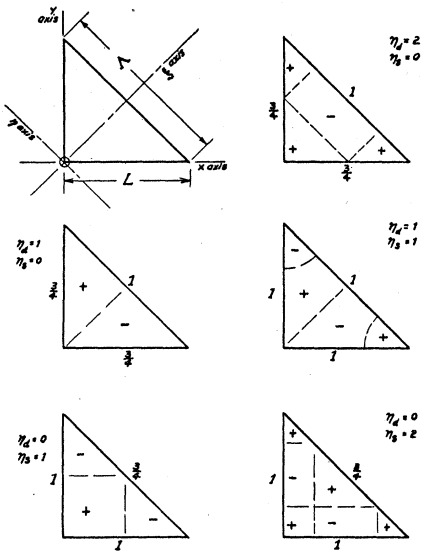

FIG. 27. Location of pressure nodes and values of wave type factor e_N for normal modes in a triangular room. Quantum numbers are n_d and n_s, and the corresponding values of e_N are written near the related walls.

waves, the waves which travel back and forth along a radius (the r-axial waves, where $n_\varphi=0$) have a wall coefficient for the circular walls only one-half of the normal coefficient because such waves focus their energy at the center of the room and have less than the average energy near these walls. In fact, for wave-lengths short compared to the room dimensions, most of the modes have a value of e_N for the circular walls, which is approximately $\frac{1}{2}$; only the modes for which n_r is very small have e_N's larger than unity. Therefore, for sound in the center of the room, acoustic material placed on the circular walls is roughly half as effective in damping out the sound as it would be if placed on the flat walls. For the sound close to the circular walls, however, absorbing material on these walls is much more effective than normal.

Similar studies of a room in the shape of a half-cylinder, with the additional plane wall along the cylindrical axis and studies of a hemispherical wall show that the rules:

For the flat walls,

$e_N=\frac{1}{2}$ for waves tangent to the walls (n_z or $n_\varphi=0$),

$e_N=1$ for waves striking the walls (n_z or $n_\varphi>0$).

For the curved walls,

$e_N>1$ for waves tangent to the walls ($n_r\ll n_\varphi$),

$e_N\simeq\frac{1}{2}$ for waves striking the walls ($n_r\geqslant n_\varphi$);

to the order of approximation considered in this section.

In general ($K9$) a curved surface which tends to focus sound at some region away from the walls will reduce the effectiveness of the acoustic material, and the greater the proportion of smooth concave surfaces, the fewer will be the locations on the walls where acoustic material will be able to produce its normal absorption, at least on the sound in the central part of the room. A similar analysis for a spherical room has been made by Schuster (S11).

46. Triangular Room

The case of a room with vertical side walls, and plane horizontal floor and ceiling, having a right isosceles triangular floor plan, is one for which exact solutions for ψ_N can be obtained although the wave equation is not separable. However (see Fig. 27), the function

$$\psi_N=(\tfrac{1}{2})\cos(\pi n_z z/L_z)T_{n_s n_d}(x,y)$$

where the function T is

$$\begin{aligned}T_{n_d,n_s}(x,y)&=\tfrac{1}{2}\{\cos[\pi(n_d+n_s)x/L]\cos(\pi n_s y/L)\\&\quad+(-1)^{n_d}\cos[\pi(n_d+n_s)y/L]\cos(\pi n_s x/L)\}\\&=\tfrac{1}{2}\{\cos[\pi(n_d+2n_s)\xi/\Lambda]\cos(\pi n_d\eta/\Lambda)\\&\quad+\cos[\pi(n_d+2n_s)\eta/\Lambda]\cos(\pi n_s\xi/\Lambda)\},\ (n_d\text{ even})\\&=\tfrac{1}{2}\{\sin[\pi(n_d+2n_s)\xi/\Lambda]\sin(\pi n_d\eta/\Lambda)\\&\quad+\sin[\pi(n_d+2n_s)\eta/\Lambda]\sin(\pi n_s\xi/\Lambda)\},\ (n_d\text{ odd})\end{aligned}\tag{7.21}$$

and where

$$\xi=\frac{1}{\sqrt{2}}(y+x),\quad \eta=\frac{1}{\sqrt{2}}(y-x);\quad \Lambda=\sqrt{2}L,$$

satisfies the boundary conditions on the diagonal wall as well as on the rectangular ones. The number of allowed frequencies less than ν for this room is about half that for a square room with the same rectangular walls, for the diagonal wall has removed the double degeneracy of most modes (i.e. the room has half the volume).

An integration of the above wave functions

provides values for the wave type factors e_N, relating the wall coefficient for a given wall and mode and the normal coefficient (8γ).

For the rectangular walls:

$$e_N=1 \quad \text{for } n_s>0,$$
$$e_N=\tfrac{3}{4} \quad \text{for } n_s=0.$$

For the diagonal wall:

$$e_N=1 \quad \text{for } n_d>0, \qquad (7.22)$$
$$e_N=\tfrac{3}{4} \quad \text{for } n_d=0.$$

For the floor and ceiling:

$$e_N=1 \quad \text{for } n_z>0,$$
$$e_N=\tfrac{1}{2} \quad \text{for } n_z=0.$$

Therefore there are waves "parallel" to a wall (one of the n's$=0$) even in this room, and for such waves the effective absorption of the material is reduced. The amount of reduction is not as great as for the rectangular room, e_N only reducing to $\frac{3}{4}$ on the side walls. Presumably a wave "parallel" to a side wall in a triangular room is not as "parallel" as a wave can be in a rectangular room. These results do show, however, that a room with plane walls not parallel to each other does not constitute a room irregular enough so that Sabine's assumptions are valid, for the decay curve in this case is still not a straight line.

A glance at Fig. 27 brings out a number of interesting points. The nodal surfaces cut a wall either at right angles or at 45 degrees. If they meet a wall at 45 degrees, the pressure is in phase over the whole of that wall, e_N has a corresponding value of $\frac{3}{4}$, and, presumably, the wave is "parallel" to that wall. If the nodal surfaces meet a wall at right angles, then the pressure over one half the wall is out of phase with the pressure over the other half, e_N has a value unity, and presumably the wave is not "parallel" to the wall. Figure 27 shows the nodal surfaces and values of e_N for some of the lower modes, including most of the typical cases.

47. Second-Order Perturbation

So far we have considered only the first-order perturbation, having tacitly assumed that the second-order term was negligibly small. This is, of course, not always the case (actually it is only true when $|Z|\lambda>4\rho c$ times the largest dimension of the room), and it will pay to investigate the higher order terms. As a matter of fact, we shall find that unless the second-order term in Eq. (7.12) is appreciable in size and is composed of many terms, there is no possibility of having ergodic wave motion in the room. The relative size of the second-order term, compared with the first-order term, will turn out to be an approximate criterion as to whether Sabine's assumptions are valid or not in the room, for a given frequency.

We first study the case where the room's shape is the simple shape R_0, the only perturbation being the effect of patches of absorbing material on the walls. The expression for the perturbed wave function is

$$\varphi(x)\simeq\Psi_N(x)-i\omega_N(c/V)$$
$$\times\sum_M{}'\left[\int\int\psi_M(X)\beta(X)\psi_N(X)dS_X\right]\frac{\psi_M(x)}{\epsilon_M(\omega_N{}^2-\omega_M{}^2)}, \qquad (7.23)$$

the prime indicating that the term $M=N$ is omitted in the summation. An application of the methods discussed in Section 33, and of Eq. (7.3), indicates that near a patch of absorbing material a rough approximation to Eq. (7.23) is

$$\varphi(x)\simeq\Psi_N(x)+i\omega_N\rho\int\int[\psi_N(X)/Z(X)]\cdot\frac{\exp(i\omega_N D/c)}{2\pi D}\cdot dS_X, \qquad (7.24)$$

where the integration is over the surface of the absorbing material near the point x, and D is the distance between points $x(x, y, z)$ in the room and point $X(X, Y, Z)$ on the wall.

This last formula is a very interesting one, which could have been obtained by the following reasoning: to the first order the pressure on the wall at point X is $-i\omega_N\rho\psi_N(X)$; the normal velocity of the wall (since it has impedance $Z(X)$ at that point) is $-i\omega_N\rho\psi_N(X)/Z(X)$. The velocity of the wall at that point sets up radiation into the room equal to the strength of the elementary source, $(-i\omega_N\rho\psi_N/Z)dS$, times $(-\exp[i\omega_N D/c]/2\pi D)$. The integration over all the elementary sources near point x is the second

term. Therefore, the first correction to the wave function ψ_N, because of the presence of absorbing material on the wall, is the radiation owing to the motion of the material (V1) (or of air into the pores of the material) induced by the standing wave ψ_N itself. The consequences of this simple result will be investigated in Chapter VIII.

To the second order in β, the equation for the frequency and damping constant, for the case in question, is

$$\xi_N^2 \simeq \omega_N^2 - \frac{i\omega_N c}{V\epsilon_N}\int\int \beta\psi_N^2 ds + \left(\frac{c\omega_N}{V\epsilon_N}\right)^2 \sum_M{}' \frac{\epsilon_N}{\epsilon_M} \frac{\left[\int\int \psi_M \beta \psi_N ds\right]^2}{(\omega_M^2 - \omega_N^2)}. \quad (7.25)$$

This equation can also be approximated by considering only the coherent part of the perturbation;

$$\xi_N^2 \simeq \omega_N^2 - \frac{i\omega_N c}{V\epsilon_N}\int\int \beta\psi_N^2 ds + \left(\frac{\omega_N^2}{V\epsilon_N}\right)\int\int dS_x \left\{\psi_N(x)\beta(x)\cdot \int\int \psi_N(X)\beta(X) \times (\exp[i\omega_N D/c]/2\pi D) dS_X\right\}, \quad (7.26)$$

where the double integration should be only over small values of D. This equation also will be discussed in detail in Chapter VIII.

48. Transition to the Ergodic State

Presumably if enough absorbing material is applied, in an irregular enough manner to the walls of a rectangular room, the wave motion could be made ergodic and the decay curve would be a straight line. This condition would be reached when we can no longer call a standing wave a pure tangential or axial wave, and when all waves have the same decay rate. From the point of view of the perturbation theory, this would be reached when every standing wave φ is a more or less random mixture of a number of different ψ_N's in about equal proportions, with sizable amounts of oblique waves present in every φ. A glance at Eqs. (7.23) and (7.25) indicates that this would be true if the last term in each expression were made up of a large number of approximately equal terms, the sum being of the same order of magnitude as the first term. When this is true, higher orders of approximation than the second will of course be needed to obtain reasonably accurate values of the wave function. Nevertheless it seems satisfactory to take the relative magnitude of the second-order term (say, in Eq. (7.25) for ξ) as a rough criterion of the presence or absence of ergodic wave motion.

Whenever this second-order term is as large as or larger than the first-order term and when it consists of a large number of different wave functions, all of about equal amplitude, then we can expect to have ergodic wave motion and to have Sabine's assumptions become valid. We will therefore be interested in obtaining simple, average values of the second-order terms in Eq. (7.25), to use as criteria for the onset of completely random motion.

The deciding factors in the second-order terms of Eq. (7.25), for instance, are the interaction integrals

$$\beta_{MN} = \int\int \psi_M \beta \psi_N dS,$$

which measure the ability of the distribution of absorbing material to "scatter" wave N into wave M. If the scattering is large enough, no wave will be just axial or tangential, all the decay constants will tend toward a common average value, and the Sabine assumptions will become valid.

For this to be true, of course, β_{MN} should differ from zero for most M's and N's; in fact, most β_{MN}'s should have roughly the same magnitude. This indicates immediately that uniform coverage of one or more walls of a regularly shaped room will *not* produce this effect; for if β is uniform over a wall (the xy wall, for instance), then all β_{MN}'s will be zero except those for which $n_x = m_x$ and $n_y = m_y$. The result will be that most of the terms in the summation over M will be zero, and the standing waves will not be random.

Similarly, any very symmetrical placing of absorbing material will result in many integrals

β_{MN} being zero. What is needed is a "completely irregular" distribution of patches of absorbing material. How this is done in practice is indicated in the work of Maxfield and Potwin (M5), Boner (B11), Meyer (6), and Volkmann (V1).

Let us consider a specific example: that of a rectangular room, with m patches of absorbing material of specific admittance $\beta=(\rho c/Z)$, each of dimensions a and b, distributed "irregularly" about the walls. The total area of material will therefore be $S_a=mab$. The first-order term in Eq. (7.25) will then become

$$-2i\omega_N c(\beta S_a/V).$$

The next quantity to compute is the mean square value of $\int\int\psi_M\beta\psi_N ds$ over one patch of material, averaged over M and N. If the patch, of dimensions a and b, is placed at random on the wall, the nodal surfaces will cut the patch at random, and the x factor of the integral will have the general form

$$\beta\int_{-a/2}^{a/2}\sin\left[(\pi n_x x/L_x)+\Phi_x\right]\times\sin\left[(\pi m_x x/L_x)+\Phi_x'\right]dx.$$

This factor is to be squared and averaged over Φ_x, Φ_x', n_x, and m_x.

Averaging first over the phase angles Φ_x and Φ_x', we obtain

$$\frac{\sin^2\left[(\pi a/2L_x)(n_x-m_x)\right]}{\left[(\pi/L_x)(n_x-m_x)\right]^2}+\frac{\sin^2\left[(\pi a/2L_x)(n_x+m_x)\right]}{\left[(\pi/L_x)(n_x+m_x)\right]^2}.$$

Averaging this, times the corresponding factor for y, over n_x, n_y, m_x, and m_y yields the approximate result for one patch,

$$\tfrac{1}{4}\beta^2\frac{a^2b^2}{1+(4ab/\lambda^2)}$$

and for all m patches,

$$(\beta_{MN}^2)_{\text{Av}}\simeq\tfrac{1}{4}\beta^2\frac{S_a^2}{1+(4S_a/m\lambda^2)}$$

where λ is the average wave-length of the sound for the Mth and Nth modes. Since the important part of the second-order sum is for $\omega_M\simeq\omega_N$, this average value is valid.

The final approximate result for a typical term in the second-order sum in Eq. (7.25) is

$$(c^2\omega_N/V^2)\beta^2\frac{S_a^2}{1+(4S_a/m\lambda^2)}\cdot\frac{1}{\omega_M-\omega_N}.$$

From Eq. (3.4), the average difference between allowed values of ω is $(2\pi^2c^3/V\omega^2)$, so that the magnitude of the largest dozen terms in the second-order sum is approximately

$$(\omega^3/4\pi^2cV)|\beta|^2\cdot\frac{S_a^2}{1+(4S_a/m\lambda^2)},$$

and the ratio between these large terms in the second-order sum and the first-order term is approximately

$$\Xi_a=\frac{\omega^2}{8\pi^2c^2}\frac{|\beta|S_a}{1+(4S_a/m\lambda^2)}=\frac{(1/2)|\beta|S_a}{\lambda^2+(4S_a/m)}. \quad (7.27)$$

This quantity can be called the *index of randomness* for waves in a rectangular room with irregularly placed patches of absorbing material. A similar formula can be obtained for rooms of other regular shape. When Ξ is smaller than unity the wave motion is not ergodic, there will be appreciable differences between the decay rates for different modes, and the decay curve will not be a straight line. When Ξ is considerably larger than unity, no wave can be a pure axial or tangential mode, the decay rates will tend to approach an average, and we can expect that the Sabine assumptions will hold. It has not yet been determined just how much larger than unity Ξ must be in order that the Sabine assumptions hold.

One can readily see that Ξ will be considerably smaller than unity for low frequencies (λ large). The usual magnitude of β for soft materials is of the order of 0.2, so that even for λ^2 smaller than $(4S_a/m)$, Ξ will not be larger than unity unless m is large; i.e., unless there are a large number of small patches. The most effective size for each patch is approximately one-half-wave-length, so that $\lambda^2\simeq(4S_a/m)$ and the resulting value of Ξ is $m(|\beta|/8)$.

For instance, for a cubical room 20 feet on a side, with square patches a half-wave-length $(\lambda/2)$ wide, of soft material having $|\beta|=0.2$, and with the average distance between patches

$(3\lambda/2)$, there will be, on the average, one patch in every $(4\lambda^2)$ area of the wall. The coefficient of randomness in this case will be $\Xi=(7.5/\lambda^2)$. In order that Ξ be larger than 4 (which is perhaps a reasonable criterion for randomness) we must have the wave-length less than about 1.5 feet, or the frequency greater than 800 cycles per sec. At 800 cycles per sec. there would need to be approximately 250 patches on the walls, one in each 9 square feet of area.

These results are quite enlightening, and tend to explain the success of the work of Maxfield and Potwin and others (B11, M5, M6, V1). However, patches of absorbing material on smooth walls are comparatively ineffective in scattering sound. We must now study the result of irregularities of room *shape* and determine the effect of these irregularities on Ξ.

49. Perturbation Caused by Change in Shape of Boundaries

The other term in Eq. (7.10) must now be taken up; that due to a change in shape between S and S_0. An example is shown in Fig. 28, where S_0 is the (x, y) plane and S "bulges" inward from S_0 in a region bounded by contour C. Inside this contour the equation for the surface S is $z=B(x, y)$, where the positive direction of z is into the room, and where B is never negative (according to our original assumptions). The unit vector normal to S_0 is $\mathbf{n}_0$, pointing in the negative z direction. The unit vector perpendicular to S is $\mathbf{n}$, at an angle $\vartheta(x, y)$ to $\mathbf{n}$. Therefore for the case under consideration the term in A_{MN} of Eq. (7.11),

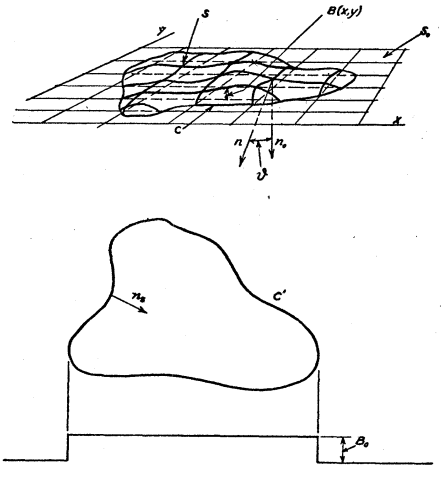

FIG. 28. Irregularities in a plane wall.

$$\frac{\partial}{\partial n}\psi_N=[\mathbf{n}\cdot\text{grad}\,\psi_N]_s=\{-[\partial\psi_N/\partial z]_s + (\text{grad}_{S_0}B)\cdot(\text{grad}_S\,\psi_N)\}\cos\vartheta,$$

where grad_{S_0} is the two dimensional gradient in the (x, y) plane, and where

$$\cos^2\vartheta=1+\text{grad}_{S_0}^2\,(B).$$

The area dS is equal to $dxdy/\cos\vartheta$, so that the first term in A_{MN} turns out to be,

$$(1/V\epsilon_M)\left\{\int\int_S\psi_M\,\text{grad}\,B\cdot\text{grad}\,\psi_N dxdy - \int\int_S\psi_M\frac{\partial}{\partial z}\psi_N dxdy\right\}, \quad (7.28)$$

where, if B is smaller than a quarter-wave-length, it is possible to use $\text{grad}_{S_0}\psi_N$ instead of $\text{grad}_S\,\psi_N$.

Since we have assumed S_0 to be a plane wall, the general form of ψ_N near this wall (z small) is

$$\psi_N=F(x, y)\cos(\pi n_z z/L_z),$$

and the value of $-(\partial\psi_N/\partial z)$ at $z=B$ is approximately

$$(\pi n_z/L_z)^2B[\psi_N]_{z=0},$$

as long as B is small compared to $(L_z/\pi n_z)$. A final approximate expression for the part of A_{MN} due to the "bump" in question is

$$A_{MN}\simeq\frac{1}{V\epsilon_M}\int\int_{S_0}\psi_M\left\{\text{grad}_{S_0}B\cdot\text{grad}_{S_0}\psi_N - \frac{\omega}{c}(\sigma+i\gamma+\sigma_B)\psi_N\right\}dxdy, \quad (7.29)$$

where $\gamma-i\sigma$ is the admittance of the bump, and where the term from $\partial\psi_N/\partial z$ has been converted into an *equivalent susceptance*

$$\sigma_B=-(\lambda/2\pi)(\pi n_z/L_z)^2B, \quad (7.30)$$

a "mass-like" susceptance as long as B is positive.

This part of the effect of change in room shape, which can be expressed in terms of σ_B, is the

effect owing to the change in total volume of the room. To show the effect we can take the case where R_0 is a rectangular room, and where the only "bump" is on one (x, y) wall, covering an area whose dimensions are large compared to a wave length. In this case the part of A_{NN} arising from σ_B is, approximately

$$(2\bar{B}/L_z)(\pi n_z/L_z)^2,$$

where $\bar{B}$ is the average of B over the whole wall. The result is valid for oblique waves $(n_z>0)$. The expression for the modification of frequency owing to this term is, to the first order

$$\xi_N^2=c^2\left[\left(\frac{\pi n_x}{L_x}\right)^2+\left(\frac{\pi n_y}{L_y}\right)^2+\left(\frac{\pi n_z}{L_z}\right)^2\right]+c^2\left(\frac{\pi n_z}{L_z}\right)^2(2\bar{B}/L_z).$$

To the first order, this extra term is equivalent to a reduction in the length of L_z by an amount $\bar{B}$.

Therefore the part of the effect of change of shape which is expressed in terms of σ_B can be handled in just the same manner as the true impedance effects were handled in the previous sub-sections. There is, in addition, a new sort of term; the part involving $\text{grad}_{S_0}\psi_N$. To show the effects of this term, let us simplify the problem somewhat further, by considering the bump to be the sort shown at the bottom of Fig. 28, with a B which changes from zero to a constant value B_0 at the edge C. In that case the expression for A_{MN} becomes

$$A_{MN}\simeq\frac{1}{V\epsilon_M}\left\{B_0\int_C\psi_M\mathbf{n}_s\cdot\text{grad}_{S_0}\psi_N ds-\frac{\omega}{c}\int\int_{S_0}\psi_M(\sigma+i\gamma+\sigma_B)\psi_N dxdy\right\},\quad(7.31)$$

where $\mathbf{n}_s$ is the vector in the (x, y) plane which is normal to the contour C; and where the first integral is a line integral around C. This first term is the effect of the edges of the bump, and we shall see that it is quite effective in producing wave scattering.

If the contour C of the edge of the bump is rectangular, of sides a and b, parallel to the x and y axes respectively, we can compute the root-mean-square value of the first term of A_{MN}. We use the same sort of calculation which already resulted in Eq. (7.26), to obtain the r.m.s. value of the first part of A_{MN} for a single bump:

$$\frac{B_0}{2V}\frac{(a+b)/\lambda}{[1+4(a+b)/\lambda]^{\frac{1}{2}}}$$

where it is assumed that neither a nor b is as large as the x or y dimension of the room R_0. If, on the other hand, b were equal to L_y, so that the bump is a raised strip of width a going across the (x, y) wall, parallel to the y axis, from one (x, z) wall to the other, then the root-mean-square value of the first part of A_{MN} in Eq. (7.29) is approximately

$$\frac{B_0}{2V}\frac{a/\lambda}{(1+4a/\lambda)^{\frac{1}{2}}},$$

for waves for which $m_y=n_y$ and $m_z=n_z$, but is zero for $m_y\neq n_y$ or $m_z\neq n_z$. If we wish all A_{MN}'s to differ from zero we must have several raised strips, on various walls, at least one of which is perpendicular to each of the three axes. Or else the irregularities should be patches extending over just part of a wall, with the patches distributed over at least three mutually perpendicular walls. If the patches are distributed irregularly enough, and if there are enough of them, the approximation series of Eq. (7.11) will not converge, and ergodic wave motion will result.

The criterion for the transition to the ergodic state will be taken from Eq. (7.11) this time. We will study the average amplitude of the coefficient of ψ_M, $c^2A_{MN}/(\omega_N^2-\omega_M^2)$, for ω_M near ω_N. If this is small, then φ will be made up primarily of one unperturbed wave ψ_N; and if the ψ_N is an axial one, φ will have a decay rate which differs appreciably from the other waves. On the other hand, if a number of coefficients of various ψ_M's are not small, then φ will be a mixture of a number of unperturbed ψ's, some of them axial and some oblique, so that *each* standing wave φ will be a mixture of axial, tangential and oblique waves; and all standing waves will have approximately equal decay rates.

50. The Index of Randomness

Suppose we have m patches of absorbing material of average admittance β and of average area S_a/m irregularly distributed over the walls; and we have n "bumps" of average height B and dimensions a (if the bump is a patch extending over just part of a wall, the dimension a can be taken to be half its perimeter; if the bump is a strip extending clear across a wall its dimension is its width a) also distributed irregularly over the walls. We also suppose that the average dimensions of patches and bumps are the same order of magnitude as the wave-length. Then, using the previous approximate results for both patches and bumps, we arrive at a very approximate value for the average amplitude of the coefficient $C^2A_{MN}/(\omega_N^2-\omega_M^2)$ in Eq. (7.11) for ψ_M's with frequencies close to ψ_N;

$$\Xi=(1/10\lambda^2)[nBa+|\beta_e|S_a] \qquad (7.30)$$

$$(a^2,\ S_a/m \text{ assumed}\simeq\lambda^2),$$

where

$$\beta_e=\gamma-i\sigma-i\sigma_B\simeq\gamma-i\sigma+(2\pi iB/\lambda),$$

if B is smaller than a half wave-length.

A somewhat more flexible formula (though no more accurate) which is equally valid for any ratio between λ and size of patch or bump, but which again requires random distribution of bumps and patches, and assumes that B is smaller than a half-wave-length, is

$$\Xi=\frac{1}{2}\left\{\frac{(nBa/\lambda)}{\lambda+4a}+\frac{|\beta_e|S_a}{\lambda^2+(4S_a/m)}\right\}. \qquad (7.31)$$

If B is larger than $(\lambda/2)$ we substitute $(\lambda/2)$ for B in the above formula.

The quantity Ξ, the index of randomness for both absorbing patches and bumps, checks with Eq. (7.27), for the second term. It can be used as a very crude measure of the presence or absence of ergodic wave motion in the room. If it is considerably less than unity, the wave motion will not be ergodic and the decay curve will not usually be a straight line; if it is considerably larger than unity, the wave motion will be random, we should expect Sabine's assumptions to be valid, and we can *only then* talk about an *absorption coefficient* for a wall material, rather than a wall coefficient for a particular wave and wall and material.

A number of interesting conclusions can be drawn from this expression. In the first place, the volume of the room does not enter explicitly into the formula for the index of randomness; to this crude approximation it takes just as many (or as few) irregularities in the room walls to create random wave motion in a small room as in a large one at a given frequency. However, since it is harder (if not impossible) to put a given number of patches and bumps in an irregular manner in a small room than in a large one, it will be more difficult to make Sabine's assumptions valid in a small room than in a large one for any given wave-length. In the second place, it is easier to obtain ergodic wave motion in any given room for a short wave-length than for a long wave-length (this is perhaps a corrolary of the first statement rather than a separate conclusion).

As an example, let us use material of acoustic admittance $|\beta|\simeq(1/5)$, which is a fairly "soft" material. For bumps we can use rectangular strips extending across three or more walls, some vertical and some horizontal, with a thickness B of about 6 inches. For a frequency of 1000 c.p.s. ($\lambda=1$ foot) we should have the strips only a foot wide, and the absorbing material cut into separate pieces about a foot on a side. To obtain ergodic wave motion, we would have to use more than 100 patches of absorbing material, irregularly placed, or we could use more than 40 strips, breaking up the wall shape (in order to make Ξ larger than 2).

For a frequency of 250 c.p.s. ($\lambda=4$ feet) we could cut our patches into $4'\times4'$ squares, and our raised strips could be 4 feet wide (both could be somewhat smaller without reducing their effectiveness appreciably). Again, we would need more than 100 such patches of the absorbing material to produce ergodic motion; or we would need more than 160 strips. It is obvious that it would be fairly easy to obtain ergodic wave motion in a room of moderate size ($10'\times20'\times30'$) at 1000 c.p.s., but that it would be difficult to crowd in enough larger patches or bumps to make it completely ergodic at 250 c.p.s. It is also obvious that it is usually easier to produce random wave motion by means of bumps than it is by patches of absorbing material. This is not surprising since a raised bump would be

expected to scatter sound more efficaciously than a flat patch of absorbing material.

Experimental verification of the theory just outlined is very fragmentary. A few experiments with small scale "rooms" have been made to check the general aspects of the perturbation theory. In one set of experiments (B8) the enclosure had dimensions of the order of one foot, so that even the lowest frequencies were not too low for easy measurement. Individual normal modes were set up in this room and the corresponding distribution of pressure was measured so as to obtain the nodes and loops in the pressure pattern. The shape of the room was varied from a rectangular one to a trapezoidal one. Rectangular "bumps" and "dents" were also applied to one or the other of the walls.

The distribution of pressure in the first ten or twenty normal modes and the values of the resonant frequencies were compared with the results obtained by the perturbation theory discussed in this chapter (B10).

In general there was good agreement between theory and experiment although the second-order term in the perturbation had to be used in order to obtain satisfactory agreement. Figure 29 shows one case, the top diagram showing the shape of the room and the measured equi-pressure contours in the room for one of the modes. The other three curves show the check between experimental and calculated pressure values. For this type of perturbation (trapezoidal room), the first-order terms vanish since the volume of the room was held constant. For other types of change of room shape, the first-order terms are important, and the calculation is somewhat simpler.

Much more experimental work needs to be done before we can be sure of the range of validity of the perturbation theory. At present we must use it since it provides the only means of computing complex rooms, but we are not yet certain how far we can trust it.

The general results obtained in the present section, and here deduced theoretically from the behavior of the index of randomness, have already been applied in architectural-acoustical design by a number of authorities in this field (B11, M5, V1); and some experimental study of the diffusing effect of cylinders has been made

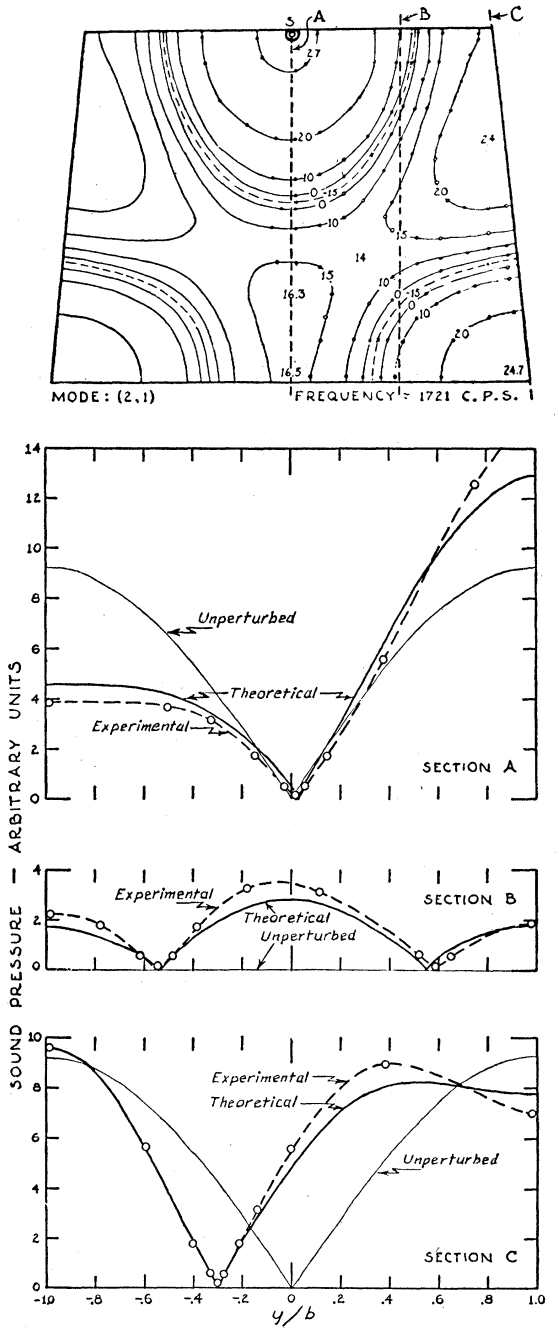

FIG. 29. Distribution of pressure measured in a standing wave in a trapezoidal room. Lower curves compare experimental results (dotted line) with second-order perturbation calculations (solid line marked theoretical). From reference B10.

experimentally by Sabine (S6). In this case the applications came before the theory, the designs being based empirically on a wide range of prac-

tical experience gained in designing auditoriums and measuring their properties. It is gratifying that the results of the theory as outlined here agree more or less with the practical conclusions drawn from these applications. It is possible that the theory will clarify these principles and make it possible to apply them in a more quantitative manner.

It has long been noticed that two rooms with the same reverberation time do not necessarily have the same acoustical behavior. An additional property has been rather vaguely called the "liveness" of the room (H2). It has something to do with the ability of the room to "hold" the sound and at the same time disperse it thoroughly. (Cf. footnote 4.)

There is now a general tendency to increase the reverberation time over that previously considered to be necessary, but to make it as flat with frequency as possible (cf. Fig. 3-B). In addition, a considerable effort is now made to disperse the sound thoroughly. No large, flat surfaces of hard material are allowed. Walls are covered with an irregularly spaced pattern of "bumps" or patches of absorbing material. The irregularities in the wall surface are made as random as possible. All of these tendencies indicate a general agreement with the principles derived in this chapter. It is to be hoped that further investigation will extend and clarify this agreement.

VIII. FREE-WAVE CALCULATIONS FOR ROOMS HAVING RANDOM WAVE MOTION

Rooms which are irregular enough in wall-shape or which have enough absorbing material distributed irregularly about the walls, can have ergodic wave motion for frequencies above a certain lower limit. For such rooms and frequencies, *each* standing wave consists of a random combination of plane waves, traveling in different directions, so that the system of nodes and loops is irregularly arranged; the decay rate for each wave is roughly equal to that of every other wave of about the same resonance frequency; only then do the Sabine assumptions hold.

In this case only can we be sure that whenever sound is present, every portion of the wall surface is struck by sound waves from all possible directions; and only in this case can we talk about an "absorption coefficient," independent of room and of normal mode, dependent only on material. Only in this case can we consider the sound striking each part of the wall as made up of a large number of plane waves, randomly distributed in direction.

When ergodic conditions hold and we *can* deal with plane waves traveling in all possible directions, the problem becomes somewhat simplified again. We can study the absorption or reflection of a plane wave from some part of the wall and then obtain the behavior for the ergodic case by averaging over all possible directions of incidence of the wave.

51. Reflection of a Plane Wave from a Uniform Wall

To illustrate this technique, and at the same time to obtain the formulas necessary to compute the relationship between the Sabine absorption coefficient and the wall impedance, we shall first discuss (K8, H4, P6) the reflection of a plane wave from a plane wall of uniform impedance $Z=R-iX=\rho c\zeta=\rho c/\beta=|Z|e^{-i\varphi}$. The angle of incidence is ϑ, and the velocity potential is

$$\psi=e^{i(\omega/c)(x\sin\vartheta-z\cos\vartheta-ct)}+Ae^{i(\omega/c)(x\sin\vartheta+z\cos\vartheta-ct)}$$

where z is the perpendicular distance to the wall, x the distance along the wall parallel to the plane of incidence, and A is the amplitude (complex) of the reflected wave.

We determine A by requiring that the ratio between the pressure at the surface

$$p_s=-i\omega\rho(1+A)e^{i(\omega/c)(x\sin\vartheta-ct)},$$

and the negative normal velocity at the surface

$$u_s=-(i\omega\cos\vartheta/c)(1-A)e^{i(\omega/c)(x\sin\vartheta-ct)},$$

equals Z, the wall impedance. The resulting equation for A yields

$$A=\frac{\zeta\cos\vartheta-1}{\zeta\cos\vartheta+1}=\frac{\cos\vartheta-\beta}{\cos\vartheta+\beta}=e^{-2\pi\Upsilon(\vartheta)}=e^{-2\pi\tau+2\pi i\upsilon}, \quad (8.1)$$

where

$$\coth[\pi\Upsilon(\vartheta)]=\coth[\pi(\tau-i\upsilon)]=\zeta\cos\vartheta=(|Z|/\rho c)e^{-i\varphi}\cos\vartheta.$$

$$\tanh[\pi\Upsilon(\vartheta)]=\beta\sec\vartheta.$$

The quantity $e^{-2\pi\tau}$ represents the reduction in amplitude of the reflected wave, $2\pi\upsilon$ is the change of phase on reflection.

If the incident plane wave has unit intensity, $(|p_i|^2/2\rho c)=1$, the pressure amplitude at the wall is the amplitude

$$(2\rho c)^{\frac{1}{2}}(1+A)=(2\rho c)^{\frac{1}{2}}\frac{2\zeta\cos\vartheta}{\zeta\cos\vartheta+1}$$

$$=(2\rho c)^{\frac{1}{2}}\frac{2\cos\vartheta}{\cos\vartheta+\beta}=(8\rho c)^{\frac{1}{2}}e^{-\pi\Upsilon}\cosh(\pi\Upsilon), \quad (8.2)$$

and the normal velocity amplitude is the amplitude of

$$(2/\rho c)^{\frac{1}{2}}\cos\vartheta(1-A)=(2/\rho c)^{\frac{1}{2}}\frac{2\cos\vartheta}{\zeta\cos\vartheta+1}$$

$$=(2/\rho c)^{\frac{1}{2}}\frac{2\beta\cos\vartheta}{\cos\vartheta+\beta}=(8/\rho c)^{\frac{1}{2}}e^{-\pi\Upsilon}\sinh(\pi\gamma). \quad (8.3)$$

When the wall is rigid ($\beta=0$, $\Upsilon=0$), the pressure amplitude at the wall is twice the amplitude of the incident wave and the normal velocity at the wall is, of course, zero. As the wall is made softer ($|\beta|>0$), the pressure amplitude at the wall, in general, decreases, and the normal velocity increases in amplitude.

The intensity of the reflected wave is

$$|p_r|^2/2\rho c=|A|^2=\frac{(\cos\vartheta-\gamma)^2+\sigma^2}{(\cos\vartheta+\gamma)^2+\sigma^2}=e^{-4\pi\tau}, \quad (8.4)$$

where $\beta=\gamma-i\sigma$. The fraction of the incident intensity which is absorbed is

$$\alpha(\vartheta)=1-|A|^2=1-e^{-4\pi\tau}$$

$$=\frac{4\gamma\cos\vartheta}{(\cos\vartheta+\gamma)^2+\sigma^2}, \quad (8.5)$$

which is the wall coefficient for a plane wave at an angle of incidence of ϑ. Its value as function of $(|Z|/\rho c)$, φ and ϑ can easily be computed from Eq. (8.5). We note that it has its maximum value for an angle of incidence ϑ such that $(|Z|/\rho c)\cos\vartheta=1$; the harder the wall the nearer the angle for maximum absorption comes to 90° (grazing incidence). Exactly at grazing incidence, of course, *free* waves are not absorbed at all.

Equation (8.5) has been checked experimentally by measurement of incident and reflected sound intensity of free waves on large samples, by Cremer (C7) and Willig (W10). A modification of this free-wave method has yielded preliminary results in substantial agreement with theory (P6). In this method, measurements were made on the maxima and minima in the interference pattern set up in front of the absorbing material by the incident and reflected waves, for various angles of incidence. Equation (8.5) has also been used (H7) in the interpretation of damping of modes of vibration in a rectangular chamber, with one wall completely covered with material. Each mode is associated with a particular angle of incidence, given by the n's, so one can study damping for all angles by appropriate choice of frequency and room dimensions. The free-wave theory gives a close approximation in this case, with the notable exception of waves at "grazing" incidence. However, a standing wave analysis must be used for the rigorous solution of this case, as was shown in Chapter V.

Willig (W10) developed a miniature pressure gradient microphone in order to discriminate, by directionality, between the incident and reflected waves. The directionality was adequate for measurements between 15 and 75° angles of incidence. He also obtained a value at normal incidence by the tube method. He fitted the points to a curve computed by Eq. (8.5), choosing a value of γ for best fit, and assuming $\sigma=0$, i.e., a real impedance. The experimental error was a minimum for $\alpha=0.75$, and became quite large for α less than 0.2 and greater than 0.9 because these involved small differences between large quantities. The experimental results fit the calculated curves within the experimental errors, giving adequate confirmation of the theory in this case.

52. Sabine Coefficient and Wall Impedance

In order to obtain the Sabine absorption coefficient, we need only obtain the average value of $\alpha(\vartheta)$, given in Eq. (8.5), over all angles of incidence, weighting each direction by the relative amount of energy falling on a unit area

at that direction. The result is

$$\alpha_{\text{stat}}=\frac{1}{\pi}\int_0^{2\pi}d\phi\int_0^{\pi}\alpha(\vartheta)\cos\vartheta\sin\vartheta d\vartheta$$

$$=8\gamma\int_0^1\frac{x^2dx}{x^2+2\gamma x+\gamma^2+\sigma^2}$$

$$=8\gamma\left\{1-\gamma\ln\left[1+\frac{2\gamma+1}{|\beta|^2}\right]+\frac{\gamma^2-\sigma^2}{\sigma}\tan^{-1}\left[\frac{\sigma}{|\beta|^2+\gamma}\right]\right\} \qquad (8.6)$$

$$=8\frac{\cos\varphi}{w}\left\{1-\frac{\cos\varphi}{w}\ln\left[1+2w\cos\varphi+w^2\right]+\frac{\cos 2\varphi}{w\sin\varphi}\tan^{-1}\left[\frac{w\tan\varphi}{w+\sec\varphi}\right]\right\}$$

$$\to 8\frac{\cos\varphi}{w}\left[1-\frac{2\cos\varphi}{w}\ln(w)+\frac{\varphi\cos 2\varphi}{w\sin\varphi}\right] \quad (w\to\infty)$$

$$\to\frac{8}{3}w\cos\varphi\left[1-\frac{3}{2}w\cos\varphi\right] \quad (w\to 0),$$

where $w=(|Z|/\rho c)$; $\cos\varphi/w=\gamma$; $w\cos\varphi=(R/\rho c)$; $w\sin\varphi=(X/\rho c)$. Figure 30 gives a contour plot of α_{stat} as a function of $w=(|Z|/\rho c)$, the specific impedance amplitude, and φ, the phase angle, of the wall.

Equation (8.6) and Figure 30 give the relationship between the wall impedance and the Sabine absorption coefficient. This quantity is measured by reverberation measurements *only when the wave motion in the reverberant room is completely randomized.* Ergodic wave motion occurs in most large auditoriums at all usual frequencies, so that α_{stat} can be used in most auditorium design problems. On the other hand there is a considerable body of evidence to indicate that ergodic wave motion *is not attained in most acoustic measurement chambers until the frequency is above 2000* c.p.s. At lower frequencies the normal coefficient $\alpha_p=8\cos\varphi/w=8\gamma$ is usually obtained from the measurements. Consequently, in designing acoustic treatment for large auditoriums *it is better to use* α_{stat} *computed by* Eq. (8.6) *or*

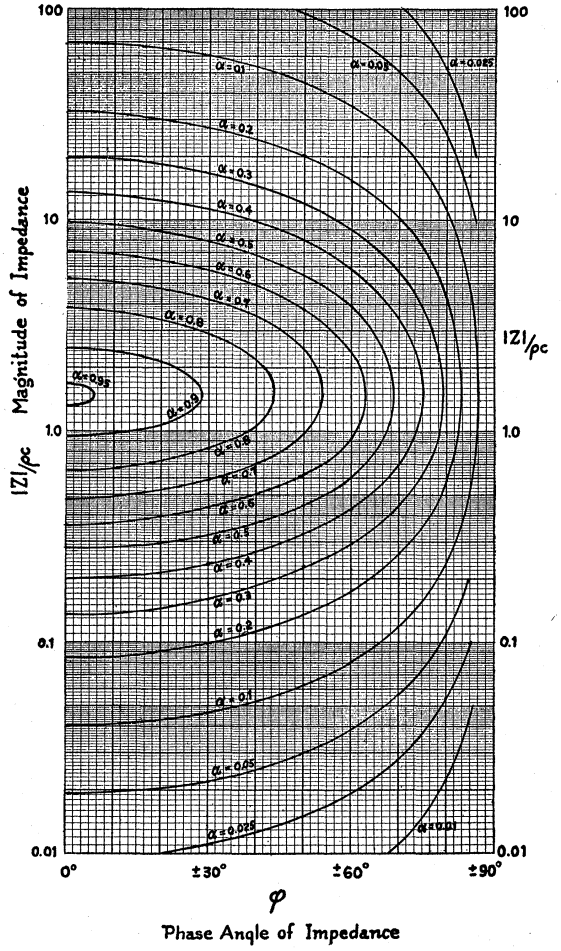

FIG. 30. Sabine absorption coefficient α_{stat} as function of wall impedance magnitude and phase angle. Only to be used in cases where ergodic wave motion is attained.

Fig. 30 from the measured impedance of the material, rather than to use the coefficients measured at present in reverberation chambers (at least for frequencies below 2000 c.p.s.) In general the normal coefficient α_p is larger than α_{stat}, so that the coefficients at present measured in acoustic chambers are usually larger than the Sabine coefficient, which characterizes the material's absorbing ability in large, irregularly shaped rooms (E5, S7, S14).

53. Reflection of Spherical Wave from Plane Wall

Some analyses of reverberation have utilized the image method to obtain the successive

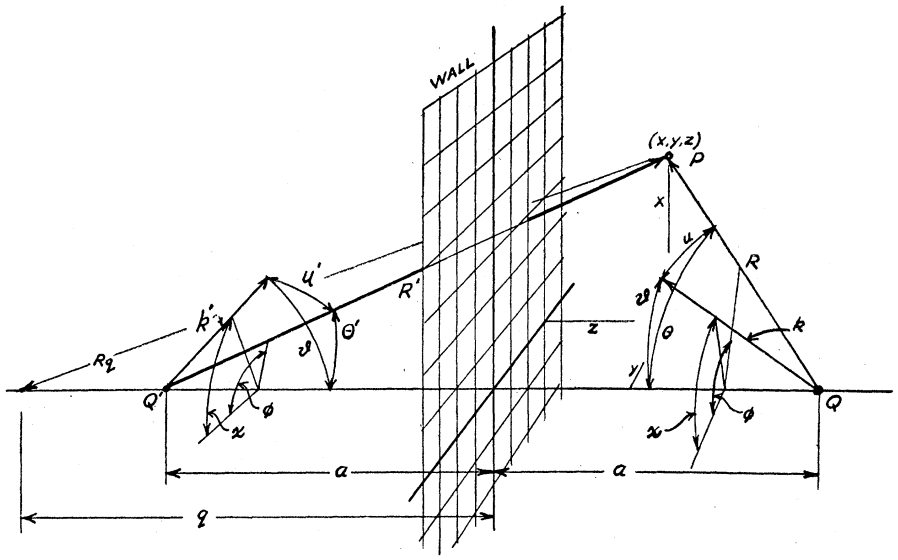

FIG. 31. Angles and distances involved in computing the reflection of a spherical wave from an absorbing wall.

reflections of a spherical wave from the walls of a rectangular room. Unfortunately this useful method is accurate *only when the walls are perfectly rigid;* when the wall impedance is not infinite *the reflected wave cannot be expressed in terms of a simple image.* To show this, we utilize the equation

$$\psi_i=\frac{e^{ikR}}{4\pi R}=\frac{k}{4\pi i}\int_1^{i\infty}e^{ikRz}dz=\frac{k}{8\pi^2 i}\int_0^{2\pi}d\chi \times\int_{i\infty-\pi/2}^{0}e^{ikR\cos u}\sin\vartheta d\vartheta$$

$$=(k/8\pi^2 i)\iint_s e^{i\mathbf{k}\cdot\mathbf{R}}d\Omega, \qquad (8.7)$$

where $k=(\omega/c)=(2\pi/\lambda)$, the angles and lengths involved are shown in Fig. 31, $d\Omega$ is the element of solid angle for k, and the subscript s beneath the integral signs indicates that the axial angle is integrated from 0 to 2π, and the polar angle is integrated from $i\infty-(\pi/2)$ to 0.

Equation (8.7) expresses the spherical velocity potential at P due to a simple unit source at Q, in terms of an integral of plane waves $e^{i\mathbf{k}\cdot\mathbf{R}}$ over different directions of k. We can now use the results of Section 51 to fit the boundary conditions at the wall, $z=0$. For each elementary plane wave $e^{i\mathbf{k}\cdot\mathbf{R}}d\Omega$ there is a reflected wave $[(\cos\vartheta-\beta)/(\cos\vartheta+\beta)]e^{i\mathbf{k}\cdot\mathbf{R}}d\Omega$. The amplitude of this reflected wave is not independent of the angle of incidence (because the factor contains $\cos\vartheta$) so that the wave emanating from the image point Q' is *not spherically symmetric.* This means that the intensity of the reflected wave at P depends on the angle θ'. Therefore any argument which assumes that the reverberent sound can be represented by a multiplicity of simple images is likely to lead to fallacious results. The analyses of Sabine (S2), Norris (N1), Eyring (E3), Millington (M7), and Sette (S12) are subject to this criticism.

The reflected wave is

$$\psi_r=\frac{k}{8\pi^2 i}\iint_s\frac{\cos\vartheta-\beta}{\cos\vartheta+\beta}e^{i\mathbf{k}'\cdot\mathbf{R}'}d\Omega'$$

$$=\frac{k}{8\pi^2 i}\int_0^{2\pi}d\chi\int_{i\infty-\pi/2}^{0}e^{-2\pi\Upsilon(\vartheta)+ikR'\cos u'}\sin\vartheta d\vartheta. \qquad (8.8)$$

This integral cannot be expressed in simple form. When β is small ($|Z|\gg\rho c$), an approximation which is good for R' larger than the wavelength is

$$\psi_r\simeq\frac{\cos\theta'-\beta}{\cos\theta'+\beta}\frac{e^{ikR}}{4\pi R'}=e^{-2\pi\Upsilon(\theta')+ikR'}/4\pi R'. \qquad (8.9)$$

To this approximation the reflected wave at P has the same reduction in intensity on reflection as would a plane wave with angle of incidence θ'. As P is moved farther from the line QQ' the angle θ' changes, and the factor $e^{-2\pi T(\theta')}$ changes; again illustrating the fact that the reflected wave is not spherically symmetric.

When the susceptibility is negative (X positive), the reflected wave can be expressed in terms of a simple source at Q' *plus a line source* extending along the axis from Q' to minus infinity:

$$\psi_r=\frac{e^{ikR'}}{4\pi R'}+2ik\beta\int_a^\infty e^{ik\beta(q-a)}\frac{\exp(ikR_q)}{4\pi R_q}dq, \quad (8.10)$$

where $\beta=\gamma-i\sigma$, $\sigma<0$, and q, R_q and a are shown in Fig. 31.

When $|\beta|$ is large ($|Z|<\rho c$), we can expand the reflected wave in a spherical harmonic series about Q:

$$\psi_r=\left[1-\beta\ln\frac{\beta+1}{\beta-1}\right]\frac{e^{ikR'}}{4\pi R'}-\frac{2k\beta}{4\pi}\sum_{n=1}^{\infty}(-i)^n(2n+1)\times Q_n(\beta)P_n(\cos\theta')h_n(kR'), \quad (8.11)$$

where Q_n is the Legendre function of the second kind, and h_n is the spherical Bessel function of the third kind. This expansion is valid for all values of β except for real values between $+1$ and -1, but its convergence is poor except for $|\beta|$ large.

54. Edge Corrections

Equation (8.6) gives the relation between the Sabine absorption coefficient and the wall impedance. With rooms of sufficient size and irregularity for ergodic wave motion to be set up, and with the wall impedance uniform over fairly large patches of the walls, the damping coefficient can be computed by means of Eq. (2.2), where the coefficient α_{stat}, for each patch, is multiplied by the area of the patch, exactly as was done by Sabine. We realize, of course, that the value of α_{stat} was computed from the impedance by assuming that the wall was infinite and had a uniform impedance. Near the boundary of a patch of material, diffraction effects will occur, and the absorption will not be the same as it is far from the boundary.

It is the purpose of this section to compute approximate edge corrections which can be added to the Sabine formula to give a more nearly correct expression for the reverberation time in rooms with random wave motion (these edge corrections are *not* valid in rooms where the wave motion is not random; the methods of Chapter VII must then be used). It turns out that the edge correction is an addition to the *area* of the patch, proportional to the perimeter of the patch, the length of boundary. It should be pointed out that those parts of the patch which end in a room edge (or within $\lambda/2$ of the edges) need no edge correction; so that a wall completely covered with acoustic material has no edge correction. Only those parts of the boundary which are on the flat part of the wall will count as "perimeter" in computing the edge correction.

To show how diffraction changes the absorption, let us consider the simplest case, that of a plane wave of unit intensity impinging normally on a plane wall (the x, y plane), the positive half ($x>0$) having impedance Z_+ and the negative half ($x<0$) having impedance Z_-. If the wall impedance were everywhere infinite, the pressure wave would be

$$p_0=(2\rho c)^{\frac{1}{2}}[e^{-i(\omega/c)z}+e^{+i(\omega/c)z}]e^{-i\omega t}=2(2\rho c)^{\frac{1}{2}}\cos(\omega z/c)e^{-i\omega t}, \quad (8.12)$$

and the normal velocity *into* the wall, $u_0=(i/\rho\omega)(\partial p_0/\partial z)_{z=0}$, would be zero.

Since the wall is not rigid, u_0 is not zero, and the wall vibrates (or, at least, air moves in and out of the pores). This motion generates a pressure wave p_1, additional to p_0, which modifies the wave to fit the boundary conditions. The total pressure at some point is then p_0+p_1, and, by the definition of the impedance, the air velocity at the surface is $u_0=(\beta/\rho c)(p_0+p_1)_{z=0}$. This motion generates the wave p_1:

$$p_1(x,y,z)=i(\omega/c)\int_{-\infty}^{\infty}dy'\int_{-\infty}^{\infty}dx'[\beta(x',y')e^{i\omega R/c}/2\pi R][p_0(x',y',0)+p_1(x',y',0)], \quad (8.13)$$

where $R^2=(x-x')^2+(y-y')^2+z^2$. Each element of surface $dx'dy'$ produces a wave which contributes to p_1. Equation (8.13) is an integral equation for p_1, which would give the exact solution if it were solved exactly, but which can usually only be solved approximately.

In the simple case we are considering, $\beta(x, y)$ depends only on x($\beta=\beta_+$ for $x>0$; $\beta=\beta_-$ for $x<0$), and we can integrate directly over y, obtaining for the pressure p_1 at the surface of the wall:

$$p_1(x)=-(\omega/2c)\int_{-\infty}^{\infty}\beta(x')[p_0(x')+p_1(x')]$$
$$\times\{J_0[\omega(x-x')/c]+iN_0[\omega|x-x'|/c]\}dx', \quad \text{at } z=0, \quad (8.14)$$

where J_0 and N_0 are the Bessel and Neumann functions of zero order.

Since p_0 at $z=0$ is equal to $2(2\rho c)^{\frac{1}{2}}e^{-i\omega t}$, independent of x, and since β only changes value at $x=0$, we can utilize the formula,

$$(\omega/c)\int_0^{\infty}\{J_0[\omega(x-x')/c]+iN_0[\omega|x-x'|/c]\}dx'$$
$$=(\omega/c)\int_{-x}^{\infty}\{J_0[\omega v/c]+iN_0[\omega|v|/c]\}dv$$
$$=\begin{cases}1-Ji_0(-\omega x/c)-iNi_0(-\omega x/c) & (x<0)\\ 1+Ji_0(\omega x/c)+iNi_0(\omega x/c) & (x>0)\end{cases} \quad (8.15)$$
$$=Fr(\omega x/c)+iFi(\omega x/c),$$

where

$$Ji_0(\mu)=\int_0^{\mu}J_0(u)du; \quad Ji_0(0)=0; \quad Ji_0(\infty)=1,$$
$$Ni_0(\mu)=\int_0^{\mu}N_0(u)du; \quad Ni_0(0)=0; \quad Ni_0(\infty)=0.$$

A plot of $Fr(z)$ and $Fi(z)$ is given in Fig. 32. We note that

$$\int_{-\infty}^{0}Fr(z)dz=0; \quad \int_0^{\infty}Fi(z)dz=-\frac{\pi}{2},$$

which will be useful later.

The final form of the integral equation for $p_1(x)$ at $z=0$ is therefore

$$p_1(x)=-(2\rho c)^{\frac{1}{2}}\{\beta_+[Fr(\omega x/c)+iFi(\omega x/c)]$$
$$+\beta_-[Fr(-\omega x/c)+iFi(-\omega x/c)]\}e^{-i\omega t}$$
$$-(\omega/2c)\int_{-\infty}^{\infty}\beta(x')p_1(x')\{J_0[\omega(x-x')/c]$$
$$+iN_0[\omega|x-x'|/c]\}dx', \quad (8.16)$$

where

$$[Fr(-z)+iFi(-z)]=2-[Fr(z)+iFi(z)].$$

When $(\omega x/c)$ is large compared to unity ($x\gg\lambda/2\pi$), $Fr(\omega x/c)\simeq 2$, $Fr(-\omega x/c)\simeq 0$, $Fi(\pm\omega x/c)\simeq 0$, and an approximate solution of Eq. (8.16) is

$$p_1\simeq-2(2\rho c)^{\frac{1}{2}}\beta_+e^{-i\omega t}-\beta_+p_1,$$

or

$$p_1\simeq-(2\rho c)^{\frac{1}{2}}[2\beta_+/(1+\beta_+)]e^{-i\omega t}, \quad (8.17)$$

so that the total pressure at the wall surface, far to the right of the junction line $x=0$ is

$$p_0+p_1\simeq(2\rho c)^{\frac{1}{2}}[2/(1+\beta_+)]e^{-i\omega t},$$

which is to be compared with Eq. (8.2) (the present case is for $\vartheta=0$). Similar expressions, with β_- inserted instead of β_+, hold for $-x\gg 2\pi/\lambda$.

A first approximation to p_1 can be obtained by setting it equal to these values, with a discontinuity at $x=0$;

$$p_1\simeq\begin{cases}-(2\rho c)^{\frac{1}{2}}[2\beta_+/(1+\beta_+)]e^{-i\omega t}, & (x>0)\\ -(2\rho c)^{\frac{1}{2}}[2\beta_-/(1+\beta_-)]e^{-i\omega t}, & (x<0).\end{cases} \quad (8.18)$$

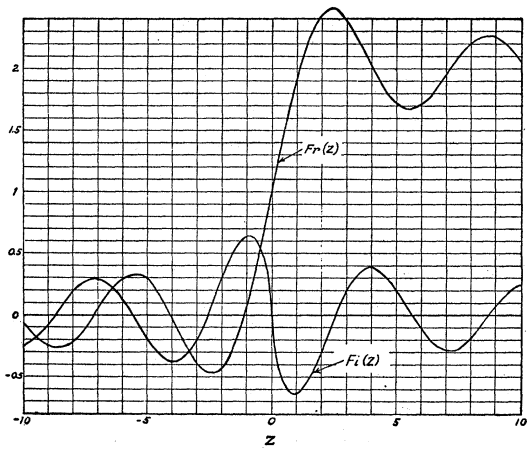

FIG. 32. Diffraction functions involved in calculation of edge corrections.

This approximation completely disregards diffraction effects, and the resulting expression for the absorption would neglect edge corrections.

A closer approximation, one which takes into account diffraction effects to the first order, is obtained by substituting Eq. (8.18) into the integral on the right-hand side of Eq. (8.16). After a bit of manipulation, the next approximation turns out to be:

$$p_1(x)\simeq-(2\rho c)^{\frac{1}{2}}\left\{\frac{\beta_+}{1+\beta_+}[Fr(\omega x/c)+iFi(\omega x/c)]+\frac{\beta_-}{1+\beta_-}[Fr(-\omega x/c)+iFi(-\omega x/c)]\right\}e^{i\omega t}, \quad (8.19)$$

for $z=0$. The total pressure at the wall surface is, to this approximation,

$$p_0+p_1\simeq\begin{cases}(2\rho c)^{\frac{1}{2}}\left\{\dfrac{2}{1+\beta_-}+\left[\dfrac{\beta_-}{1+\beta_-}-\dfrac{\beta_+}{1+\beta_+}\right][Fr(\omega x/c)+iFi(\omega x/c)]\right\}e^{-i\omega t} & (x<0)\\ (2\rho c)^{\frac{1}{2}}\left\{\dfrac{2}{1+\beta_+}+\left[\dfrac{\beta_+}{1+\beta_+}-\dfrac{\beta_-}{1+\beta_-}\right][Fr(-\omega x/c)+iFi(-\omega x/c)]\right\}e^{-i\omega t} & (x>0).\end{cases} \quad (8.20)$$

The power dissipated into the wall per unit incident intensity per unit area of wall at the distance x from the boundary line is $\gamma|p_0+p_1|^2/2\rho c=\alpha(0)$. When both $|\beta_+|$ and $|\beta_-|$ are smaller than unity ($|Z|>\rho c$) a fair approximation to $\alpha(0)$ is

$$\alpha(0)\simeq\begin{cases}\dfrac{4\gamma_-}{(1+\gamma_-)^2+\sigma_-{}^2}[1+(\gamma_--\gamma_+)Fr(\omega x/c)\\ \quad+(\sigma_--\sigma_+)Fi(\omega x/c)] & (x<0)\\ \dfrac{4\gamma_+}{(1+\gamma_+)^2+\sigma_+{}^2}[1+(\gamma_+-\gamma_-)Fr(-\omega x/c)\\ \quad+(\sigma_+-\sigma_-)Fi(-\omega x/c)] & (x>0).\end{cases} \quad (8.21)$$

The first factor is just the expression for the wall coefficient for normal incidence ($\vartheta=0$) for the wall far to the right or far to the left of the boundary line $x=0$. When this is averaged over all angles of incidence, the Sabine coefficient is obtained. The second and third terms in the square brackets are the correction terms due to diffraction effects near the boundary, the quantities *Fr* and *Fi* being small except within a wave-length (or so!) of this boundary. When the expression is integrated to obtain the total absorption of the wall, the first term is the usual coefficient multiplied by the total area of material, the second and third terms are edge corrections to be added to the area of each material having a "free" boundary. A "free" boundary is one which is well away from room edges: one which is closer than a half-wave-length from an edge of a room over most of its extent is not counted as a "free" boundary. For instance, if a patch of material covers half a wall, clear to the edges of the room, then only the boundary down the middle of the wall is a free boundary.

By using the expressions for the integrals of *Fr* and *Fi*, we finally obtain the following approximate rules for applying edge corrections in rooms with random wave motion. The usual expression for the total absorption holds: we multiply the Sabine coefficient (computed by means of Eq. (8.6) or Fig. 31) for each patch of material by the *effective* area of each patch. The effective area is the actual area of the patch plus

$$(\lambda/4)(\sigma_+-\sigma_-)=\frac{\lambda\rho c}{4}\left[-\frac{X_+}{R_+{}^2+X_+{}^2}+\frac{X_-}{R_-{}^2+X_-{}^2}\right] \quad (8.22)$$

times the length of free boundary. Here λ is the wave-length of the sound, $\gamma_+-i\sigma_+$ the admittance of the patch under consideration (R_+ and X_+ the corresponding acoustic resistance and reactance) and $\gamma_--i\sigma_-$ is the admittance of the material adjoining the patch on the other side of the free boundary in question. It is assumed that $|Z|>\rho c$.

We note that corresponding to each boundary

separating two materials on a wall (provided the line is not too close to a room corner), there are *two* edge corrections of equal magnitude and opposite sign, one for the area of material on one side of the boundary and the other for the area of material on the other side. The correction for the material of larger susceptance (σ larger) is positive, that for the material of less positive susceptance is negative. The sum of the effective areas is just equal to the total wall area. Since $\sigma=-\rho cX/(R^2+x^2)$ measures the compliance (reciprocal of the stiffness of a wall), we can say that the effective areas of the more compliant patches are somewhat larger than their actual areas and those for the less compliant patches are reduced somewhat. Equation (8.22) is derived for normal incidence; the correction for oblique waves will differ somewhat from this.

For example, take a patch of material of resistance $R=1.5(\rho c)$ and reactance $-2(\rho c)$. The Sabine absorption coefficient is approximately 0.75, and the specific susceptance is 0.33. Suppose a $10'\times10'$ patch of this material be mounted on a wall of impedance $(14+20i)(\rho c)$, ($\alpha_{\text{stat}}=0.15$, $\sigma=0.03$), with its edges far from the room corners. At 500 cycles the effective area of the patch will be 106 square feet, and the effect of diffraction will be to add 4.5 sabines to the absorption of the patch and to subtract 1 sabine from the absorption of the rest of the wall. At lower frequencies, if the wall impedances remain the same (which they will not!) the relative size of the correction will increase.

ACKNOWLEDGMENTS

Valuable help has been rendered the authors by many colleagues. Among them are Professor V. O. Knudsen, whose encouragement and general advice have been particularly inspiring. Many thanks are due Dr. H. Feshbach, Dr. R. L. Brown, Mr. Cyril M. Harris, and Mr. J. R. Pellam, for painstaking and intensive checking of the manuscript, and for many cogent suggestions. We are also indebted to Misses C. Lane and M. Hatch for careful typing and preparation of the textual matter.

55. Glossary of Symbols Used

The more commonly used symbols are listed here, with reference to the section or sections where the symbol is defined. Only symbols used in more than one section are included here.

Symbol	*Meaning*	*Units*	*Defined in sections number*
a	Room absorption factor	cm² or ft.²	32
a_p	Normal absorption factor	cm² or ft.²	33
A	Amplitude of ψ	cm²/sec.	14, 25
	Indicial admittance		37
B	Expansion coeff. for Q	sec.$^{-1}$	29
c	Velocity of sound in air	cm/sec.	10, 17
e	Wave type factor		27, 44
G	Normalizing amplitude for ψ		27, 28
i, j	Imaginary units, $i=(-1)^{\frac{1}{2}}$, $j=-i$		10
I	Intensity of sound	ergs/sec. cm²	3.1
j	Imaginary units	$-i$	10
J	Bessel function		
k	Damping constant		6, 16, 27, 32
k_{ON}	Natural damping constant		37
K	Constant in reverberation formula		3.1, 4, 6
	Effective stiffness of panel		21
L	Dimensions of room	cm or ft.	14
	Thickness of wall material	cm or ft.	17
m	Density factor for material		17
M	Effective mass of panel		21
n	Integer		14
	Real part of index of refraction		17
N	Quantum number trio	(n_x, n_y, n_z)	27
P	Porosity of material (Percent of volume which is pore space)		17
q	Imaginary part of index of refraction		17
	Source function	sec.$^{-1}$	29
Q	Source amplitude	sec.$^{-1}$	29
Q_0	Strength of simple source	cm³/sec.	29
r	Resistivity factor for materials	g/cm sec.	17, 24

Symbol	Meaning	Units	Defined in sections number
R	Acoustic resistance	Press./velocity	10
S	Area of wall surface	cm² or ft.²	
t	Time	sec.	
T	Reverberation time	sec.	3.1, 4
u	Vector velocity of air x component of air velocity	cm/sec.	14, 25
U	Unity or step function		37
v	y component of air velocity	cm/sec.	14
V	Volume of room	cm³ or ft.³	
w	z component of air velocity	cm/sec.	14
W	Energy density of sound	erg/cm³	6
x, y, z	Rectangular coordinates	cm or ft.	
X	Acoustic reactance	Press./velocity	10
Z	Acoustic impedance	Press./velocity	10, 27
α	Absorption or wall coefficient		4, 10
α_p	Normal wall coefficient		10, 32
α_t	Tangential wall coefficient		32
α_s	Supplementary wall coefficient		32
α_{stat}	Sabine or statistical absorption coefficient		4, 10, 52
β	Specific admittance	$=(\rho c/Z)=\gamma-i\sigma$	10, 27
γ	Specific conductance Resistivity parameter for material		10, 27 17
Γ	Impedance parameter for material Phase angle for ξ		19 37
Δ	$=4\pi\mu\kappa$		27
ϵ	Normalizing number	$(\frac{1}{8}, \frac{1}{4}, \frac{1}{2}, 1)$	14, 28
ζ	Specific impedance	$(Z/\rho c)$	10
η	Frequency parameter	$(2L/\lambda)$	25
ϑ	Angle of incidence		51
θ	Normalizing phase angle for ψ		27, 28
κ	Attenuation parameter		25
λ	Wave-length	cm or ft.	
Λ	Normalizing constant		28
μ	Wave number parameter		25
ν	Frequency	sec.$^{-1}$	14
ξ	Characteristic value $(\omega+ik)$		27, 37
Ξ	Index of randomness		47
π	$=3.1416$		
Π	Power of source	ergs/sec.	6
ρ	Mean density of air	g/cm³	10
σ	Specific susceptance Frequency parameter for material		10, 27 19
Σ	Summation sign		
τ, v	Reflected wave parameters		51
Υ	$=\tau-iv$		51
φ	Phase angle for Z	$Z=\lvert Z\rvert e^{-i\varphi}$	10, 27
φ_i	Angle of incidence		17
Φ	Phase angle for velocity potential		25, 37
χ	Characteristic value for ψ,	$=(\mu-i\kappa)$	25
ψ	Velocity potential	cm²/sec.	14, 25
Ψ	Total velocity potential	cm²/sec.	29, 37
ω	Angular frequency	$=(2\pi\nu)$	10, 27
ω_{ON}	Natural frequency		37
Ω	$=\mu^2-\kappa^2$		27

56. Bibliography

The following references cover most of the material discussed in this review. For a more complete Bibliography on this subject, see Watson, "Bibliography of Acoustics of Buildings," J. Acous Soc. Am. **2**, 14 (1931), and Cumulative Index, J. Acous. Soc. Am. Vols. 1–10 (1939), which are referred to as References A in the text.

(A1) F. Aigner, "*Experimentelle Studie über d. Nachhall*," Akad. Wiss. Wien **123**, 1489 (1914).

(A2) C. A. Andree, "Effect of position on the absorption of materials for the case of a cubical room," J. Acous. Soc. Am. **3**, 535 (1932).

(B1) G. v. Bekesy, "Uber die Horsamkeit kleiner Musikraume," Ann. d. Physik **19**, 665 (1934).

(B2) L. L. Beranek, "Precision Measurement of acoustical impedance," J. Acous. Soc. Am. **12**, 3 (1940).

(B3) L. L. Beranek, "Acoustical impedance of commercial materials and the performance of rectangular rooms with one treated surface," J. Acous. Soc. Am. **12**, 14 (1940).

(B4) L. L. Beranek, "Acoustic impedance of porous materials," J. Acous. Soc. Am. **13**, 248 (1942).

(B5) N. B. Bhatt, "The effect of an absorbing wall on the decay of normal frequencies," J. Acous. Soc. Am. **11**, 67 (1939).

(B6) R. H. Bolt, "Frequency distribution of eigentones in a three-dimensional continuum," J. Acous. Soc. Am. **10**, 228 (Jan. 1939); "Angular distribution theory," J. Acous. Soc. Am. **11**, 74 (1939).
(B7) R. H. Bolt and A. A. Petrauskas, "An acoustic impedance meter for rapid field measurements," J. Acous. Soc. Am. **15**, 79A (1943).
(B8) R. H. Bolt, "Normal modes of vibration in room acoustics;" "Experimental investigations in non-rectangular enclosures," J. Acous. Soc. Am. **11**, 184 (1939).
(B9) R. H. Bolt and R. L. Brown, "Variable boundary impedance," J. Acous. Soc. Am. **12**, 31 (1940).
(B10) R. H. Bolt, H. Feshbach, and A. M. Clogston, "Perturbation of sound waves in irregular rooms," J. Acous. Soc. Am. **14**, 65 (1942).
(B11) C. P. Boner, "Performance of broadcast studios designed with convex surfaces of plywood," J. Acous. Soc. Am. **13**, 244 (1942).
(B12) R. L. Brown, R. H. Bolt, and P. M. Morse, "Acoustic impedance and sound absorption," J. Acous. Soc. Am. **12**, 217 (1940).
(B13) R. L. Brown and R. H. Bolt, "Measurement of flow resistance of porous acoustic materials," J. Acous. Soc. Am. **13**, 337 (1942).
(B14) E. Buckingham, Bull. Bur. Stand. **20**, 193 (1925).

(C1) V. L. Chrisler, "Acoustical work of the National Bureau of Standards," J. Acous. Soc. Am. **7**, 79 (1935).
(C2) V. L. Chrisler, "Sound absorption coefficients," J. Acous. Soc. Am. **6**, 115 (1934).
(C3) C. W. Clapp and F. A. Firestone, "The acoustic wattmeter, an instrument for measuring sound energy flow," J. Acous. Soc. Am. **13**, 12 (1941).
(C4) I. B. Crandall, *Theory of Vibrating Systems and Sound* (D. Van Nostrand Company, New York, 1927).
(C5) H. Cremer and L. Cremer, "The theoretical derivations of the laws of reverberation," Akustische Zeits. **2**, 225, 296 (1937).
(C6) L. Cremer, "The physical basis of room acoustics," Zeits. f. tech. Physik **17**, 528 (1936).
(C7) L. Cremer, "Nachhallzeit und Dämpfungsmass bei streifendem Einfall," Akustische Zeits. **5**, 57 (1940).

(D1) A. H. Davis, "Reverberation equations for two adjacent rooms connected by incompletely sound-proof partition," Phil. Mag. **50**, 75–80 (1925).
(D2) A. H. Davis, "The basis of acoustic measurements by reverberation methods," Phil. Mag. **2**, 543 (1926).
(D3) A. H. Davis and E. J. Evans, "Measurement of absorbing power of materials by the stationary wave method." Proc. Roy. Soc. **A127**, 89–110 (1930).
(D4) I. Dreisen, "The orientation of natural acoustic vibrations in a room with concentrated absorbents and of anomalous shapes," Tech. Phys. USSR **3**, 743 (1936).

(E1) E. A. Eckhardt, "Acoustics of rooms," J. Frank. Inst. **195**, 799 (1923).
(E2) L. P. Eisenhart, "Separable Euclidean coordinates," Ann. Math. **35**, 284 (1934).
(E3) C. F. Eyring, "Reverberation time in 'dead' rooms," J. Acous. Soc. Am. **1**, 217–241 (1930).
(E4) C. F. Eyring, "Conditions under which residual sound in reverberent rooms may have more than one rate of decay," J. Soc. Mot. Pict. Eng. **15**, 528 (1943).
(E5) C. F. Eyring, "Symposium discussion," J. Acous. Soc. Am. **11**, 104 (1939).

(F1) H. Feshbach and A. M. Clogston, "Perturbation of boundary conditions," Phys. Rev. **59**, 189 (1941).
(F2) H. Feshbach, "On the perturbation of boundary conditions," Phys. Rev. **65**, 307 (1944).
(F3) H. Fletcher and J. C. Steinberg, "Articulation testing methods," J. Acous. Soc. Am. **1**, No. 2, Pt. 2 (1930).
(F4) A. D. Fokker, "Sabine's formule voor den nagalm," Physica **7**, 198 (1927).
(F5) W. S. Franklin, "Derivation of equation of decaying sound in a room," Phys. Rev. **16**, 372 (1903).

(G1) A. Gemant, "Resistance to airflow in sound absorbers," Preuss. Akad. Wiss. **17**, 579 (1933).

(H1) W. M. Hall, "An acoustic transmission line for impedance measurements," J. Acous. Soc. Am. **11**, 140 (1939).
(H2) R. L. Hanson, "Liveness of rooms," J. Acous. Soc. Am. **3**, 318 (1932).
(H3) J. Henry, "Acoustics applied to public buildings," Smithsonian Reports (1854 and 1856).
(H4) P. R. Heyl, V. L. Chrisler, and W. F. Snyder, "The absorption of sound at oblique angles of incidence," Bur. Stand. J. of Research **4**, 289 (1930).
(H5) F. V. Hunt, "On frequency modulated signals in reverberation measurements," J. Acous. Soc. Am. **5**, 127 (1933).
(H6) F. V. Hunt, "Apparatus and technique for reverberation measurements," J. Acous. Soc. Am. **8**, 34 (1936).
(H7) F. V. Hunt, "Investigation of room acoustics by steady state transmission measurements," J. Acous. Soc. Am. **10**, 216 (1939).
(H8) F. V. Hunt, "Absorption coefficient problem," J. Acous. Soc. Am. **11**, 38 (1939).
(H9) F. V. Hunt, L. L. Beranek, and D. Y. Maa, "Analysis of sound decay in rectangular rooms," J. Acous. Soc. Am. **11**, 80 (1939).
(H10) Kodi Husimi, "On the asymptotic distribution of frequencies of a Hohlraum and the surface tension of an ideal gas," Proc. Phys. Math. Soc. Japan **21**, 759 (1939).

(J1) A. Jager, "Zur theorie des Nachhalls," Akad. Wiss. Wien 2a, **120**, 613 (1911).
(J2) J. Jeans, "On the partition of energy between matter and aether," Phil. Mag. **10**, 91 (1905).
(J3) R. C. Jones, "Theory of fluctuations in decay of sound," J. Acous. Soc. Am. **11**, 324 (1940).

(K1) V. O. Knudsen, "Acoustics of music rooms," J. Acous. Soc. Am. **2**, 434 (1931).
(K2) V. O. Knudsen, "Absorption of sound in air," J. Acous. Soc. Am. **3**, 126 (1931).
(K3) V. O. Knudsen, *Architectural Acoustics* (John Wiley & Sons, Inc., New York, 1932).
(K4) V. O. Knudsen, "Measurement of sound absorption in a room," Phil. Mag. **5**, 1240 (1928).
(K5) V. O. Knudsen, "Resonance in small rooms," J. Acous. Soc. Am. **4**, 20–37 (1932).
(K6) V. O. Knudsen, "The absorption of sound in air, in oxygen, and in nitrogen," J. Acous. Soc. Am. **5**, 112 (1933).
(K7) V. O. Knudsen, "Recent developments in architectural acoustics," Rev. Mod. Phys. **6**, 1 (1934).
(K8) V. Kuhl and E. Meyer, "Untersuchungen über die Winkel- und Frequenz-abhängigheit der Schallschluckung von Pyorösen Stoffen," Preuss. Akad. Wiss. **26**, 416 (1932).
(K9) K. Kurhihara, "Distribution of sound energy in an enclosed space," Proc. Phys. Math. Soc. Japan **10**, 71 (1928).

(L1) M. von Laue, "Die Freiheitsgrade von Strahlenbündeln," Ann. d. Physik **44**, 1197 (1914).
(L2) S. Lifschitz, "Mean intensity of sound in an auditorium, and optimum reverberation," Phys. Rev. **27**, 618 (1926).
(L3) S. Lifschitz, "Acoustics of large auditoriums," J. Acous. Soc. Am. **4**, 113 (1932).
(L4) S. Lifschitz, "Apparent duration of sound perception and musical optimum reverberation," J. Acous. Soc. Am. **7**, 213 (1936).
(L5) D. P. Loye and R. L. Morgan, "Acoustic tube for measuring the sound absorption coefficients of small samples," J. Acous. Soc. Am. **13**, 261 (1942).

(M1) D. Y. Maa, "The distribution of eigentones in a rectangular chamber at lower frequency ranges," J. Acous. Soc. Am. **10**, 258 (1939).
(M2) D. Y. Maa, "Non-uniform acoustical boundaries in rectangular rooms," J. Acous. Soc. Am. **12**, 39 (1940).
(M3) D. Y. Maa, "Flutter echoes," J. Acous. Soc. Am. **13**, 170 (1941).
(M4) W. A. MacNair, "Optimum reverberation time for auditoriums," J. Acous. Soc. Am. **1**, 242 (1930).
(M5) J. P. Maxfield and C. C. Potwin, "A modern concept of acoustical design," J. Acous. Soc. Am. **11**, 48 (1939).
(M6) E. Meyer, "Reverberation and absorption of sound," J. Acous. Soc. Am. **8**, 155 (1937).
(M7) G. Millington, "A modified formula for reverberation," J. Acous. Soc. Am. **4**, 69 (1932).
(M8) A. Monna, "Absorption of sound by porous substances," Physica **5**, 129 (1938); Rev. d acoustique **7**, 126 (1938).
(M9) K. C. Morrical, "A modified tube method for measurement of sound absorption," J. Acous. Soc. Am. **8**, 162 (1931).
(M10) R. M. Morris, G. M. Nixon, and J. S. Parkinson, "Variations in absorption coefficients as obtained by the reverberation chamber method," J. Acous. Soc. Am. **9**, 234 (1938).
(M11) P. M. Morse, *Vibration and Sound* (McGraw-Hill Book Company, Inc., New York, 1936) in particular, Chapter VIII.
(M12) P. M. Morse, "Some aspects of the theory of room acoustics," J. Acous. Soc. Am. **11**, 56 (1939).
(M13) P. M. Morse, "Transmission of sound inside pipes," J. Acous. Soc. Am. **11**, 205 (1939).

(N1) R. F. Norris, "A derivation of the reverberation formula," Appendix II in *Architectural Acoustics* by V. O. Knudsen (John Wiley & Sons, Inc., New York, 1932).

(O1) H. F. Olsen and B. Kreuzer, "The reverberation time bridge," J. Acous. Soc. Am. **2**, 78 (1930).

(P1) E. T. Paris, "Sound absorption coefficients measured by reverberation and stationary wave methods," Nature **120**, 806, 880 (1927).
(P2) E. T. Paris, "On the reflection of sound from a porous surface," Proc. Phys. Soc. **115**, 407–419 (1927).
(P3) E. T. Paris, "On the stationary wave method of measuring sound absorption at normal incidence," Proc. Phys. Soc. **39**, 269–295 (1927).
(P4) E. T. Paris, "Resonance in pipes stopped with imperfect reflectors," Phil. Mag. **4**, 907–917 (1927).
(P5) E. T. Paris, "On the coefficient of sound-absorption measured by the reverberation method," Phil. Mag. **5**, 489–497 (1928).
(P6) E. T. Paris, "Oblique reflection of sound," Nature **9**, 126 (1930).
(P7) J. S. Parkinson, "Area and pattern effects in the measurement of sound absorption," J. Acous. Soc. Am. **2**, 112 (1930).
(P8) H. L. Penman and E. G. Richardson, "The absorption of porous materials at normal incidence," J. Acous. Soc. Am. **4**, 322 (1933).
(P9) J. R. Power, "Measurement of absorption in rooms with sound absorbing ceilings," J. Acous. Soc. Am. **10**, 98 (1938).

(R1) A. V. Rabinovich, "Effect of distance in the broadcasting studio," J. Acous. Soc. Am. **7**, 199 (1936).
(R2) L. G. Ramer, "Absorption of strips, effects of width and location," J. Acous. Soc. Am. **12**, 323 (1941).
(R3) Rayleigh, "The law of complete radiation," Phil. Mag. **49**, 539 (1900).
(R4) Rayleigh, *Theory of Sound* (The Macmillan Company, New York, Vol. II, Chap. 13, 1929).
(R5) M. Rettinger, "Note on reverberation characteristics," J. Acous. Soc. Am. **6**, 51 (1934).
(R6) M. Rettinger, "On the theory of sound absorption of porous materials," J. Acous. Soc. Am. **6**, 188 (1935).
(R7) M. Rettinger, "Theory of sound absorption of porous materials, flexible and non-flexible," J. Acous. Soc. Am. **8**, 53 (1936).
(R8) G. M. Roe, "Frequency distribution of normal modes," J. Acous. Soc. Am. **13**, 1 (1941).

(S1) W. C. Sabine, *Collected Papers on Acoustics* (Harvard University Press, 1922).
(S2) W. C. Sabine, *Collected Papers on Acoustics* (Harvard University Press, 1929) p. 43.
(S3) P. E. Sabine, "Diffraction effects in sound absorption measurements," Phys. Rev. **19**, 402 (1922).
(S4) P. E. Sabine, "What is measured in sound absorption measurements?" J. Acous. Soc. Am. **6**, 239 (1935).
(S5) P. E. Sabine, "The beginnings of architectural acoustics," J. Acous. Soc. Am. **7**, 242–248 (1936).
(S6) P. E. Sabine, "The effect of cylindrical pillars in a reverberation chamber," J. Acous. Soc. Am. **10**, 1 (1938).
(S7) P. E. Sabine, "Architectural acoustics, its past and its future," J. Acous. Soc. Am. **11**, 21 (1939).
(S8) P. E. Sabine, "Specific normal impedance and sound absorption coefficients of materials," J. Acous. Soc. Am. **12**, 317 (1941).
(S9) H. J. Sabine, "Notes on acoustic impedance measurements," J. Acous. Soc. Am. **14**, 143 (1942).
(S10) K. Schuster and E. Waetzmann, "Uber den Nachhall in geschlossenen Raumen," Ann. d. Physik **1**, 671 (1929).
(S11) K. Schuster, "Berechnung der Schalldichte in einem Kugelformigen Raume," Ann. d. Physik **1**, 696 (1929).
(S12) W. H. Sette, "A new reverberation time formula," J. Acous. Soc. Am. **4**, 193 (1933).
(S13) G. T. Stanton, F. C. Schmidt, and W. J. Brown, "Reverberation measurements in auditoriums," J. Acous. Soc. Am. **4**, 95–105 (1934).
(S14) G. T. Stanton, "Correlation of sound absorption coefficients with field measurements," J. Acous. Soc. Am. **11**, 45 (1939).
(S15) M. J. O. Strutt, "On the acoustics of large rooms," Phil. Mag. **8**, 236–250 (1929).
(S16) M. J. O. Strutt, "Acoustics of large halls," Zeits. f. angew. Math. u. Mech. **10**, 360–368 (1930).

(T1) H. O. Taylor, "A direct method of finding the value of materials as sound absorbers," Phys. Rev. **2**, 270 (1913).

(T2) H. O. Taylor and C. W. Sherwin, "Sound absorption and attenuation by the flue method," J. Acous. Soc. Am. **9**, 331–335 (1938).

(V1) J. E. Volkmann, "Polycylindrical diffusers in room acoustical design," J. Acous. Soc. Am. **13**, 234 (1942).

(W1) F. R. Watson, *Acoustics of Buildings* (John Wiley & Sons, Inc., New York, 1941).

(W2) F. R. Watson, "Acoustics of auditorium; optimum time of reverberation," Arch. **55**, 251 (1927).

(W3) R. B. Watson, "The modulations on sound decay curves," J. Acous. Soc. Am. **13**, 82A (1941).

(W4) E. C. Wente and E. H. Bedell, "The measurement of acoustic impedance and the absorption coefficient of porous materials," Bell Sys. Tech. J. **7**, 1–10 (1928).

(W5) E. C. Wente and E. H. Bedell, "Chronographic method of measuring reverberation time," J. Acous. Soc. Am. **1**, 422 (1930).

(W6) E. C. Wente, E. H. Bedell, and K. D. Swartzel, "High speed level recorder for acoustic measurements," J. Acous. Soc. Am. **6**, 121 (1935); See also Bedell and Swartzel, J. Acous. Soc. Am. **6**, 130 (1935).

(W7) E. C. Wente, "Acoustical instruments," J. Acous. Soc. Am. **7** (1935).

(W8) E. C. Wente, "Characteristics of sound transmission in rooms," J. Acous. Soc. Am. **7**, 123 (1935),

(W9) H. Weyl, "Das asymptotische Verteilungsgesetz der Eigenwerte linearer partieller Differentialgleichungen," Math. Ann. **71**, 441 (1911).

(W10) F. J. Willig, "Comparison of sound absorption coefficients obtained experimentally by different methods," J. Acous. Soc. Am. **10**, 293 (1939).

(W11) E. Wintergerst, "Theorie der Schalldurchlässigkeit von einfachen und zusammengesetzten Wänden," Schalltechnik. **4**, 85 (1931).